Analysis and prediction of plant functional traits in contrasting environments: information for next-generation ecosystem models

By

Henrique Furstenau Togashi

Supervised by
I. Colin Prentice
Owen K. Atkin
Ian J. Wright
Suzanne M. Prober
Craig Macfarlane
Michael J. Liddell

A thesis submitted to Macquarie University
for the degree of
Doctor of Philosophy

Faculty of Science and Engineering
Department of Biological sciences
February 2016

MACQUARIE
University
SYDNEY·AUSTRALIA

I certify that the work in this thesis has not previously been submitted for a degree nor has it been submitted as part of requirements for a degree to any other university or institution other than Macquarie University. I also certify that the thesis is an original piece of research and it has been written by me. Any help and assistance that I have received in my research work and the preparation of the thesis itself have been appropriately acknowledged. In addition, I certify that all information sources and literature used are indicated in the thesis.

Henrique Furstenau Togashi

Acknowledgements

I thank Macquarie University for supporting me through the International Macquarie University Research Excellence Scholarship (iMQRES) during the past three and a half years. I also extend my gratitude to the Terrestrial Ecosystem Research Network (TERN) organisation and to the Ecosystem Modelling and Scaling Infrastructure (eMAST) facility for financial support and for funding my fieldwork in Australia.

It has been a great opportunity to work with Professor Colin Prentice, my primary supervisor. Colin is a very influential scientist in Earth System Modelling, and a great supervisor. He was always available when I needed help, and always encouraged me to work towards novel science. His ideas and guidance led me to expand my understanding of science greatly. Colin's network permitted me to work with and learn from leading scientists in plant physiology and biogeography. His prestige and hard work were essential to obtain grants that allowed me to go on fascinating campaigns to collect plant data. I am so grateful to Colin, and I can't think of anyone who could be a better mentor, offering so many amazing opportunities for a student to learn.

I thank Professor Owen Atkin, my associate supervisor and an internationally recognised scientist, who taught me a great deal about ecophysiology and leaf gas exchange methods. He was as important as Colin in obtaining the grants that made my fieldwork possible. He was also present in the early campaigns, making sure we were successful in collecting the data. His positive criticism on part of my work was crucial for my development as a scientist. Owen also organised a TERN workshop in which I had the great opportunity to expand my network by meeting the Australian leading scientists

in the area.

My other associate supervisors also had a very important role in my progress. I am grateful to Dr Ian Wright for many discussions about my results. I thank Dr Suzanne Prober and Dr Craig Macfarlane, who provided scientific and field support to my work at the Great Western Woodlands; and Professor Mike Liddell during my work at Robson Creek.

Thanks to Dr Brad Evans who was my employer over last year at eMAST. He shared his knowledge in obtaining and creating products from gridded data, motivated me to learn the python programming language, how to create spatial products following international standards, along with how to manage complex databases. His input was fundamental to my learning in a wide variety of extremely useful scientific skills.

I am thankful to my lab colleagues, Guangqi Li, Dr Rhys Whitley, Anna Ukkola, Dr Ines Hessler, Dr Wang Han, Ian Marang, Shuang Zhou, Ning Dong, Yasmin Hageer, Douglas Kelley, Annika Herbert, Dr Kevin Willis, and Farzana Raihan. They helped me on the most diverse kinds of tasks including science discussions, fieldwork, writing grant applications, and setting up the required computer tools to process and analyse data.

I am grateful to Dr Keith Bloomfield for the discussions about ecophysiology, for managing the field campaigns in Australia, for reviewing part of my work, and for his hospitality in my trips to Canberra. Dr Lasantha Weerasinghe contributed in early stages of the Australian fieldwork and also helped me understand more about ecophysiology and leaf gas exchange. Thanks to Professor David Ellsworth for his comments on some of my results, for inviting me to participate in some of his research group activities, and for answering my questions of plant physiology.

I would like to thank Professor Tomas Domingues, Professor Maurizio Mencuccini, Professor Santi Sabate, Dr Lucas Cernusak, Dr Sean Gleason and Dr Daniel Falster for their scientific input on, and giving ideas, about my data. I also recognise scientific contribution in part of my work from Professor Jon Lloyd, Professor Derek Eamus, Professor David Forrester, Dr Paul Drake, Dr Paul Feikema and Dr Kim Brooksbank. I acknowledge support on fieldwork by Jack Egerton, Lingling Zhu, Danielle Creek,

Desmond Ng, Aurore Penillard, Lucy Hayes, Jinlong Zhang, Professor Sandy Harrison, Professor Jian Ni (funds and network), and Dr Marina Scalon. Dr Matt Bradford contributed fundamental data as well as identified all tree species I collected in Robson Creek. My thanks to Stephanie McCaffery for supervision in the digestion of leaves for nitrogen and phosphorus analysis; and to Professor Brian Atwell, Muhammad Masood and Ray Duell for all laboratory support. Diego Barneche, thanks for the great help with R scripts.

I want to thank the entire Biological Sciences Department of Macquarie University including, but not restricted to, Teresa Potalivo, Marie Howitt, Laura McMillan, Professor Marie Herberstein, Samantha Newton, and especially Veronica Peralta who booked my student trips and resolved most of my paperwork. Thanks also to Jane Yang and Ana Borba from the Higher Degree Research team at Macquarie University.

Last, but not least, I have to mention my family that always accepted all my decisions, particularly my choice of living overseas for so long. Gabriela, Rafael, Akira, Erica, Vera, and Yoko, I would not have finished this thesis without your support. Thank you.

Abstract

Three empirical plant-trait studies are presented, based on new field data plus extensive data analysis. All aim to provide information to improve the basis of dynamic global vegetation models (DGVMs), by exploring neglected ecophysiological processes.

The first study investigates a key model parameter, the leaf area (LA) to cross-sectional sapwood-area (SA) ratio, in Australian evergreen woody plants. It confirms the pipe model, which states that SA at any point should scale isometrically with LA distal to that point. But although the LA:SA ratio is reported to vary with hydroclimate, aridity determined only upper and lower bounds of LA:SA. Great variation among species in similar environments exists and may reflect variation in stem hydraulics.

The second study refutes the common model assumption that photosynthetic traits of evergreen plants are fixed in time. If it were true, carboxylation capacity (V_{cmax}) should increase with temperature following Rubisco kinetics. The study employs a theoretical framework to predict, instead, that V_{cmax} should acclimate to temperature: increasing, but less steeply. Repeat sampling of plants in the semi-arid Great Western Woodlands, during the warm and cool seasons, revealed that V_{cmax} (and other photosynthetic parameters) show thermal acclimation as predicted.

The third study focuses on tropical rainforests in Australia and China, occupying a relatively narrow range of climates, to examine the association of plant functional traits (including growth traits such as maximum height as well as field-measured photosynthetic traits) with species' successional 'roles'. Consistent relationships were found,

providing key information for modelling forest dynamics.

Each study tackles an aspect of DGVMs that so far has involved simplifying assumptions, such as assigning fixed trait values to functional types without considering variability across environments, seasons, and species. To take account of such variation, DGVM development will require targeted empirical studies like those presented here.

Contents

List of Figures

List of Tables

1

Introduction

1.1 Current knowledge about the impacts of vegetation and human activity on climate

1.1.1 Human activity and alterations in climate and the global carbon cycle

Anthropogenic carbon emissions during the Industrial Era have unequivocally increased the atmospheric carbon dioxide (CO_2) concentration and contributed decisively to present (and likely future) climate change. Carbon dioxide is the most important long-lived greenhouse gas and anthropogenic emissions of CO_2 are the principal human contribution to the radiative forcing of climate since the Industrial Revolution. The main causes of anthropogenic CO_2 emission are fossil fuel combustion and land use

change (deforestation), with a small additional contribution from cement production (Ciais *et al.*, 2014). Analyses of the European Project for Ice Coring in Antarctica (EPICA) provide evidence that the current atmospheric concentration of CO_2 (∼400 ppm) is the highest in 800,000 years (Monnin *et al.*, 2001). Prior to 1750, atmospheric CO_2 concentration ranged between ∼180 and ∼300ppm during glacial and interglacial periods respectively (Petit *et. al*, 1999; Monnin *et. al*, 2001; MacFarling Meure *et. al*, 2006). The ongoing increase in atmospheric CO_2 concentration is an important driver required to account for the observed increase of temperatures at a continental scale at a rate of 0.13°C (±0.03) per decade over the last 50 years (1956 - 2005), which is approximately twice the average rate over the last 100 years (1906 - 2005) (Solomon *et al.*, 2007). The global rise in temperature has driven an intensification of the hydrological cycle due to an increase in water vapour evaporated from the oceans and land. A general concept, that many wet regions are becoming wetter while some dry areas getting drier, has been proposed ('rich get richer, poor get poorer' hypothesis), however, the magnitude of these changes remains somewhat unclear (Allan *et al.*, 2010; Friedlingstein *et al.*, 2014). A recent study has shown that the picture is more complicated than this and a simple intensification of existing patterns of the land surface is not sustained (Greve *et al.*, 2014). Uncertainty extends to future projections, which are unanimous about near-ubiquitous global warming but vary considerably in their regional distribution of changes in rainfall. This lack of precise understanding of hydrological change and its distribution across the continents creates problems in anticipating and planning effective responses to the impacts of climate change, which potentially include alterations in agricultural practices and food security, fire regimes, extreme weather events, biodiversity and conservation practices, the spread of infectious diseases and environmental challenges to economic growth.

Mitigation of and optimal adaptation to climate change require a firm quantitative understanding of the global carbon cycle (and the fates of other greenhouse gases, including methane and nitrous oxide, whose abundances are being modified by human activities) and the various fluxes of CO_2 between ocean, atmosphere and land that help to determine the atmospheric concentration of CO_2 under any given emissions scenario.

From a quantitative perspective, the global carbon cycle can be considered as a series of carbon 'reservoirs' in the Earth system (Ciais *et al.*, 2014), which dynamically exchange carbon with one each other. The annual exchange fluxes of carbon between the ocean and atmosphere, and between the land and atmosphere, are extremely large - more than an order of magnitude larger than the total added to the atmosphere annually by human activities - and thus any perturbation of these fluxes can have a profound impact. The largest carbon reservoirs are in sedimentary rocks (a small part of the lithospheric reservoir is in the form we know as fossil fuels) and the deep ocean. The sedimentary reservoir was almost isolated from the 'fast' reservoirs of atmospheric CO_2 until the Industrial Revolution, which was spurred by the discovery of fossil fuels and their potential to generate useful energy. The natural exchange of carbon between the sedimentary reservoir and the atmosphere, ocean and land involves rock weathering, subduction and volcanism and takes place exceedingly slowly, causing variations in CO_2 on a multi-million year time scale but having essentially negligible effects on a human time scale. In contrast, fossil fuel burning is responsible for a transfer of 8.7±0.5 Pg C y^{-1} (1 Pg = 1015 g or 1 billion tonnes) from the lithosphere to the atmosphere, while the annual gross exchange of carbon between land ecosystems (as organic carbon in vegetation and soils) and atmospheric CO_2 is estimated to have been almost 110 Pg C before the Industrial Revolution (Ciais *et al.*, 2014) and is now estimated to be in the range 120 to 130 Pg C yr^{-1} (Beer *et al.*, 2010; Piao *et al.*, 2013; Reichstein *et al.*, 2013). The flux has increased as the land has been taking up, on average, about a quarter of total anthropogenic emissions from fossil fuel burning and land use change. The processes involved in the land-atmosphere exchange of carbon are almost entirely biological: photosynthesis (also called gross primary production) by green plants, almost balanced by autotrophic respiration and heterotrophic respiration due to microbial and fungal decomposers, plus a small contribution from wildfire. The fact that the land is taking up a part of the anthropogenic CO_2 emission implies that there is a slight imbalance in the fluxes, such that the rate of global photosynthesis is increasing faster than the combined rate of heterotrophic respiration and combustion of biomass (Ciais *et al.*, 2014). Thus, terrestrial ecosystems constitute an important

'sink' for anthropogenic CO_2 which has significantly reduced the rate of global climate change (Shevliakova *et al.*, 2009).

1.1.2 State of the art in land-surface and vegetation modelling

Atmosphere-ocean general circulation models (AOGCMs) - often called GCMs or simply 'climate models' - and, more recently, Earth System models (ESMs) that include biological and chemical components, are the principal tools used to project future climate change and (in the case of ESMs) the future of the global carbon cycle and atmospheric CO_2. The latest results of these models form the backbone of successive Assessment Reports by the Intergovernmental Panel on Climate Change (IPCC) (Houghton *et. al*, 1990; 1995; 2001; Solomon *et. al*, 2007; Stocker *et. al*, 2013; Ciais *et. al*, 2014; Friedlingstein *et. al*, 2014). Models of land-atmosphere CO_2 exchange based on dynamic representations of ecosystem processes (known as Dynamic Global Vegetation Models or DGVMs: Prentice and Cowling, 2013; Prentice *et al.*, 2007) were used to project future CO_2 uptake under continuing climate change by Cramer *et al.* (2001) and results of such modelling were described in the IPCC Third Assessment Report (Prentice *et al.*, 2001). Coupled climate-carbon cycle models, in which GCMs were combined with process-based representations of land- and ocean-atmosphere exchanges, were presented by Cox *et al.* (2000) and Friedlingstein *et al.* (2006), and reported in the IPCC Fourth Assessment Report (Solomon *et al.*, 2007). By the Fifth Assessment Report, results were available from many ESMs with the carbon cycle as a fully integrated component (Ciais *et al.*, 2014). The direction of development of the carbon cycle model components has been characterized by a progressive increase in complexity which has not, however, been matched by convergence: there were large differences among the projections of different models as presented by Cramer *et al.* (2001) and a similar range of future predictions characterizes the latest ensemble of ESMs considered by the IPCC (Ciais *et al.*, 2014). This lack of consensus seems to reflect a lack of agreement on how various land processes should be modelled, thus providing a key motivation for this thesis.

Several types of model have been used from about the 1980s onwards to represent

land ecosystem processes. Terrestrial biogeochemistry models (TBMs) (e.g. McGuire *et al.*, 2001) have the main objective of simulating land-atmosphere carbon exchanges but typically keep biome distributions fixed, applying different sets of parameter values to each biome. Biogeography models (e.g. Prentice *et. al*, 1992; Haxeltine and Prentice 1996) have the main objective of simulating biome distributions by consideration of the climatic controls of different Plant Functional Types (PFTs). The earliest such models did not consider land-atmosphere carbon exchanges explicitly, although later models included this aspect (Prentice *et al.*, 2007). Land-surface models (LSMs) were developed originally to provide the physical land-surface component of GCMs, and as such typically focus on 'fast' processes (for example, a diurnal cycle of evapotranspiration is required to represent the physics of land-atmosphere exchanges) while typically treating the distribution of vegetation, and often other aspects such as phenology, constant. More recent LSMs have included CO_2 as well as water and energy exchanges (see e.g. Prentice *et al.*, 2015; Sellers *et al.*, 1986). Finally vegetation dynamics models (Shugart, 1984) have usually been regionally specific and focused on simulating the course of vegetation succession and response to disturbance, but often with relatively crude representations of physical and physiological processes. Today's DGVMs represent a merger of these four strands of model development (Prentice *et al.*, 2007). They serve two major functions: simulation of land-surface dynamics coupled to GCMs (Potter and Klooster 1999; Sitch *et. al*, 2008; Prentice *et. al*, 2011), and as self-contained models predicting past and future mechanisms of change in vegetation cover, as result of alterations in climate and in atmospheric chemical composition (Potter and Klooster, 1999; Wang *et al.*, 2014). Many models now include, for example, land use change, coupled N and P cycling (Wang *et al.*, 2007), emissions of reactive trace gases (Arneth *et al.*, 2011) and anthropogenic fire regimes (Thonicke *et. al*, 2010; Kloster *et. al*, 2012).

Most contemporary land models make use of the standard model of photosynthesis by Farquhar *et al.* (1980). This model represents the dependence of photosynthesis on the intercellular concentration of CO_2 (c_i), which is a key variable required for the process-based simulation of CO_2 effects on vegetation and the carbon cycle. This is one

component of contemporary land process models that is generally agreed upon, as the model is well known to provide a very good approximation of the behaviour of photosynthesis with respect to environmental changes under controlled conditions. However, the model (a) requires certain important (and variable) quantities to be known - they can be measured, but for global modelling they have to be predicted somehow - and (b) also requires a 'closure' (because there is no universally accepted model for stomatal behaviour) to predict the value of c_i, given the ambient CO_2 concentration (c_a). These 'details' are in fact immensely important, as we shall see.

1.1.3 New opportunities for Dynamic Global Vegetation Models

The huge challenge faced by early attempts to model the global land surface in all its daunting complexity was to produce realistic results with the help of remarkably limited data that could be used either to develop the model or to evaluate the results (Prentice *et al.*, 2015). This situation has now greatly improved, as a very large body of empirical data on leaf and plant traits and rates has accumulated over the past two decades (Wright *et. al*, 2004; Kattge *et. al*, 2011; Torello-Raventos *et. al*, 2013; Bradford *et. al*, 2014). However, model development has not fully capitalized on this 'data revolution'. What has happened is that models have became increasingly complex, and 'realistic' in the sense that they represent an increasing fraction of the processes known to influence ecosystems - a trend that has not been matched by increasing reliability or robustness (Prentice *et al.*, 2015). Models generally still require a long list of parameters to be specified for each of a number of PFTs, while the controls of these parameters are often incompletely understood and/or inadequately quantified. The situation demands to be rectified because the differences among model predictions are stark. For example, modelled positive responses of global net primary production (NPP) to atmospheric CO_2 concentration vary more than five times and models even diverge on the sign of the response of global NPP to climate (Solomon *et al.*, 2007; Wang *et al.*, 2014). The causes of such differences are difficult to diagnose, because of the models' sheer complexity and

the lack of a common framework that could facilitate process-by-process comparisons (Medlyn *et al.*, 2015). These problems are now stimulating a re-think of land models with a view to providing a much stronger and more transparent basis in observations (Smith *et al.*, 2013) and theory (Wang *et al.*, 2014).

One key to making better, more robust models resides in the now extensive field of empirical research on plant traits and their correlations with one another and with environmental variables, of which the leaf economics spectrum (Wright *et al.*, 2004) provides a classic example. The idea of optimization by natural selection, which is assumed to act by eliminating inefficient combinations of traits (Prentice *et al.*, 2015), is key to the development of theoretical insights and modelling principles in plant trait research. It is expected that plant traits should respond to climatic influences (Reich, 2014) because the optimal trait combinations are likely to be different in different growth environments. However, this is a nascent science. The 'periodic table of PFTs' (Steffen, 1996) has yet to emerge. Meanwhile, there is a great deal of work to be done in trying to establish general simplifying principles that can be supported by measurements in the field.

1.2 Plant Functional Types and forest dynamics

From their earliest stages of development, DGVMs have adopted PFT classification systems designed principally to facilitate representation of the global-scale distribution of different biomes (Prentice *et al.*, 1992, 2007). But PFT classifications have a long history prior to the development of numerical models. Raunkiær's (1934) 'life form' classification was specifically based on plant traits that ensure persistence through seasons unfavourable for growth (Harrison *et al.*, 2010). After several decades when plant functional geography was largely neglected, new PFT classifications started to appear in the 1980s (Box, 1981; Woodward, 1987). However, most PFT classifications in current models are simplified relative to Raunkiær's. They are usually defined in terms of: (a) life form (often just woody versus non-woody), (b) leaf type (broad- or needle-leaf), (c) phenological type (deciduous or evergreen), (d) photosynthetic pathway (C3,

C4) and (e) climatic ranges as broad climatic classes such as boreal, tropical, desert. This conventional approach to PFT classification has served its purpose in enabling the development of the first generation of DGVMs, but is also fraught with limitations (Prentice and Cowling, 2013). In particular, the common modelling approach that assigns fixed values of leaf-level traits such as carboxylation capacity (V_{cmax}) and nitrogen content per unit leaf area (N_{area}) to PFTs does not adequately describe the plasticity of such traits nor, crucially, the adaptive importance of trait variation within PFTs.

The last few years have seen rapidly increasing interest in the development of models based on continuous trait variation (Pavlick *et al.*, 2013; Scheiter *et al.*, 2013; Verheijen *et al.*, 2013; Fisher *et al.*, 2015), which in principle could account for the large and systematic variations that can be found in many quantitative traits along environmental gradients, both within and between PFTs (Meng *et al.*, 2015). But models that represent trait variation as a continuum within conventionally defined PFTs still struggle with the coarse and approximate definitions of PFTs. Models capitalise on well-understood distinctions among photosynthetic pathways, but they also need more explicit principles for the assignment of values for quantitative traits with adaptive significance (see e.g. Ali *et al.*, 2015).

Another neglected aspect of PFT classification concerns niche differences among co-existing species in complex communities. Classifications of tree species according to shade tolerance (Whitmore, 1982) and growth rate characteristics (pioneer versus climax) (Swaine and Whitmore, 1988) define species' various 'roles' in forest dynamics. Such classifications have been used to specify parameter values in regionally specific 'gap models' (Botkin et al., 1972; Shugart, 1984). Most DGVMs however do not consider these distinctions and little recent research has been done on the relationship between dynamical roles and the functional traits used in DGVMs. Fyllas *et al.* (2012), focusing on Amazonian tropical rainforests, examined the relationship between 'roles' in vegetation dynamics and a series of quantitative traits. Chapter 4 here adopts the simple fourfold species' role classification popularized by Shugart (1984). This classification subdivides two continua of variation - shade tolerance (requiring, versus

not requiring, a gap for regeneration) and size at maturity (producing, versus not producing, a gap upon mortality). This work extends the approach of Fyllas *et al.* (2012) to include photosynthetic trait measurements.

1.3 Physiological basis of photosynthesis described by models

1.3.1 The Farquhar model and Fick's law

Plant growth is based on the space-time integral of carbon uptake, also called GPP. Autotrophic carbon uptake is the result of the process of photosynthesis. Estimating terrestrial GPP is crucial to quantifying the land-surface component of the global carbon cycle (Wang *et al.*, 2014). Photosynthesis is regulated by the key control variable c_i which depends in part on the stomatal conductance (g_s), which simultaneously controls the entry of CO_2 into the leaf and the loss of water (transpiration) from the leaf (Farquhar and Sharkey, 1982). The coupling of photosynthesis and transpiration through stomatal behaviour is central to simulation of both the global carbon cycle and the global hydrological cycle.

Farquhar *et al.* (1980) introduced the standard biochemical model of photosynthesis in C3 plants (the FvCB model). In this model, photosynthesis (A) is taken to proceed at the slower of two rates. One of these (W_c) refers to the catalytic rate of conversion of the enzyme ribulose 1.5 - bisphosphate carboxylase/oxygenase (Rubisco), assuming a saturating supply of substrate (RuBP). The maximum velocity of carboxylation is generally called V_{cmax}. The Rubisco-limited rate of photosynthesis is described by the following equation:

$$W_c = V_{cmax}\left[\frac{c_i - \Gamma^*}{c_i + K}\right] - R_d \tag{1}$$

where c_i is the leaf-intercellular partial pressure of CO_2. Here $K = K_c(1 + O/K_o)$, where the partial pressure of intercellular oxygen is represented by O, K_c and K_o are

respectively the Michaelis-Menten constants of Rubisco for CO_2 and oxygen (O_2). Γ^* is the photorespiratory compensation point of CO_2, where assimilation exactly matches photorespiration (i.e. the net CO_2 exchange is zero). The kinetic properties of Rubisco are conservative among C3 species and so this general relationship, with prescribed values of K_c and K_o (which are functions of temperature), has a very wide field of application (Von Caemmerer 2000; Sharkey *et. al*, 2007). R_d (or R_{day}) is the rate of mitochondrial respiration in the presence of light, which is a small and approximately constant fraction of V_{cmax}.

Equation (1) formally assumes infinite mesophyll conductance (g_m), which is a measure of the ability of CO_2 to diffuse through physical barriers inside the leaf including air, cell walls, lipid membranes, liquid cytoplasm and stroma. The mesophyll conductance is expected to affect values of Γ^* and c_i (Von Caemmerer, 2000) and the assumption of infinite mesophyll conductance means that in practice estimation of V_{cmax} based on photosynthesis measurements and using Equation (1) leads to an underestimation of the true value of Rubisco catalytic capacity. However, given still incomplete understanding of the controls of g_m, Equation (1) remains the standard implementation in the FvCB model.

The second limiting rate (W_j) is the rate of regeneration of RuBP. The rate of electron transport (J) is crucial here because electron transport supports $NADP^+$ reduction to NADPH, required for the regeneration of RuBP. This limitation is described by:

$$W_j = J\left[\frac{c_i - \Gamma^*}{4c_i + 8\Gamma^*}\right] - R_d \tag{2}$$

A maximum rate of electron transport (J_{max}) can be estimated from leaf gas-exchange measurements under saturating light and CO_2, using equation (2). J is then a function of J_{max} and is most commonly quantified by the non-rectangular hyperbola (Von Caemmerer, 2000):

$$J = \frac{\phi I + J_{max} - \sqrt{(\phi I + J_{max})^2 - 4\phi\theta I J_{max}}}{2\theta} \tag{3}$$

where I is the photosynthetic photon flux density (PPFD), ϕ is the intrinsic quantum yield and θ is the curvature of the light response.

Typically, photosynthesis at high PPFD is Rubisco-limited for $c_i < 200$ ppm and RuBP-regeneration-limited for $c_i > 300$ ppm CO_2. Between 200 and 300 ppm there is a 'transition zone' where the two rates are co-limiting. The standard approach to measuring photosynthesis involves developing response curves (A-c_i curves) where photosynthesis is recorded under saturating PPFD at different levels of c_a. From A-c_i curves, it is possible to estimate V_{cmax} and J_{max}.

Sharkey (1985) introduced a third (W_t) limitation to the biochemical processes of photosynthesis when high CO_2, high light and low temperature yield results inconsistent with the FvCB model. This third limitation, known as triose phosphate limitation (TPU), is rarely observed in field. It occurs when the leaf's capacity to release phosphate in the chloroplast during the synthesis of sucrose and starch is smaller than the capacity for triose phosphate production in the Calvin cycle. As a result, phosphate becomes limiting to photosynthesis, and assimilation becomes insensitive to both CO_2 and O_2. This situation is described by:

$$W_t = 3TPU - R_d \tag{4}$$

where TPU is the triose phosphate utilization rate. This standard implementation has been further corrected for 'reversed' O_2 and CO_2 sensitivities observed empirically (Harley and Sharkey, 1991).

Equations (1) and (2) are functions of c_i, but c_i is itself a function of the rate of photosynthesis and of the stomatal conductance to CO_2 (g_s). The assimilation rates (A), and the c_i value consistent with it, are given by the coordinates of the intersection of the A-c_i curve and the straight line that describes the relationship between c_i and g_s according to Fick's law of diffusion (Figure 1.1). The A function is also known as 'demand function' (Leuning, 1990) while the 'supply function' describes the Fick's law

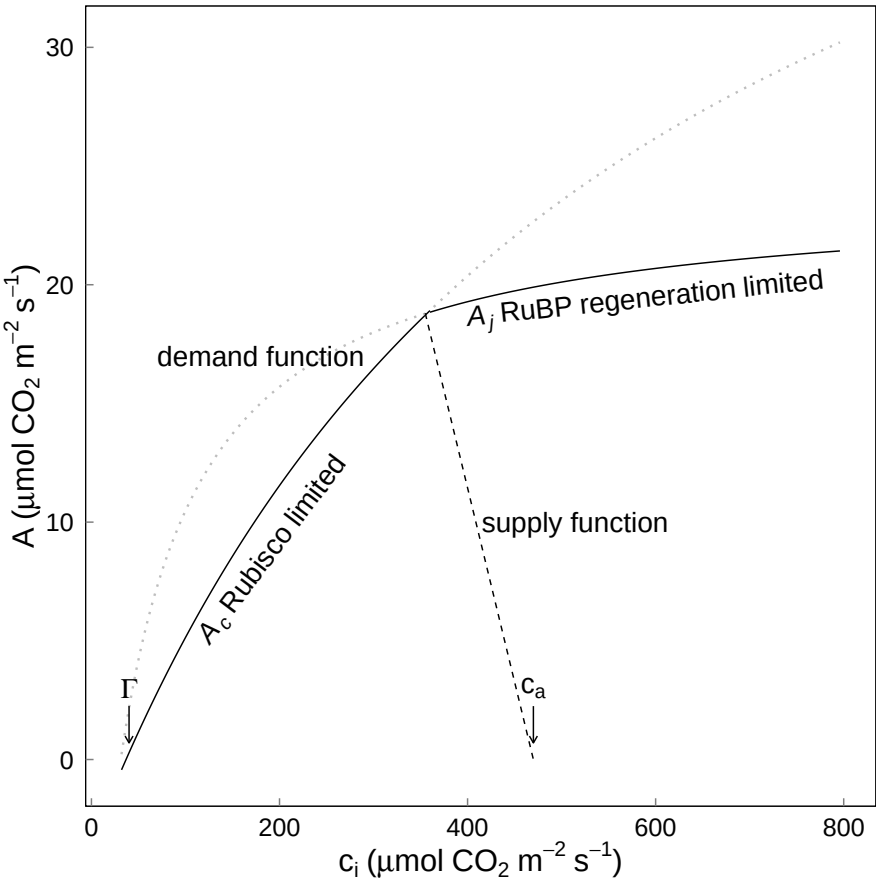

FIGURE 1.1: Assimilation (A) plotted against the leaf-intercellular partial pressure of CO_2 (c_i) (*Prunus turneriana* measured at Robson Creek - see section 1.4 and chapter 4). Solid lines are modelled W_c and W_j (demand function). Dotted grey lines are assimilation if W_c and W_j were not co-limiting. The dashed line describes CO_2 diffusion from the atmosphere to the intercellular spaces (supply function)

limitation of A by g_s:

$$A = g_s(c_a - c_i) \tag{5}$$

where c_a is the atmospheric partial pressure of CO_2. If g_s is not limiting (infinite), the supply function is a vertical line through $c_i = c_a$ (Farquhar and Sharkey, 1982).

1.3.2 The evolutionary attractor framework

The quantification of photosynthetic parameters in a straightforward, robust and realistic modelling framework opened the doors for microeconomic analogies to the photosynthetic process, in which water, nitrogen, and carbon can be viewed as currencies to be acquired, stored, and spent (Wright *et al.*, 2003). The economic analogy applied to the concept of optimization by natural selection permitted the formulation of quantitative, testable hypotheses in an 'evolutionary attractor framework' (Givnish 1986; Westoby *et. al*, 2012; Prentice *et. al*, 2014), also referred to as 'optimality modelling'. According to this approach, measures of plant efficiency should be maximized by strategies that permit the highest photosynthetic revenue to be obtained with the lowest construction and maintaining costs, under specific sets of environmental constraints. However, although the basic idea is powerful, it is not necessarily clear *a priori* what measures should be optimized, or indeed what can be optimized; for example, some of the terms in the FvCB model are considered to be close to evolutionarily 'hard-wired' constraints - for example the intrinsic quantum yield (φ) does not represent a thermodynamic constraint but rather the empirical fact that this quantity, when properly measured, varies little at least among wild C3 plants (Skillman *et. al*, 2005; Long and Bernacchi 2003). Thus, the evolutionary attractor framework provides a way to formulate general hypotheses that may hold great promise for simplifying DGVMs; but they have to be tested with field measurements. That is the purpose of this thesis. Specifically, the thesis addresses the following explicit hypotheses, which represent under-studied aspects of plant ecophysiology that are nonetheless of great importance for the correct representation of plant processes in DGVMs:

- That the ratio of leaf area to the cross-sectional sapwood area supplying that area (LA:SA) should be invariant with plant size (the pipe model: Shinozaki *et al.*, 1964), but should vary systematically with hydroclimate.
- That photosynthetic capacity at constant growth PPFD should acclimate to temperature on a seasonal time scale, in such a way that photosynthesis on average remains co-limited by Rubisco capacity and electron transport (the 'coordination hypothesis': Maire *et al.*, 2012).

- That different 'roles' of species in complex tropical forests - climax, large and small pioneer, and subcanopy species - should exhibit leaf and plant trait combinations consistent with the 'coordination hypothesis' and the 'least-cost' theory (Prentice *et al.*, 2014) which proposes that c_i:c_a should decline with increasing water transport costs.

The theory behind each of these hypotheses is described in the following sections.

1.3.3 The least-cost theory and the trade-offs of V_{max}, c_i:c_a, leaf N and the Huber value

The 'least-cost' theory was introduced by Wright *et al.* (2003) and refined by Prentice *et al.* (2014). Carbon assimilation is considered as the 'product' and the costs of production are considered as (1) a carbon cost proportional to the transpiration (E) required to support a given rate of assimilation ($a.E/A$ where a is a water-transport 'cost factor') and (2) a carbon cost proportional to maintaining Rubisco capacity ($b.V_{cmax}/A$ where b is a carboxylation 'cost factor'). Prentice *et al.* (2014) hypothesized that plants minimize the sum of these two costs:

$$Cost = a\,\frac{E}{A} + b\,\frac{V_{cmax}}{A} \tag{6}$$

Applying Fick's law for transpiration, and given that the stomatal conductance to water vapour is 1.6 times higher than stomatal conductance to CO_2 (g_s), we have:

$$E = 1.6 g_s D \tag{7}$$

where D is the leaf-to-air vapour pressure deficit. The supply function for photosynthesis can be re-arranged to demonstrate photosynthetic relationships to the CO_2 diffusion gradient represented by the ratio c_i:c_a:

$$A = g_s c_a \left(1 - \frac{c_i}{c_a}\right) \tag{8}$$

Equations 7 and 8 contain the common parameter g_s suggesting a trade-off between c_i:c_a, assimilation A, transpiration E and atmospheric aridity D. Prentice *et al.* (2014) showed that there is an optimal value (χ_0) of the c_i:c_a ratio, which can be simplified (provided A is much higher than R_d and c_i much higher than Γ^*) to the following expression:

$$\chi_0 = \frac{\xi}{\xi + \sqrt{D}} \tag{9}$$

where $\xi = \sqrt{(bK/1.6a)}$. This is identical with the equation presented in Medlyn *et al.* (2011), but derived in a more explicit way by Prentice *et al.* (2014) as the solution to the minimisation problem posed by equation (6). Note that the formal assumption $A >> R_d$ is only used in this thesis in the derivation of the optimal c_i:c_a ratio where it has very little effect - whereas the fact that R_d is nonetheless a significant 'cost' is part of the underpinning of the least-cost theory. The formal assumption $c_i >> \Gamma^*$ is not a requirement of the theory but rather a convenient approximation as fully expressed in equation (8) of Prentice *et al.* (2014).

Equation (9) predicts that the c_i:c_a ratio should have a positive relationship to K and a negative relationship to vapour pressure deficit (D). K is known to increase steeply with temperature (Bernacchi *et al.*, 2003). In addition, a should decrease with temperature because the declining viscosity of water with increasing temperature (Roderick and Berry, 2001) means that the maintenance costs of sapwood (for a given water flow) are less at higher temperatures. Therefore, χ_0 increases with temperature both due to the increasing cost of photosynthesis (higher V_{cmax} is required to support a given assimilation rate) and the declining cost of water transport. Both factors speak for a shift in the balance of investments towards water transport, resulting in a higher optimal value of c_i:c_a. Prentice *et al.* (2014) also presented field evidence in support of the positive relationship between c_i:c_a and temperature, and the negative relationship between c_i:c_a and aridity as predicted by equation (9).

Plant transpiration E can be expressed by a simple relationship that derived from Darcy's Law to describe the water flow, combined with Fick's law to describe water

loss at the leaf surface (Whitehead *et al.*, 1984):

$$E = \frac{v_h \, \Delta\Psi \, k_s \, \rho}{\eta \, l} \tag{10}$$

where the so-called Huber value (v_h) is the ratio of the cross-sectional sapwood area and the (one-sided) leaf area supplied by it (the inverse of the Huber value, the leaf area to sapwood area ratio LA:SA, was adopted in this thesis). Sapwood permeability (k_s) is a wood property independent of the properties of water (Reid *et al.*, 2005). The water potential gradient $\Delta\Psi$ is the difference between soil water potential (or pre-dawn leaf water potential) and leaf water potential. The total path length is l. More conservative (physical) quantities in equation (10) are the density of water ρ and the temperature-dependent viscosity of water η. If LA:SA is negatively correlated to E, and thus to D (equations 7 and 10), we would also expect the optimal ratio of stomatal conductance to photosynthetic capacity to be reduced in drier environments (Wright *et. al*, 2004; Prentice *et. al*, 2014). In drier environments, usually a larger sapwood area per unit area of transpiring leaf has to be maintained if photosynthetic rates are to equal those achieved in wetter environments (Westoby *et al.*, 2012). Additionally, equation (10) suggests that LA:SA and k_s should be correlated. This relationship has been empirically proved by Gleason *et al.* (2012) and it is revisited in Chapter 2 of this thesis.

The Huber value is a powerful predictive trait for several reasons:

- Its trade-offs with other traits are well-defined theoretically (Whitehead *et. al*, 1984; Westoby *et. al*, 2012; Li *et. al*, 2014).
- Its value is predicted by the pipe model (Shinozaki *et al.*, 1964) to be constant, implying an isometric relationship between LA and SA, in any part of the tree (permitting up scaling from small branches to whole trees) or between trees of the same species but different size.
- Xylem tapering renders hydraulic conductivity approximately independent of path length, thus tending to maintaining v_h constant (Tyree and Ewers, 1991).

- The Huber value should reflect plant strategies of water use ranging from 'conservative' (high-density wood, low-calibre conducting elements) to 'aggressive' (low-density wood, high-calibre conducting elements) (Gleason *et al.*, 2012).
- Huber values can be measured straightforwardly in the field by scanning leaves and by subtracting the cross-sectional area of a branch/trunk from the pith cross-sectional area (Gleason *et al.*, 2012).

Trade-offs between the Huber value and other traits have been modelled in other contexts. The mass of carbon in sapwood ($W_{.s}$) is a parameter included in a model developed by Prentice *et al.* (2014) and Wang *et al.* (2014) to calculate net primary production (NPP) and relates to v_h as follows (Li *et al.*, 2014):

$$W_{.s} = L\, A_c\, v_h\, \rho_s\, H_f \tag{11}$$

where L is the leaf area index within the crown, A_c is the projected crown area, ρ_s is the density of the wood, and H_f is the mean foliage height. Assuming the 'initial' sapwood area (for a small tree) is equal to the stem cross-sectional area, Li *et al.* (2014) derived from equation (11) a simple identity:

$$L\, c\, v_h = 1 \tag{12}$$

where c is the initial ratio of crown area to stem cross- sectional area. Thus, for whole-tree growth modelling, knowing any two of the variables L, c and v_h is sufficient to predict the third.

Yet despite all these reasons to study LA:SA, as well as its obvious importance for modelling (as it determines the support costs associated with maintaining leaf area), the available data are still quite limited. Most studies of variation in LA:SA have ben carried out on gymnosperms, and few comparative studies have been undertaken involving multiple angiosperm species. There is evidence that this parameter adjusts in the expected manner (declining with aridity) to spatial variation in D within gymnosperm species (Mencuccini and Grace, 1995), but no information seems to be

available concerning the generality (or otherwise) of this response.

Another important trait (and one that is very commonly measured) is the leaf nitrogen content per unit area (N_{area}). The least-cost theory predicts a trade-off between V_{cmax} and the c_i:c_a ratio, and to a first approximation, N_{area} is related to V_{cmax} (for any given temperature; as the amount of Rubisco, and therefore the quantity of N, required to support a given level of enzyme activity declines with increasing temperature). Thus, a general prediction of least-cost theory is that N_{area} should increase with aridity, all else equal. However the expected response to temperature is more complex because it includes a predicted increase (due to the increased V_{cmax} needed to support a given assimilation rate at higher temperature) and a decrease (due to the increased catalytic activity of photosynthetic enzymes; as further elaborated in the next section). Moreover, the relationship between N_{area} and V_{cmax} is indirect, and approximate, with some indication of higher N requirements per unit V_{cmax} in dry climates (Prentice *et al.*, 2014). Thus, a proportional relationship between V_{cmax} (even at standardized temperature) and N_{area} cannot be taken for granted; it is better to measure both quantities, as has been done here.

1.3.4 The coordination hypothesis

The 'coordination hypothesis' was introduced by Chen *et al.* (1993) to explain a long-known and widely observed phenomenon: the decline of leaf N with depth in closed canopies. The basic idea is that plants allocate N, coordinating both V_{cmax} and J_{max} to attain a balance where $W_c = W_j$ for typical daytime conditions. Maire *et al.* (2012) confirmed this finding for sunlit leaves, also showing its link to N_{area}, for a range of plant species grown under different environmental conditions. Although originally (and from today's perspective, puzzlingly) presented as an alternative to optimality models (Chen *et al.*, 1993; Maire *et al.*, 2012), the coordination hypothesis can easily be understood in the evolutionary attractor framework as co-limitation implies an optimal balance of investment in light capture, electron transport and carboxylation capacities. Excess investment in any of these functions would have no positive impact on assimilation and should therefore, from first principles, be disfavoured. And indeed, Chen

et al. (1993) already showed that the vertical distributions of carbon assimilation and nitrogen distribution resulting from their mechanistic interpretation of the hypothesis were closely similar to the predictions of optimal models (see also Hirose and Werger 1987; Anten 2005).

Nitrogen used for carbon assimilation should be allocated to leaves until W_c and W_j are balanced and for that reason V_{cmax} and J_{max} are expected to be pairwise proportional (Chen *et al.*, 1993). Empirically, V_{cmax} and J_{max} have been shown to be strongly correlated and the ratio between them to be fairly conservative (Wullschleger 1993; Domingues *et. al*, 2010), although somewhat dependent on growth temperature (Kattge and Knorr, 2007). Thus, the coordination hypothesis suggests the possibility that this observed conservatism - analogously to the well-known conservatism of the c_i:c_a ratio - might be theoretically explicable in the evolutionary attractor framework and perhaps that the modest temperature dependence of this ratio - analogously to the well-established decline of c_i:c_a with aridity - might be predictable as well. However, this possibility is not pursued here.

1.3.5 Acclimated responses, least-cost, coordination and PFTs

Plants are expected to optimise carbon revenue and minimize costs, in a highly plastic response to environmental conditions. Although it is recognized that plants have to adapt to temperature, water availability, vapour pressure deficit and light, how these environmental factors will limit and determine plant acclimation are still not entirely understood (Niinemets and Valladares, 2004). Assuming that optimal use of limiting resources results from canopy photosynthetic acclimation, leaf level photosynthesis models may be directly up scaled to predict whole canopy photosynthesis biochemistry (Farquhar *et al.*, 1980). The spatial variation of photosynthesis acclimation to environmental factors may be dependent on attributes such as canopy position, height and level (e.g. understorey, overstorey), gap exposure and others. These characteristics will influence plants exposure to various light levels, temperature and climatic moisture, and thus will define how heterogeneous should be photosynthesis acclimation (Niinemets and Valladares, 2004). Short-term variation of the interactions between

the environmental factors should be large enough to significantly modify leaf physiology, while long-term acclimation may lead to complex and dynamic patterns of carbon assimilation among short distances in plant canopies (Niinemets and Valladares, 2004).

This thesis considers certain predictions that arise from a combination of the least-cost hypothesis with the coordination hypothesis, as follows:

- V_{cmax} should increase with increasing growth temperature (spatially or seasonally) due to the increase of K.
- V_{cmax} and J_{max} should covary, both spatially and seasonally.
- Values of V_{cmax} and J_{max} normalized to 25°C should decline with increasing growth temperature, because the catalytic capacity of Rubisco increases more steeply than K.
- Mitochondrial respiration in the dark, R_{dark} (Niinemets and Tenhunen 1997; Atkin *et. al*, 2000) and in the light, R_d should acclimate to temperature in the same way as V_{cmax} (Atkin *et. al*, 2015). Variation in respiration associated to variation in photosynthesis can be explained by chloroplast-mitochondrion interdependence in the light and dark, and energy costs associated with phloem loading (Atkin *et. al*, 2015).
- Relationships of V_{cmax}, J_{max} and R_d to N_{area} and other structural traits (tree height, wood density) (Fyllas *et al.*, 2012) within complex forest communities should be predictable, and related to species' dynamical roles (longevity and canopy access).

1.4 Fieldwork context

Fieldwork in Australia was conducted in two contrasting environments during two seasons: summer and winter in the south west of the Great Western Woodlands (GWW); and dry and wet seasons in Far North Queensland (FNQ). The GWW (−30.46, 120.82) site is located near Credo, 60 km north-west of Kalgoorlie, Western Australia. The FNQ site (−17.11, 145.63) is located near Tinaroo, 10 km north-east of Atherton, Queensland. The GWW has a semi-arid climate and the vegetation is an intact mosaic

of temperate woodland, shrubland and mallee. The mean annual rainfall (MAP) is 380±108 mm (Hutchinson, 2014c), the mean annual temperature (MAT) is 20±0.4°C (Hutchinson, 2014a,b) and altitude is 420 m. The FNQ - Robson Creek site is a preserved tropical forest at 700 metres a.s.l. with mean annual rainfall (MAP) of 1813±472 mm (Hutchinson, 2014c) and mean annual temperature (MAT) of 20±0.4°C (Hutchinson, 2014a,b).

The GWW and FNQ research sites are part of the Australian Supersite network (ASN) which in turn is a facility of the Terrestrial Ecosystem and Research Network (TERN). The ASN includes ten sites, representing the major Australian biomes. The sites selected in this thesis are the most environmentally contrasting in the entire ASN. There is an OzFlux eddy-covariance flux measurement tower at each SuperSite, and ongoing research is developing detailed data sets on flora, fauna and biophysical processes at every site. The fieldwork in the GWW and FNQ-Robson Creek was part of a larger project to quantify leaf traits in eight out of ten SuperSites and in selected Ausplots Rangelands sites including the north-south 'Transect for Environmental Monitoring and Decision Making' (TREND). The fieldwork in GWW and FNQ was funded by TERN Ecosystem Modelling and Scaling Infrastructure (eMAST, refer: http://www.emast.org.au), directed by Dr Bradley Evans and chaired by Professor Colin Prentice. This research was jointly planned by Colin Prentice (Department of Biological Sciences, Macquarie University; and AXA Chair of Biosphere and Climate Impacts, Grand Challenges in Ecosystems and the Environment and Grantham Institute - Climate Change and the Environment, Department of Life Sciences, Imperial College London), Professor Andy Lowe (Centre for Conservation Science and Technology, University of Adelaide), Professor Owen Atkin (Division of Plant Sciences, Research School of Biology and ARC Centre of Excellence in Plant Energy Biology, Research School of Biology, Australian National University), A. Professor Michael Liddell (College of Science, Technology and Engineering, Centre for Tropical Environmental and Sustainability Studies), Dr Craig Macfarlane (CSIRO Wembley WA Land and Water Flagship) and Dr Suzanne Prober (CSIRO Wembley WA Land and Water Flagship).

Fieldwork in southeast China was conducted in five areas of preserved tropical

forest near Kunming (21.61, 101.58) and near the Xishuangbanna Tropical Botanical Garden (21.91, 101.27), Yunnan (YUN) during the winter dry season. Altitude ranges between ∼500 and 1000m, MAT ranges from 19.6±06°C to 21.7±07°C and MAP from 1427±297 mm to 1662±302 mm. The sampling in this area is part of a long-term collaborative project led by Professor Jian Ni (Chinese Academy of Sciences - China), Professor Sandy Harrison (Macquarie University - Australia, and University of Reading - UK) and Colin Prentice (Macquarie University - Australia, and Imperial College London - UK). This project has measured leaf traits of main vascular species of 47 sites in eastern China ranging from subtropical broad-leaved evergreen and temperate-deciduous forests to grasslands and desert. This fieldwork was funded by the Key Program (grant no. 30590383) of the National Natural Science Foundation of China and a State Key Laboratory of Vegetation and Environmental Change program (Chinese Academy of Sciences): 'Responses of important functional process of old-growth forests to environmental changes'.

1.5 Thesis approach

This thesis aims to provide empirical information needed to improve the representation of key biological processes related to terrestrial carbon and water cycling in Dynamic Global Vegetation Models (DGVMs). The representation of the ecophysiological processes of carbon assimilation, and plant traits influencing these processes is simplistic in most current DGVMs, which have not benefited fully from the 'data revolution' that has hugely increased the amount and variety of data available to support a stronger scientific basis for next-generation modelling. Still less has current model development, much of which is now located in climate modelling centres, engaged with field ecologists or been involved in the data analysis. There is an important gap to be filled.

In this thesis, only evergreen plants were considered because they are overwhelmingly dominant in Australian vegetation and in tropical moist forests; and because further considerations come into play when trying to model deciduous phenologies, which would extrapolate the limits proposed in this single thesis. The field sampling

criterion was to use top-canopy sunlit, newly mature and fully expanded leaves. This work has not explored the potential effect of leaf age on photosynthetic properties of leaves. In theory, leaf nitrogen nutrient levels should decrease with an increase in leaf age, caused by reallocation rather than uncontrolled deterioration (Field and Mooney, 1983). Together with leaf shading and exposition to sunlight, leaf ageing can be a major factor to cause non-uniform distribution of nitrogen (Hirosaka *et al.*, 1994). Additionally, leaf age increase (and decrease in nitrogen) is also expected to reduce photosynthetic capacity and stomatal conductance (Field and Mooney, 1983).

The coordination hypothesis and the least-cost theory are used here to provide a theoretical framework to explain the economics of carbon assimilation. Notwithstanding some important theoretical advances, based on the evolutionary attractor framework or 'optimality modelling' (Chen *et. al*, 1993; Wright *et. al*, 2003; Maire *et. al*, 2012; Prentice *et. al*, 2014), there is a pressing need for more field-based empirical work to test the explicit predictions of theory: potentially providing a rationale for the radical simplification of future DGVMs.

The thesis is divided into three principal, self-contained chapters (the second, third and fourth chapters) each of which has been conceived and written as a journal article, either published, in review or submitted.

The second chapter explores the least-cost theory prediction that the leaf area (LA) to cross-sectional sapwood area (SA) ratio should decrease toward drier climates. LA and SA are two critically important traits for the function of trees, which respectively determines tree water use and light interception, and the tree's ability to supply water to the leaves. This relationship has been tested and verified in gymnosperms (Mencuccini and Grace 1995; Delucia *et. al*, 2000) but information in angiosperms is notably scarce. In order to address this gap, this chapter assembles and analyses a large dataset from 184 evergreen angiosperm tree species spanning contrasting environments in Australia, from deserts to tropical forests. The dataset was gathered from field observations, published and unpublished data contribution, and literature compilation. A quantile regression approach was implemented to define what parts of the spectrum LA:SA can be explained by climatic moisture. I also investigated the

pipe model (the prediction that the sapwood cross-sectional area of a stem or branch at any point should scale isometrically with the area of leaves distal to that point). I further test with a smaller subset the least-cost theory prediction that leaf hydraulic conductivity (Gleason *et al.*, 2012) is a key trait to improve the explanation of the relationship between LA:SA and climatic moisture.

The third chapter addresses a crucial issue for DGVMs. Most of these models work on the 'simplifying' assumption that key photosynthetic traits, such as carboxylation and electron-transport capacities measured at a standard air temperature, are constant (within PFTs) in time and space. This assumption neglects the potential for optimal acclimation of photosynthetic and respiratory traits to variations in growth temperature, and therefore, can lead to incorrect model estimates (and implicitly, predictions of suboptimal behaviour by plants) where rate limitations respond passively to enzyme kinetics. Temperature acclimation is predicted by combining the coordination hypothesis (that Rubisco- and electron-transport limited rates of photosynthesis are co-limiting under typical daytime conditions) with the least-cost theory prediction that the ratio of intercellular to ambient CO_2 concentration increases with temperature, due to lower water viscosity and higher photorespiratory losses. This chapter uses linear regression between log-transformed photosynthetic parameters (V_{cmax}, J_{max}, R_{dark}) and temperature observed in field, and does the same for the same parameters after standardisation to 25°C. *Prima facie* evidence for optimal acclimation is obtained in the form of rates that increase with temperature (compensating for the increase of K) while temperature-standardized rates decrease - consistent with the coordination hypothesis prediction of reduced allocation of N to Rubisco at higher temperatures, which is predicted to outweigh the effect of K on the optimal rates. This chapter also shows that the slopes of the relationships found are broadly consistent with quantitative expectations based on optimality principles.

The fourth chapter addresses the representation of functional and structural plant traits in tropical moist forests. By focusing on a narrow climatic range and comparing species occupying a wide range of niches, this work draws attention to the significance of ecophysiological differences that are related to vegetation dynamical roles. Multivariate

analysis methods are used to establish the dimensions of trait variation, to cluster species according to traits, and to partition trait variance into climatic (between-site) and vegetation-dynamic contributions. The analysis demonstrates both the consistency (within and between species) of key trait-trait relationships and the predictability of relationships between certain traits (including V_{cmax} and c_i:c_a) and vegetation-dynamic roles, based on height and canopy access, from the standpoint of the least-cost theory and the coordination hypothesis.

All three data chapters had plant traits (such as LA:SA, V_{cmax}, J_{max}, and others) $\log_{10}$ transformed unless indicated. Log transformations are widely used for pairwise and multiple correlations between plant traits because relationships between log-normalised traits can be analysed straightforwardly by simple correlation (Wright *et al.*, 2002).

The final chapter summarises key findings in this thesis, and discusses limitations and future research directions.

1.6 Candidate's role

Chapter 2 has been published as: Togashi, Henrique. F.; Prentice, I. Colin.; Evans, Brad. J.; Forrester, D. Ian.; Drake, Paul.; Feikema, Paul.; Brooksbank, Kim.; Eamus, Derek; Taylor, Daniel. (2015), Morphological and moisture availability controls of the leaf area-to-sapwood area ratio: analysis of measurements on Australian trees. *Ecology and Evolution*. DOI: 10.1002/ece3.1344. This work originated from Colin Prentice's idea of predicting the ratio LA:SA from measures of climatic moisture (MI, alpha, VPD). I conducted an extensive literature review to compile data from Australia that could be used, collected LA:SA for ten species at FNQ-Robson Creek, and contacted over 50 researchers who could contribute data (five did). I analysed all the data (occasionally guided by Colin Prentice), performed all statistical and graphical analyses, wrote the first draft, and modified the manuscript after comments from all authors and journal reviewers. The idea of including leaf hydraulic conductance from a smaller dataset was inspired by a comment from Derek Eamus.

Chapter 3 is in revision, having been submitted to *Functional Plant Biology* as: Togashi, Henrique F.; Prentice, I. Colin; Atkin, Owen K.; Macfarlane, Craig; Prober, Suzanne M.; Bloomfield, Keith J. Thermal Acclimation of leaf photosynthetic traits in an evergreen woodland consistent with the coordination hypothesis. This work originated from my idea of investigating the responses of photosynthesis to temperature. Colin Prentice identified in this idea a good opportunity to test some assumptions of the coordination hypothesis and least-coast theory. I collected all the data in the field, performed all statistical and graphical analyses, processed and analysed the data (occasionally guided by Colin Prentice), wrote the first draft, and modified the manuscript after comments from all authors. Colin Prentice suggested the idea of quantifying the prediction of acclimated versus kinetic slopes, and its algebraic formulation.

Chapter 4 is approaching readiness for submission to *Perspectives in Plant Ecology, Evolution and Systematics* as: Togashi, Henrique F.; Prentice, I. Colin; Atkin, Owen K.; Bradford, Matt; Harrison, Sandy P.; Boomfield, Keith J.; Evans; Bradley J.; Liddell, Michael J.; Wang, Han; Weerasinghe, Lasantha K.; Cao, Kun-fang; Zexin, Fan.

Functional trait variation related to gap dynamics in tropical moist forests: a perspective for vegetation modelling. The idea for this work came from a gap in the representation of Plant Functional Types (PFTs) in ecosystem models, identified by Colin Prentice. His idea was to advance the PFT framework adopted in models (Fyllas *et al.*, 2012) using leaf gas exchange measurements. I collected the data in China and part of the data in Queensland. Colin Prentice negotiated additional data from Queensland with Jon Lloyd; I negotiated additional data from Cape Tribulation with Owen Atkin and Lasantha Weerasinghe. I performed all statistical and graphical analyses, processed and analysed the data (occasionally guided by Colin Prentice), wrote the first draft, and modified the manuscript after comments from authors. I developed the spectrum approach based on Wright *et al.* (2004) and Baraloto *et al.* (2010). I acknowledge Jon Lloyd, Ni Jian, and Zhu Hua for providing data and they may wish to become co-authors.

Glossary of terms

A	Net rate of CO_2 uptake per unit leaf area (µmol m^{-2} s^{-1})
a	Water-transport 'cost factor' (dimensionless)
A_c	Projected crown area (m^2)
b	Carboxylation 'cost factor' (dimensionless)
c	Initial ratio of crown area to stem cross-sectional area (dimensionless)
c_a	Ambient partial pressure of CO_2 (µmol mol^{-1})
c_i	Leaf-intercellular partial pressure of CO_2 (µmol mol^{-1})
D	Leaf-to-air vapour pressure deficit (KPa)
E	Plant transpiration (µmol m^{-2} s^{-1})
g_m	Mesophyll conductance (µmol m^{-2} s^{-1})
g_s	stomatal conductance (µmol m^{-2} s^{-1})
H_f	Mean foliage height (m)

I (or PPFD)	Photosynthetic photon flux density (µmol m^{-2} s^{-1})
J	Rate of electron transport (µmol m^{-2} s^{-1})
J_{max}	Maximum electron transport rate (µmol m^{-2} s^{-1})
K_c	Michaelis-Menten constants of Rubisco for CO_2 (µmol mol^{-1})
K_o	Michaelis-Menten constants of Rubisco for O_2 (µmol mol^{-1})
k_s	Sapwood permeability (cm s^{-1})
L	Leaf area index (dimensionless)
LA:SA	Ratio of leaf area to the cross-sectional sapwood area (dimensionless)
N_{area}	Leaf nitrogen per unit area (m^2 g^{-1})
O	Leaf-intercellular partial pressure of O_2 (µmol mol^{-1})
P_{area}	Leaf phosphorus per unit area (m^2 g^{-1})
R_d (or R_{day})	Rate of mitochondrial respiration in the presence of light (µmol m^{-2} s^{-1})
TPU	Triose phosphate utilization rate (µmol m^{-2} s^{-1})
V_{cmax}	Maximum carboxylation capacity rate (µmol m^{-2} s^{-1})
v_h	Huber value (dimensionless)
$W_{.s}$	Mass of carbon in sapwood (Kg)
W_c	Rubisco limited rate of carboxylation (µmol m^{-2} s^{-1})
W_j	RuBP limited rate of carboxylation (µmol m^{-2} s^{-1})
W_t	Triose phosphate utilization limited rate of carboxylation (µmol m^{-2} s^{-1})
$\Delta\Psi$	Water potential gradient (MPa)
Γ^*	Photorespiratory compensation point of CO_2 (µmol mol^{-1})
η	Temperature-dependent viscosity of water (Pa s)
θ	Curvature of the light response (dimensionless)
ρ	Density of water (kg m^-3)
ρ_s	Density of the wood (kg m^-3)
ϕ	Intrinsic quantum yield (dimensionless)
χ_0	Time averaged c_i:c_a ratio (dimensionless)

1.7 References

Ali, A, Xu, C, Rogers, A, Fisher, R, Wullschleger, S, McDowell, N, Massoud, E, Vrugt, J, Muss, J, Fisher, J, Reich, P, Wilson, C . A global scale mechanistic model of the photosynthetic capacity. *Geoscientific Model Development Discussions (Online)*, 8 (8), 2015.

Allan, R. P, Soden, B. J, John, V. O, Ingram, W, and Good, P. Current changes in tropical precipitation. *Environmental Research Letters*, 5(2):025205, 2010.

Anten, N. P. R. Optimal photosynthetic characteristics of individual plants in vegetation stands and implications for species coexistence. *Annals of Botany*, 95(3): 495–506, 2005.

Arneth, A, Schurgers, G, Lathiere, J, Duhl, T, Beerling, D, Hewitt, C, Martin, M, and Guenther, A. Global terrestrial isoprene emission models: sensitivity to variability in climate and vegetation. *Atmospheric Chemistry and Physics*, 11(15):8037–8052, 2011.

Atkin, O. K, Holly, C, and Ball, M. C. Acclimation of snow gum (*Eucalyptus pauciflora*) leaf respiration to seasonal and diurnal variations in temperature: the importance of changes in the capacity and temperature sensitivity of respiration. *Plant, Cell & Environment*, 23(1):15–26, 2000.

Atkin, O. K, Bloomfield, K. J, Reich, P. B, Tjoelker, M. G, Asner, G. P, Bonal, D, Bönisch, G, Bradford, M. G, Cernusak, L. A, Cosio, E. G, Creek, D, Crous, K. Y, Domingues, T. F, Dukes, J. S, Egerton, J. J. G, Evans, J. R, Farquhar, G. D, Fyllas, N. M, Gauthier, P. P. G, Gloor, E, Gimeno, T. E, Griffin, K. L, Guerrieri, R, Heskel, M. A, Huntingford, C, Ishida, F. Y, Kattge, J, Lambers, H, Liddell, M. J, Lloyd, J, Lusk, C. H, Martin, R. E, Maksimov, A. P, Maximov, T. C, Malhi, Y, Medlyn, B. E, Meir, P, Mercado, L. M, Mirotchnick, N, Ng, D, Niinemets, Ü, O'Sullivan, O. S,

Phillips, O. L, Poorter, L, Poot, P, Prentice, I. C, Salinas, N, Rowland, L. M, Ryan, M. G, Sitch, S, Slot, M, Smith, N. G, Turnbull, M. H, VanderWel, M. C, Valladares, F, Veneklaas, E. J, Weerasinghe, L. K, Wirth, C, Wright, I. J, Wythers, K. R, Xiang, J, Xiang, S, and Zaragoza-Castells, J. Global variability in leaf respiration in relation to climate, plant functional types and leaf traits. *New Phytologist*, 206(2):614–636, 2015.

Baraloto, C, Timothy Paine, C, Poorter, L, Beauchene, J, Bonal, D, Domenach, A, Hérault, B, Patino, S, Roggy, J, and Chave, J. Decoupled leaf and stem economics in rain forest trees. *Ecology Letters*, 13(11):1338–1347, 2010.

Beer, C, Reichstein, M, Tomelleri, E, Ciais, P, Jung, M, Carvalhais, N, Rödenbeck, C, Arain, M. A, Baldocchi, D, Bonan, G. B, Bondeau, A, Cescatti, A, Lasslop, G, Lindroth, A, Lomas, M, Luyssaert, S, Margolis, H, Oleson, K. W, Roupsard, O, Veenendaal, E, Viovy, N, Williams, C, Woodward, F. I, and Papale, D. Terrestrial gross carbon dioxide uptake: Global distribution and covariation with climate. *Science*, 329(5993):834–838, 2010.

Bernacchi, C. J, Pimentel, C, and Long, S. P. *In vivo* temperature response functions of parameters required to model RuBP-limited photosynthesis. *Plant, Cell & Environment*, 26(9):1419–1430, 2003.

Botkin, D. B, Janak, J. F, and Wallis, J. R. Some ecological consequences of a computer model of forest growth. *The Journal of Ecology*, pages 849–872, 1972.

Box, E. O. Predicting physiognomic vegetation types with climate variables. *Vegetatio*, 45(2):127–139, 1981.

Bradford, M. G, Murphy, H. T, Ford, A. J, Hogan, D. L, and Metcalfe, D. J. Long-term stem inventory data from tropical rain forest plots in Australia. *Ecology*, 95(8): 2362–000, 2014.

Chen, J-L, Reynolds, J, Harley, P, and Tenhunen, J. Coordination theory of leaf nitrogen distribution in a canopy. *Oecologia*, 93(1):63–69, 1993.

Ciais, P, Sabine, C, Bala, G, Bopp, L, Brovkin, V, Canadell, J, Chhabra, A, DeFries, R, Galloway, J, and Heimann, M. Carbon and Other Biogeochemical Cycles. *Climate Change 2013: The Physical Science Basis. Contribution of Working Group I to the Fifth Assessment Report of the Intergovernmental Panel on Climate Change*, pages 465–570. Cambridge University Press, 2014.

Cox, P. M, Betts, R. A, Jones, C. D, Spall, S. A, and Totterdell, I. J. Acceleration of global warming due to carbon-cycle feedbacks in a coupled climate model. *Nature*, 408(6809):184–187, 2000. 10.1038/35041539.

Cramer, W, Bondeau, A, Woodward, F. I, Prentice, I. C, Betts, R. A, Brovkin, V, Cox, P. M, Fisher, V, Foley, J. A, Friend, A. D, Kucharik, C, Lomas, M. R, Ramankutty, N, Sitch, S, Smith, B, White, A, and Young-Molling, C. Global response of terrestrial ecosystem structure and function to CO_2 and climate change: results from six dynamic global vegetation models. *Global Change Biology*, 7(4):357–373, 2001.

Delucia, E. H, Maherali, H, and Carey, E. V. Climate-driven changes in biomass allocation in pines. *Global Change Biology*, 6(5):587–593, 2000.

Domingues, T. F, Meir, P, Feldpausch, T. R, Saiz, G, Veenendaal, E. M, Schrodt, F, Bird, M, Djagbletey, G, Hien, F, Compaore, H, Diallo, A, Grace, J, and Lloyd, J. O. N. Co-limitation of photosynthetic capacity by nitrogen and phosphorus in west Africa woodlands. *Plant, Cell & Environment*, 33(6):959–980, 2010.

Farquhar, G. D, von Caemmerer, S, and Berry, J. A. A biochemical model of photosynthetic CO_2 assimilation in leaves of C_3 species. *Planta*, 149(1):78–90, 1980.

Farquhar, G. D and Sharkey, T. D. Stomatal conductance and photosynthesis. *Annual Review of Plant Physiology*, 33(1):317–345, 1982.

Field, C. and Mooney, H. A. Leaf age and seasonal effects on light, water, and nitrogen use efficiency in a California shrub *Oecologia*, 2-3(56):348–355, 1983.

Fisher, R, Muszala, S, Verteinstein, M, Lawrence, P, Xu, C, McDowell, N, Knox, R, Koven, C, Holm, J, Rogers, B, Lawrence, D, and Bonan, G. Taking off the training

wheels: the properties of a dynamic vegetation model without climate envelopes. *Geoscientific Model Development Discussions*, 8(4), 2015.

Friedlingstein, P, Cox, P, Betts, R, Bopp, L, Von Bloh, W, Brovkin, V, Cadule, P, Doney, S, Eby, M, and Fung, I. Climate-carbon cycle feedback analysis: Results from the C4MIP model intercomparison. *Journal of Climate*, 19(14):3337–3353, 2006.

Friedlingstein, P, Meinshausen, M, Arora, V. K, Jones, C. D, Anav, A, Liddicoat, S. K, and Knutti, R. Uncertainties in CMIP5 climate projections due to carbon cycle feedbacks. *Journal of Climate*, 27(2):511–526, 2014.

Fyllas, N. M, Quesada, C. A, and Lloyd, J. Deriving plant functional types for Amazonian forests for use in vegetation dynamics models. *Perspectives in Plant Ecology, Evolution and Systematics*, 14(2):97–110, 2012.

Givnish, T. J. *On the Economy of Plant Form and Function: Proceedings of the Sixth Maria Moors Cabot Symposium, Evolutionary Constraints on Primary Productivity, Adaptive Patterns of Energy Capture in Plants, Harvard Forest, August 1983*, volume 6. Cambridge University Press, 1986.

Gleason, S. M, Butler, D. W, Ziemińska, K, Waryszak, P, and Westoby, M. Stem xylem conductivity is key to plant water balance across Australian angiosperm species. *Functional Ecology*, 26(2):343–352, 2012.

Greve, P, Orlowsky, B, Mueller, B, Sheffield, J, Reichstein, M, and Seneviratne, S. I. Global assessment of trends in wetting and drying over land. *Nature Geoscience*, 7 (10):716–721, 2014.

Harley, P and Sharkey, T. An improved model of C_3 photosynthesis at high CO_2: Reversed O_2 sensitivity explained by lack of glycerate reentry into the chloroplast. *Photosynthesis Research*, 27(3):169–178, 1991.

Harrison, S. P, Prentice, I. C, Barboni, D, Kohfeld, K. E, Ni, J, and Sutra, J. Ecophysiological and bioclimatic foundations for a global plant functional classification. *Journal of Vegetation Science*, 21(2):300–317, 2010.

Haxeltine, A and Prentice, I. C. A general model for the light-use efficiency of primary production. *Functional Ecology*, 10(5):551–561, 1996.

Hirosaka, K, Terashima, I, and Katoh, S. Effects of leaf age, nitrogen nutrition and photon flux density on the distribution of nitrogen among leaves of a vine (*Ipomoea tricolor* Cav.) grown horizontally to avoid mutual shading of leaves. *Oecologia*, 97 (4):451–457, 1994.

Hirose, T and Werger, M. J. Nitrogen use efficiency in instantaneous and daily photosynthesis of leaves in the canopy of a *Solidago altissima* stand. *Physiologia Plantarum*, 70(2):215–222, 1987.

Houghton, J, Ding, Y, Griggs, M, Noguer, P, Van Der Linden, X, Xiaosu, D, and Maskell, K. (eds.) *Climate change 2001: The scientific basis. Contribution of working group I to the third assessment report of the intergovernmental panel on climate change (IPCC)*. Cambridge University Press, Cambridge, Great Britain, New York, NY, USA and Melbourne, Australia, 2001.

Houghton, J, Jenkins, G, and Ephraums, J. (eds.) *Climate Change: The IPCC Scientific Assessment (1990). Report prepared for Intergovernmental Panel on Climate Change by Working Group I*. Cambridge University Press, Cambridge, Great Britain, New York, NY, USA and Melbourne, Australia, 1990.

Houghton, J, Meira Filho, L, Callander, B, Harris, N, Kattenberg, A, and Maskell, K. (eds.) *Climate change 1995: The science of climate change: Contribution of working group I to the second assessment report of the intergovernmental panel on climate change*. Cambridge University Press, Cambridge, Great Britain, New York, NY, USA and Melbourne, Australia, 1995.

Hutchinson, M. Daily maximum temperature: Anuclimate 1.0, 0.01 degree, Australian coverage, 1970-2012, 2014a. http://www.emast.org.au

Hutchinson, M. Daily minimum temperature: Anuclimate 1.0, 0.01 degree, Australian coverage, 1970-2012, 2014b. http://www.emast.org.au

Hutchinson, M. Daily precipitation: Anuclimate 1.0, 0.01 degree, Australian coverage, 1970-2012, 2014c. http://www.emast.org.au

Kattge, J, Díaz, S, Lavorel, S, Prentice, I. C, Leadley, P, Bönisch, G, Garnier, E, Westoby, M, Reich, P. B, Wright, I. J, Cornelissen, J. H. C, Violle, C, Harrison, S. P, Van Bodegom, P. M, Reichstein, M, Enquist, B. J, Soudzilovskaia, N. A, Ackerly, D. D, Anand, M, Atkin, O, Bahn, M, Baker, T. R, Baldocchi, D, Bekker, R, Blanco, C. C, Blonder, B, Bond, W. J, Bradstock, R, Bunker, D. E, Casanoves, F, Cavender-Bares, J, Chambers, J. Q, Chapin Iii, F. S, Chave, J, Coomes, D, Cornwell, W. K, Craine, J. M, Dobrin, B. H, Duarte, L, Durka, W, Elser, J, Esser, G, Estiarte, M, Fagan, W. F, Fang, J, Fernández-Méndez, F, Fidelis, A, Finegan, B, Flores, O, Ford, H, Frank, D, Freschet, G. T, Fyllas, N. M, Gallagher, R. V, Green, W. A, Gutierrez, A. G, Hickler, T, Higgins, S. I, Hodgson, J. G, Jalili, A, Jansen, S, Joly, C. A, Kerkhoff, A. J, Kirkup, D, Kitajima, K, Kleyer, M, Klotz, S, Knops, J. M. H, Kramer, K, Kühn, I, Kurokawa, H, Laughlin, D, Lee, T. D, Leishman, M, Lens, F, Lenz, T, Lewis, S. L, Lloyd, J, Llusià, J, Louault, F, Ma, S, Mahecha, M. D, Manning, P, Massad, T, Medlyn, B. E, Messier, J, Moles, A. T, Müller, S. C, Nadrowski, K, Naeem, S, Niinemets, ü, Nöllert, S, Nüske, A, Ogaya, R, Oleksyn, J, Onipchenko, V. G, Onoda, Y, Ordoñez, J, Overbeck, G, Ozinga, W. A, Patino, S, Paula, S, Pausas, J. G, Penuelas, J, Phillips, O. L, Pillar, V, Pooter, H, Poorter, L, Poschlod, P, Prizing, A, Proulx, R, Rammig, A, Reinsch, A, Reu, B, Sack, L, Salgado-Negret, B, Sardans, J, Shiodera, S, Shipley, B, Siefert, A, Sosinski, E, Soussana, F, Swaine, E, Sweson, N, Thompson, K, Thornton, P, Waldram, M, Weiher, E, White, M, White, S, Wright, S. J, Yguel, B, Zaehle, S, Zanne, A. E, and Wirth, C. Try – a global database of plant traits. *Global Change Biology*, 17(9): 2905–2935, 2011.

Kattge, J and Knorr, W. Temperature acclimation in a biochemical model of photosynthesis: a reanalysis of data from 36 species. *Plant, Cell & Environment*, 30(9): 1176–1190, 2007.

Kloster, S, Mahowald, N. M, Randerson, J. T, and Lawrence, P. J. The impacts of climate, land use, and demography on fires during the 21st century simulated by CLM-CN. *Biogeosciences*, 9(1):509–525, 2012.

Leuning, R. Modelling stomatal behaviour and and photosynthesis of eucalyptus grandis. *Functional Plant Biology*, 17(2):159–175, 1990.

Li, G, Harrison, S. P, Prentice, I. C, and Falster, D. Simulation of tree-ring widths with a model for primary production, carbon allocation, and growth. *Biogeosciences*, 11 (23):6711–6724, 2014.

Long, S and Bernacchi, C. Gas exchange measurements, what can they tell us about the underlying limitations to photosynthesis? procedures and sources of error. *Journal of Experimental Botany*, 54(392):2393–2401, 2003.

MacFarling Meure, C, Etheridge, D, Trudinger, C, Steele, P, Langenfelds, R, Van Ommen, T, Smith, A, and Elkins, J. Law dome CO_2, CH_4 and N_2O ice core records extended to 2000 years bp. *Geophysical Research Letters*, 33(14):L14810, 2006.

Maire, V, Martre, P, Kattge, J, Gastal, F, Esser, G, Fontaine, S, and Soussana, J.-F. The coordination of leaf photosynthesis links C and N fluxes in C_3 plant species. *PLoS ONE*, 7(6):e38345, 2012.

McGuire, A, Stich, S, Clein, J, Dargaville, R, Esser, G, Foley, J, Heimann, M, Joos, F, Kaplan, J, Kicklighter, D, Meier, R, Melillo, J, Moore III, B, Prentice, I, Ramankutty, N, Reichenau, T, and Schloss, A. Carbon balance of the terrestrial biosphere in the twentieth century: Analyses of CO_2, climate and land use effects with four process-based ecosystem models. *Global Biogeochemical Cycles*, 15(1):183–206, 2001.

Medlyn, B. E, Duursma, R. A, Eamus, D, Ellsworth, D. S, Prentice, I. C, Barton, C. V. M, Crous, K. Y, De Angelis, P, Freeman, M, and Wingate, L. Reconciling the optimal and empirical approaches to modelling stomatal conductance. *Global Change Biology*, 17(6):2134–2144, 2011.

Medlyn, B. E, Zaehle, S, De Kauwe, M. G, Walker, A. P, Dietze, M. C, Hanson, P. J, Hickler, T, Jain, A. K, Luo, Y, and Parton, W. Using ecosystem experiments to improve vegetation models. *Nature Climate Change*, 5(6):528–534, 2015.

Mencuccini, M and Grace, J. Climate influences the leaf area/sapwood area ratio in Scots pine. *Tree Physiology*, 15(1):1–10, 1995.

Meng, T, Wang, H, Harrison, S, Prentice, I, Ni, J, and Wang, G. Responses of leaf traits to climatic gradients: adaptive variation *vs*. compositional shifts. *Biogeosciences Discussions*, 12(9), 2015.

Monnin, E, Indermühle, A, Dällenbach, A, Flückiger, J, Stauffer, B, Stocker, T. F, Raynaud, D, and Barnola, J.-M. Atmospheric CO_2 concentrations over the last glacial termination. *Science*, 291(5501):112–114, 2001.

Niinemets, Ü and Tenhunen, J. D. A model separating leaf structural and physiological effects on carbon gain along light gradients for the shade-tolerant species *Acer saccharum*. *Plant, Cell & Environment*, 20(7):845–866, 1997.

Niinemets, Ü and Valladares, F. Photosynthetic acclimation to simultaneous and interacting environmental stresses along natural light gradients: optimality and constraints. *Plant Biology*, 254(6):254–268, 2004.

Pavlick, R, Drewry, D. T, Bohn, K, Reu, B, and Kleidon, A. The jena diversity-dynamic global vegetation model (JEDI-DGVM): a diverse approach to representing terrestrial biogeography and biogeochemistry based on plant functional trade-offs. *Biogeosciences*, 10:4137–4177, 2013.

Petit, J. R, Jouzel, J, Raynaud, D, Barkov, N. I, Barnola, J. M, Basile, I, Bender, M, Chappellaz, J, Davis, M, Delaygue, G, Delmotte, M, Kotlyakov, V. M, Legrand,

M, Lipenkov, V. Y, Lorius, C, Pepin, L, Ritz, C, Saltzman, E, and Stievenard, M. Climate and atmospheric history of the past 420,000 years from the Vostok ice core, Antarctica. *Nature*, 399(6735):429–436, 1999.

Piao, S, Sitch, S, Ciais, P, Friedlingstein, P, Peylin, P, Wang, X, Ahlström, A, Anav, A, Canadell, J. G, Cong, N, Huntingford, C, Jung, M, Levis, S, Levy, P. E, Li, J, Lin, X, Lomas, M. R, Lu, M, Luo, Y, Ma, Y, Myneni, R. B, Poulter, B, Sun, Z, Wang, T, Viovy, N, Zaehle, S, and Zeng, N. Evaluation of terrestrial carbon cycle models for their response to climate variability and to CO_2 trends. *Global Change Biology*, 19(7):2117–2132, 2013.

Potter, C. S and Klooster, S. A. Dynamic global vegetation modelling for prediction of plant functional types and biogenic trace gas fluxes. *Global Ecology and Biogeography*, 8(6):473–488, 1999.

Prentice, I. C and Cowling, S. A. Dynamic Global Vegetation Models. *Encyclopedia of Biodiversity*, pages 607–689. Academic Press, Waltham, 2nd edition, 2013.

Prentice, I. C, Harrison, S. P, and Bartlein, P. J. Global vegetation and terrestrial carbon cycle changes after the last ice age. *New Phytologist*, 189(4):988–998, 2011.

Prentice, I. C, Liang, X, Medlyn, B. E, and Wang, Y. P. Reliable, robust and realistic: the three R's of next-generation land-surface modelling. *Atmospheric Chemistry and Physics*, 15(10):5987–6005, 2015.

Prentice, I. C, Cramer, W, Harrison, S. P, Leemans, R, Monserud, R. A, and Solomon, A. M. Special paper: a global biome model based on plant physiology and dominance, soil properties and climate. *Journal of biogeography*, pages 117–134, 1992.

Prentice, I. C, Farquhar, G, Fasham, M, Goulden, M. L, Heimann, M, Jaramillo, V, Kheshgi, H, LeQuéré, C, Scholes, R. J, and Wallace, D. W. The Carbon Cycle and Atmospheric Carbon Dioxide. *Climate Change 2001: The Scientific Basis. Contributions of Working Group I to the Third Assessment Report of the Intergovernmental*

Panel on Climate Change, pages 185-237. Cambridge University Press, Cambridge, UK, 2001.

Prentice, I. C, Bondeau, A, Cramer, W, Harrison, S. P, Hickler, T, Lucht, W, Sitch, S, Smith, B, and Sykes, M. T. Dynamic Global Vegetation Modeling: quantifying terrestrial ecosystem responses to large-scale environmental change. *Terrestrial ecosystems in a changing world*, pages 175–192. Springer Berlin Heidelberg, 2007.

Prentice, I. C, Dong, N, Gleason, S. M, Maire, V, and Wright, I. J. Balancing the costs of carbon gain and water transport: testing a new theoretical framework for plant functional ecology. *Ecology Letters*, 17(1):82–91, 2014.

Raunkiær, C. *The Life Forms of Plants and Statistical Plant Geography*. Clarendon Press, 1934.

Reich, P. B. The world-wide 'fast–slow' plant economics spectrum: a traits manifesto. *Journal of Ecology*, 102(2):275–301, 2014.

Reichstein, M, Bahn, M, Ciais, P, Frank, D, Mahecha, M. D, Seneviratne, S. I, Zscheischler, J, Beer, C, Buchmann, N, Frank, D. C, Papale, D, Rammig, A, Smith, P, Thonicke, K, van der Velde, M, Vicca, S, Walz, A, and Wattenbach, M. Climate extremes and the carbon cycle. *Nature*, 500(7462):287–295, 2013.

Reid, D. E. B, Silins, U, Mendoza, C, and Lieffers, V. J. A unified nomenclature for quantification and description of water conducting properties of sapwood xylem based on Darcy's law. *Tree Physiology*, 25(8):993–1000, 2005.

Roderick, M. L and Berry, S. L. Linking wood density with tree growth and environment: a theoretical analysis based on the motion of water. *New Phytologist*, 149(3): 473–485, 2001.

Scheiter, S, Langan, L, and Higgins, S. I. Next-generation dynamic global vegetation models: learning from community ecology. *New Phytologist*, 198(3):957–969, 2013.

Sellers, P, Mintz, Y, Sud, Y. e. a, and Dalcher, A. A simple biosphere model (sib) for use within general circulation models. *Journal of the Atmospheric Sciences*, 43(6): 505–531, 1986.

Sharkey, T. D. O_2-insensitive photosynthesis in C_3 plants : Its occurrence and a possible explanation. *Plant Physiology*, 78(1):71–75, 1985.

Sharkey, T. D, Bernacchi, C. J, Farquhar, G. D, and Singsaas, E. L. Fitting photosynthetic carbon dioxide response curves for C_3 leaves. *Plant, Cell & Environment*, 30 (9):1035–1040, 2007.

Shevliakova, E, Pacala, S. W, Malyshev, S, Hurtt, G. C, Milly, P, Caspersen, J. P, Sentman, L. T, Fisk, J. P, Wirth, C, and Crevoisier, C. Carbon cycling under 300 years of land use change: Importance of the secondary vegetation sink. *Global Biogeochemical Cycles*, 23(2), 2009.

Shinozaki, K, Yoda, K, Hozumi, K, and Kira, T. A quantitative analysis of plant form: The pipe model theory I. *Japanese Journal of Ecology*, 14(3):97–105, 1964.

Shugart, H. H. *A Theory of Forest Dynamics*. Springer-Verlag, New York, 1984.

Sitch, S, Huntingford, C, Gedney, N, Levy, P. E, Lomas, M, Piao, S. L, Betts, R, Ciais, P, Cox, P, Friedlingstein, P, Jones, C. D, Prentice, I. C, and Woodward, F. I. Evaluation of the terrestrial carbon cycle, future plant geography and climate-carbon cycle feedbacks using five dynamic global vegetation models (DGVMs). *Global Change Biology*, 14(9):2015–2039, 2008.

Skillman, J. B, Garcia, M, Virgo, A, and Winter, K. Growth irradiance effects on photosynthesis and growth in two co-occurring shade-tolerant neotropical perennials of contrasting photosynthetic pathways. *American Journal of Botany*, 92(11):1811–1819, 2005.

Smith, M. J, Purves, D. W, Vanderwel, M. C, Lyutsarev, V, and Emmott, S. The climate dependence of the terrestrial carbon cycle, including parameter and structural uncertainties. *Biogeosciences*, 10(1):583–606, 2013.

Solomon, S, Qin, D, Manning, M, Chen, Z, Marquis, M, Averyt, K, Tignor, M, and Miller, H. (eds.) *IPCC, Climate Change 2007: the physical science basis. contribution of working group i to the fourth assessment report of the intergovernmental panel on climate change.* Cambridge University Press, Cambridge, Great Britain, New York, NY, USA and Melbourne, Australia, 2007.

Steffen, W. L. A periodic table for ecology? A chemist's view of plant functional types. *Journal of Vegetation Science*, 7(3):425–430, 1996.

Stocker, T, Qin, D, Plattner, G, Tignor, M, Allen, S, Boschung, J, Nauels, A, Xia, Y, Bex, B, and Midgley, B. (eds.) *IPCC, Climate Change 2013: the physical science basis. contribution of working group i to the fifth assessment report of the intergovernmental panel on climate change.* Cambridge University Press, Cambridge, Great Britain, New York, NY, USA and Melbourne, Australia, 2013.

Swaine, M and Whitmore, T. On the definition of ecological species groups in tropical rain forests. *Vegetatio*, 75(1-2):81–86, 1988.

Thonicke, K, Spessa, A, Prentice, I, Harrison, S, Dong, L, and Carmona-Moreno, C. The influence of vegetation, fire spread and fire behaviour on biomass burning and trace gas emissions: results from a process-based model. *Biogeosciences*, 7(6):1991–2011, 2010.

Torello-Raventos, M, Feldpausch, T. R, Veenendaal, E, Schrodt, F, Saiz, G, Domingues, T. F, Djagbletey, G, Ford, A, Kemp, J, Marimon, B. S, Hur Marimon Junior, B, Lenza, E, Ratter, J. A, Maracahipes, L, Sasaki, D, Sonké, B, Zapfack, L, Taedoumg, H, Villarroel, D, Schwarz, M, Quesada, C. A, Yoko Ishida, F, Nardoto, G. B, Affum-Baffoe, K, Arroyo, L, M.J.S. Bowman, D, Compaore, H, Davies, K, Diallo, A, Fyllas, N. M, Gilpin, M, Hien, F, Johnson, M, Killeen, T. J, Metcalfe, D, Miranda, H. S, Steininger, M, Thomson, J, Sykora, K, Mougin, E, Hiernaux, P, Bird, M. I, Grace, J, Lewis, S. L, Phillips, O. L, and Lloyd, J. On the delineation of tropical vegetation types with an emphasis on forest/savanna transitions. *Plant Ecology & Diversity*, 6 (1):101–137, 2013.

Tyree, M and Ewers, F. The hydraulic architecture of trees and other woody plants. *New Phytologist*, 119(3):345–360, 1991.

Verheijen, L, Brovkin, V, Aerts, R, Bönish, G, Cornelissen, J, Kattge, J, Reich, P, Wright, I, and Van Bodegom, P. Impacts of trait variation through observed trait-climate relationships o performance of a representative earth system model: a conceptual analysis. *Biogeosciences*, 10:5497–5515, 2013.

Von Caemmerer, S. *Biochemical Models of Leaf Photosynthesis.* Csiro publishing, 2000.

Wang, H, Prentice, I. C, and Davis, T. W. Biophysical constraints on gross primary production by the terrestrial biosphere. *Biogeosciences Discussions*, 11:3209–3240, 2014.

Wang, Y, Houlton, B, and Field, C. A model of biogeochemical cycles of carbon, nitrogen, and phosphorus including symbiotic nitrogen fixation and phosphatase production. *Global Biogeochemical Cycles*, 21(1), 2007.

Westoby, M, Cornwell, W. K, and Falster, D. S. An evolutionary attractor model for sapwood cross section in relation to leaf area. *Journal of Theoretical Biology*, 303 (0):98–109, 2012.

Whitehead, D, Jarvis, P. G, and Waring, R. H. Stomatal conductance, transpiration, and resistance to water uptake in a *Pinus sylvestris* spacing experiment. *Canadian Journal of Forest Research*, 14(5):692–700, 1984.

Whitmore, T. On pattern and process in forests. *Special publications series of the British Ecological Society*, 1982.

Woodward, F. I. *Climate and Plant Distribution.* Cambridge University Press, 1987.

Wright, I. J, Reich, P. B, and Westoby, M. Leastcost input mixtures of water and nitrogen for photosynthesis. *The American Naturalist*, 161(1):98–111, 2003.

Wright, I. J, Westoby, M., and Reich, P. B. Convergence towards higher leaf mass per area in dry and nutrient-poor habitats has different consequences for leaf life span *Journal of Ecology*, 90(3):534–543, 2003.

Wright, I. J, Reich, P. B, Westoby, M, Ackerly, D. D, Baruch, Z, Bongers, F, Cavender-Bares, J, Chapin, T, Cornelissen, J. H. C, Diemer, M, Flexas, J, Garnier, E, Groom, P. K, Gulias, J, Hikosaka, K, Lamont, B. B, Lee, T, Lee, W, Lusk, C, Midgley, J. J, Navas, M.-L, Niinemets, U, Oleksyn, J, Osada, N, Poorter, H, Poot, P, Prior, L, Pyankov, V. I, Roumet, C, Thomas, S. C, Tjoelker, M. G, Veneklaas, E. J, and Villar, R. The worldwide leaf economics spectrum. *Nature*, 428(6985):821–827, 2004.

Wullschleger, S. D. Biochemical limitations to carbon assimilation in C_3 plants—a retrospective analysis of the A/c_i curves from 109 species. *Journal of Experimental Botany*, 44(5):907–920, 1993.

2

Morphological and moisture availability controls of the leaf area-to-sapwood area ratio: analysis of measurements on Australian trees

Henrique Furstenau Togashi[1], Iain Colin Prentice[1,2], Bradley John Evans[1], David Ian Forrester[3,4], Paul Drake[5,6], Paul Feikema[4], Kim Brooksbank[7], Derek Eamus[8,9], Daniel Taylor[1]

[1]Department of Biological Sciences, Macquarie University, Sydney, NSW, Australia

[2]AXA Chair of Biosphere and Climate Impacts, Grand Challenges in Ecosystems and the Environment and Grantham Institute, Climate Change and the Environment, Department of Life Sciences, Imperial College London, Silwood Park Campus, Buckhurst Road, Ascot SL5 7PY, UK

[3]Department of Forest and Ecosystem Science, The University of Melbourne, Melbourne, Australia

[4]Chair of Silviculture, Faculty of Environment and Natural Resources, Freiburg University, Germany

[5]Natural Resources Branch, Department of Parks and Wild Life, Bentley, Australia

[6]School of Plant Biology, University of Western Australia, Crawley, Australia

[7]Agricultural Resource Risk Management, Department of Agriculture and Food, Albany, Australia

[8]School of Environment, University of Technology Sydney, Sydney, Australia

[9]National Centre for Groundwater Research and Training, Sydney, Australia

This chapter is presented as the published journal article:

Togashi, Henrique F, Prentice, I. Colin, Evans, Brad J., Forrester, D. Ian, Drake, Paul, Feikema, Paul, Brooksbank, Kim, Eamus, Derek and Taylor, Daniel. (2015), Morphological and moisture availability controls of the leaf area-to-sapwood area ratio: analysis of measurements on Australian trees. *Ecology and Evolution*; 5(6). 1263:1270

Ecology and Evolution

Open Access

Morphological and moisture availability controls of the leaf area-to-sapwood area ratio: analysis of measurements on Australian trees

Henrique Furstenau Togashi[1], Iain Colin Prentice[1,2], Bradley John Evans[1], David Ian Forrester[3,4], Paul Drake[5,6], Paul Feikema[4], Kim Brooksbank[7], Derek Eamus[8,9] & Daniel Taylor[1]

[1]Department of Biological Sciences, Macquarie University, Sydney, New South Wales, Australia
[2]AXA Chair of Biosphere and Climate Impacts, Grand Challenges in Ecosystems and the Environment and Grantham Institute – Climate and Environment, Department of Life Sciences, Imperial College, London, UK
[3]Department of Forest and Ecosystem Science, The University of Melbourne, Melbourne, Victoria, Australia
[4]Chair of Silviculture, Faculty of Environment and Natural Resources, Freiburg University, Freiburg, Germany
[5]Natural Resources Branch, Department of Parks and Wild Life, Bentley, Western Australia, Australia
[6]School of Plant Biology, University of Western Australia, Crawley, Western Australia, Australia
[7]Agricultural Resource Risk Management, Department of Agriculture and Food, Albany, Western Australia, Australia
[8]School of Environment, University of Technology Sydney, Sydney, New South Wales, Australia
[9]National Centre for Groundwater Research and Training, Sydney, New South Wales, Australia

Keywords
Climatic moisture, leaf area, pipe model, plant hydraulics, sapwood area, tree morphology.

Correspondence
Henrique Furstenau Togashi, Department of Biological Sciences, Macquarie University, Sydney, Australia.
Tel: +61 2 9850 8165; Fax: +61 2 9850 8165;
E-mail: henriquetogashi@gmail.com

Funding Information
This research was funded by TERN and iMQRES/Macquarie University.

Received: 19 August 2014; Revised: 22 October 2014; Accepted: 27 October 2014

Ecology and Evolution **2015; 5(6): 1263–1270**

doi: 10.1002/ece3.1344

Abstract

1 The leaf area-to-sapwood area ratio (*LA:SA*) is a key plant trait that links photosynthesis to transpiration. The pipe model theory states that the sapwood cross-sectional area of a stem or branch at any point should scale isometrically with the area of leaves distal to that point. Optimization theory further suggests that *LA:SA* should decrease toward drier climates. Although acclimation of *LA:SA* to climate has been reported within species, much less is known about the scaling of this trait with climate among species.
2 We compiled *LA:SA* measurements from 184 species of Australian evergreen angiosperm trees. The pipe model was broadly confirmed, based on measurements on branches and trunks of trees from one to 27 years old. Despite considerable scatter in *LA:SA* among species, quantile regression showed strong ($0.2 < R1 < 0.65$) positive relationships between two climatic moisture indices and the lowermost (5%) and uppermost (5–15%) quantiles of log *LA:SA*, suggesting that moisture availability constrains the envelope of minimum and maximum values of *LA:SA* typical for any given climate.
3 Interspecific differences in plant hydraulic conductivity are probably responsible for the large scatter of values in the mid-quantile range and may be an important determinant of tree morphology.

Introduction

Trade-offs between plant functional traits are central to optimality theories developed to account for observed covariation among traits (Wright et al. 2004; Warton et al. 2006). Investigations of trait variation under different environmental conditions can yield insight into how plant strategies adapt to specific habitats and provide information for modeling plant growth in response to environmental change (Mencuccini and Bonosi, 2001). Here, we focus on the relationships between two critically important traits for the function of trees: leaf area (*LA*), which determines tree water use, light interception, and thus photosynthesis, and sapwood area (*SA*), which determines hydraulic capacity and thus the tree's ability to supply water to the leaves.

According to the "pipe model" (Shinozaki et al. 1964), the leaf area of a stem or branch should be proportional to (scale isometrically with) the sapwood cross-sectional area that sustains it (Tyree and Ewers 1991). As the construction and maintenance of sapwood entail substantial costs, optimization theory further predicts that the ratio *LA:SA* should adjust to environmental conditions in such a way as to maximize photosynthetic revenue relative to

these costs. In dry environments, high vapor pressure deficits (*vpd*) generally imply that larger transpiration rates have to be maintained in order to achieve a given rate of photosynthesis. As a result, the optimal ratio of stomatal conductance to photosynthetic capacity (minimizing the combined costs of maintaining the capacity for both transpiration and carboxylation) is lower in drier environments (Wright et al. 2004; Prentice et al. 2014). However, usually a larger sapwood area per unit area of transpiring leaf has to be maintained if photosynthetic rates are to equal those achieved in wetter environments (Westoby et al. 2012). Thus, we expected to find a trend toward systematically lower *LA:SA* ratios with increasing aridity.

We combined new field measurements of *LA:SA* ratios with published values and values from unpublished studies at sites across a range of Australian environments, from wet to semi-arid and cool-temperate to tropical climates. We used these data – which come from trees of different heights, and include measurements on whole trees as well as branches – to test the general scaling relationships between *LA* and *SA*. We then analyzed relationships between *LA:SA* and several indices of climatic moisture in order to test the predicted relationships between *LA:SA* and aridity. We confined attention to evergreen angiosperms, the dominant tree functional type in Australia. Gymnosperm wood has very different hydraulic properties, while tropical deciduous trees would be expected to respond only to wet-season conditions and therefore to show different patterns of variation with climate.

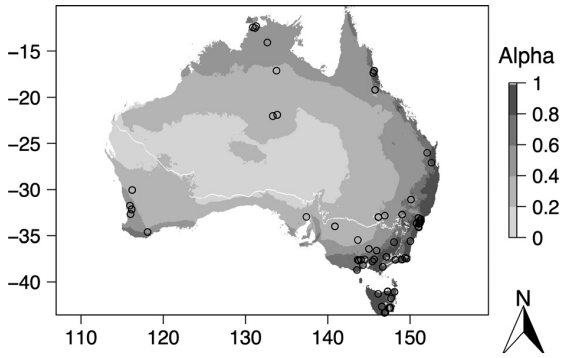

Figure 1. Geographic distribution of measured leaf area-to-sapwood area (*LA:SA*) ratios. The mapped climate variable is the Cramer–Prentice α index of moisture availability (average between 1970 and 2000) calculated from AWAP data (http://www.eoc.csiro.au/awap/). The white line shows the limit between May to September north dry season and October to April south dry season.

Methods

Measurements and data synthesis

We measured *LA* and *SA* on four branches per tree of ten evergreen angiosperm species at Robson Creek, Danbulla National Park, Queensland (17°07′S, 145°37′E). Leaf area was measured using a desktop scanner for all leaves on a sampled branch. After bark removal, the branch cross-sectional area was measured with a digital caliper at two points near the cut (methodology that includes the non-conductive part of the sapwood). The pith cross-sectional area was measured and subtracted from the branch cross-sectional area.

Data for a further 170 species were contributed from 25 sites, based on seven published and two unpublished studies. We also compiled 258 published measurements on 151 species from 43 sites (Supplementary Information Data S1 and S2). The data comprised measurements from 183 species, at the locations shown in Fig. 1. The full dataset was composed of 252 measurements on branches and 175 on whole trees. For compiled and contributed data, measurements on branches were made as described above, although with a variable number of branches sampled per tree. In some studies where the branch diameter was too small (<10 mm), the pith was considered part of the sapwood. For whole trees, cross-sectional sapwood area was measured at 1.3 m above the ground from bored cores or harvesting the tree. Leaf area in whole trees was in most cases measured from harvested trees. Data for individual height in 38 species (49 observations) were also gathered. A further subset was considered for 35 species (101 observations) for which xylem-specific hydraulic conductivity (K_s) was available simultaneously with LA:SA and climatic moisture.

Climate data

Mean *vpd* was estimated at each sampling site from the Bureau of Meteorology (BoM) 0.01-degree gridded climatology using seven models (Running and Coughlan 1988; Allen et al. 1998; Wang et al. 2004), all of which yielded similar results. For illustration, we present results obtained using the equation of Allen et al. (1998), also adopted by the Australian Bureau of Meteorology (BoM), http://www.bom.gov.au:

$$e_o = 0.6108 \exp[(17.27T)/(T + 237.3)]$$

$$vpd = (e_{o,max} + e_{o,min})/2 - e_a$$

where T is daily temperature (°C), $e_{o,\ max}$ is the saturated vapor pressure (kPa) calculated at the daily maximum temperature, $e_{o,\ min}$ is the saturated vapor pressure

calculated at the daily minimum temperature, and e_a is the mean daily actual vapor pressure, calculated from the BoM product as the average of measurements at 0900 and 1500 h.

Two additional climatic indicators of moisture availability were calculated, using Australia Water Availability Project (AWAP) gridded data (http://www.eoc.csiro.au/awap/): the moisture index (*MI*) (the ratio between precipitation and potential evaporation) and the Cramer–Prentice α index (Prentice et al. 2011) (calculated here as the ratio between actual and potential evaporation in the AWAP data). Both *MI* and α are dimensionless numbers and are conceptually related by the Budyko curve, whereby α is a saturating function of *MI*.

All moisture variables (including *vpd*) were calculated for months, years, decades, and dry seasons (the hydraulic architecture of evergreen species may sometimes present a "bottleneck" effect as response to dry season). "Dry season" was defined following the BoM convention as May to September in the north and October to April in the south. The Australian averaged rainfall gridded values for the northern dry season months were subtracted from the averaged southern dry season (1970–2000). Negative values were considered "May to September north dry season" and positive values "October to April south dry season" (Fig. 1).

Data analysis

We tested the pipe model by regressing *LA* against *SA* values for branches and trunks, between species and across environments, using standardized major axis (SMA) regression with the *smatr* package (Warton et al. 2006) in the R language (R Core Team 2012). SMA is a least-squares method which fits the first major axis to standardized data and then retransforms the data to their original scales. The method is useful for studies of the relationships between different dimensions and traits of organisms where natural variability is expected to be present in both variables, as it handles them in a symmetrical way (Warton et al. 2006).

Ordinary linear regression was used to fit bivariate relationships between log *LA:SA* and climatic moisture (α, *MI* and *vpd*). Multiple regression was used for analyses exploring the additional predictive power of plant height and for LA:SA, K_s, and climatic moisture comparisons. The *quantreg* package (Koenker 2004) in R was used to perform quantile regressions between log *LA:SA* and climate variables. Quantile regression (Koenker and Bassett 1978) provides a more complete understanding of relationships between variables than can be obtained with simple regression, allowing different slopes to apply in different quantiles of the dependent variable. Is it also particularly useful when analyzing datasets with unequal variation (Cade and Noon 2003). The coefficient of determination associated with quantile regression is based on absolute rather than squared deviations. For any given quantile τ, this "pseudo-R^2" is $R1 = 1 - F(\tau)/R(\tau)$, where $F(\tau)$ is the weighted sum of absolute deviations from the regression model and $R(\tau)$ is the weighted sum of absolute deviations from the corresponding model with zero slope (Koenker and Machado 1999).

Results

Branch to trunk allometry

Leaf area and sapwood area are both necessarily larger for whole trees than for individual branches. The two variables were strongly and positively correlated across scales (SMA regression: $\log LA = 1.08 \log SA + 3.72$, $R^2 = 0.94$, $P < 0.05$) (Fig. 2) with a slope slightly, but significantly ($P < 0.01$), larger than unity. This finding indicates that while the measurements follow a relationship close to the pipe model, there is a systematic tendency for the ratio *LA:SA* to be higher for whole trees.

A generic (cross-species) estimate of *LA:SA* was obtained by constraining the log–log slope to 1, yielding an intercept of 3.3 ($P < 0.05$) corresponding to a ratio of 2363 ± 818 m^2 m^{-2}. SMA regression also indicated equal slopes for log *LA versus* log *SA* in trunks and in branches ($P > 0.05$ for the null hypothesis of equality) but different intercepts ($P < 0.05$). Constraining the slopes to 1 yielded an intercept of 3.28 ($P < 0.05$), corresponding to a generic *LA:SA* of 1933 ± 578, for branches, and 3.49

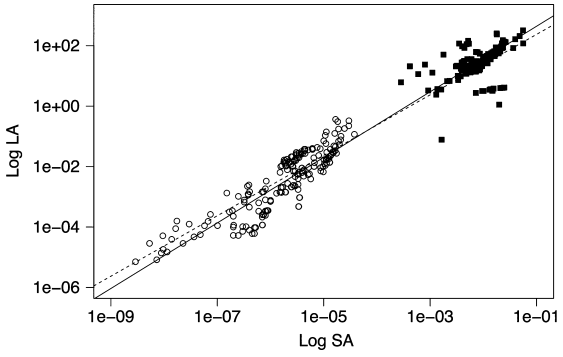

Figure 2. Standardized major axis (SMA) regression between log-transformed leaf area (log *LA*) and sapwood area (log *SA*) for 184 tree species across Australia. Units are in m^2. Open circles and filled squares are observations in branches and whole trees, respectively. The solid line represents the SMA linear regression, and the dashed line shows the line obtained when the slope was constrained to 1. The allometric equations are given in the text.

($P < 0.05$), corresponding to a generic *LA:SA* of 3093 ± 980, for whole trees.

Leaf area-to-sapwood area ratio and tree height

There was a significant positive correlation between log *LA:SA* and log tree height ($R^2 = 0.52$, $P < 0.05$) (Fig. 3). The correlation was stronger for branches only ($R^2 = 0.64$, $P < 0.05$). There was no significant relationship for whole trees (slope 0.001, $P > 0.05$) (lines not shown). The overall increase in *LA:SA* with increasing tree height seems to be ontogenetic, and not an artifact of correlation between height and climatic moisture, as there was no significant bivariate relationship between tree height and climatic moisture (*MI*, α or *vpd*). A multiple linear regression of height and each of the climatic moisture variables as predictors for *LA:SA* ($R^2 = 0.24$) returned a significant slope for height ($P < 0.05$) but a nonsignificant slope for climatic moisture ($P > 0.05$) (graphs not shown).

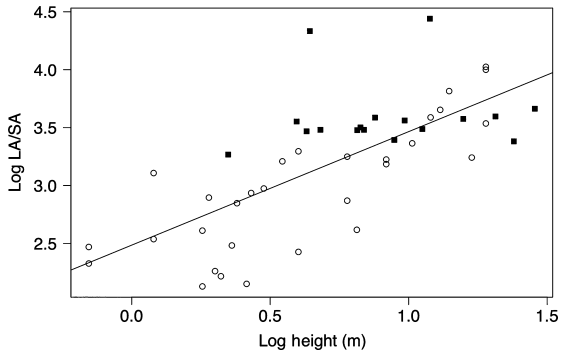

Figure 3. Relationship between log-transformed leaf area-to-sapwood area ratio (log *LA/SA*) and log tree height in 39 angiosperm tree species. Open circles and filled squares are observations in branches and whole trees, respectively.

Relationship of LA:SA to climatic moisture

The overall linear regression relationships of log *LA:SA* to annual, decadal, dry-season, and mean monthly α (Fig. 4) were not statistically significant. Linear regressions between log *LA:SA* and *MI* and mean *vpd* were also not significant. However, the upper and lower bounds of log *LA:SA* tend to increase with increasing α even though the cloud of points does not show such a relationship (Fig. 4, left panels). Quantile regressions confirmed this, with α accounting for about 0.2 of the bottom 7% ($P < 0.05$) and from 0.3 to 0.55 of the top 15% ($P < 0.05$) of the variation in *LA:SA* (Fig. 4, right panels). Similarly, *MI* accounted for 0.2 to 0.35 of the top 10% ($P < 0.05$) of the observed variation in *LA:SA* (data not shown). In contrast, dry season and monthly α and *MI* could not explain any quantiles of the relationship (data not shown). There were also no significant relationships between *LA:SA* and *vpd* ($R1 < 0.2$, $P > 0.05$) for any τ (data not shown).

These relationships were valid whether *LA:SA* was measured in branches (for the lower end) or in whole trees (for the upper end). No value of log *LA:SA* in whole trees was smaller than 2.7 ($502 < LA:SA < 58\,200$), while values of log *LA:SA* in branches were generally restricted to between 2 and 4 ($122 < LA/SA < 10\,000$). Part of the spread in values is due to the slight departure from isometry, such that whole trees have larger values than branches. Significant correlations between log *LA:SA* and α in this dataset are restricted to the upper and the lower

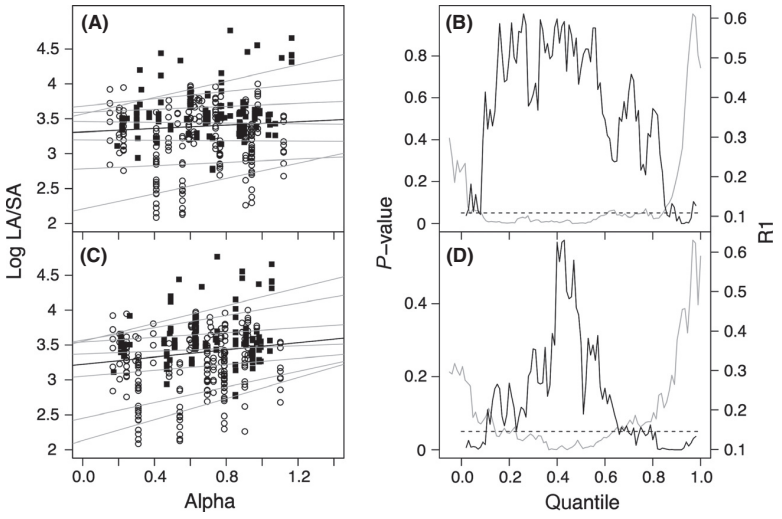

Figure 4. Filled points and open circles are *LA/SA* observations in whole trees and branches, respectively. The left panels show quantile linear regressions lines in gray (τ = 0.05, 0.1, 0.25, 0.5, 0.75, 0.9, 0.95) and ordinary least-squares linear regression line in black, for log-transformed leaf area-to-sapwood area ratio (log *LA/SA*) as a function of annual (A) and decadal (C) values of α. The right panels show the corresponding *P*-values (black) and pseudo *R*-squared (*R*1) values (gray) as a function of τ.

quantiles where there are either only whole-tree or only branch measurements, respectively. Nevertheless, when separate regressions were performed for whole trees and branches, the former yielded similar significant relationships for the upper quantiles and the latter yielded similar significant relationships for the lower quantiles.

Relationship of LA:SA to K_s and climatic moisture

K_s data were available only in the higher range of log *LA:SA* values (between 2.6 and 4). Within this range, xylem-specific hydraulic conductivity showed some predictive ability for *LA:SA*. The bivariate linear regression was significant ($P < 0.05$), and R^2 was 0.24 (Fig. 5). The positive regression slope indicates an increase in *LA:SA* with increasing K_s. Including the index α in a multiple regression increased the correlation to $R^2 = 0.34$ ($P < 0.05$). A model including an interaction term (K_s:α) also returned significant results for alpha ($P < 0.05$). Species in wetter environments present higher LA:SA at a given K_s than species in drier environments.

Discussion

LA to SA allometry in branches and whole trees

The close, near-isometric relationship (slope 1.08 ± 0.02) between leaf area and sapwood area shown in Fig. 2 is broadly consistent with the pipe model. The similar slopes and different intercepts between *LA* and *SA*, however, indicate a tendency for overall higher *LA:SA* ratios at the whole-tree scale. This conclusion is supported by our generic regression-based estimates of the *LA:SA* ratio, which are about 50% higher for whole trees than for branches. The difference could perhaps be an artifact of the assumption, made in many studies, that branches are composed entirely of sapwood (i.e., the pith is not accounted for). Alternatively, it could be explained by the variations in the relationship of *LA:SA* with tree height and climatic moisture in plant hydraulic traits.

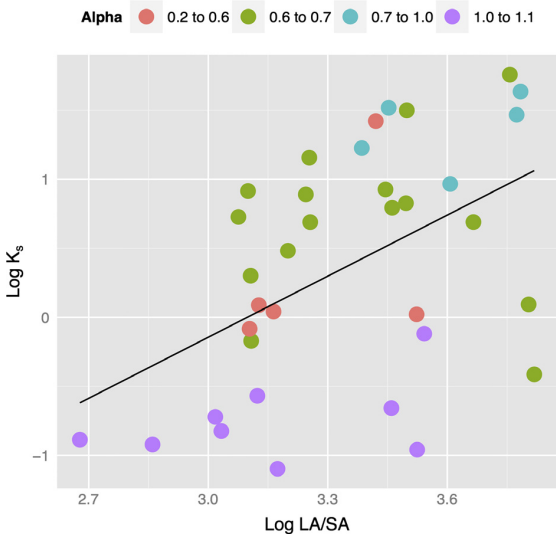

Figure 5. Linear regression of xylem-specific hydraulic conductivity (K_s) and *LA/SA*. Values of the Cramer–Prentice Alpha (α) index ($R^2 = 0.34$, $P < 0.05$) are superimposed.

Relationship of LA:SA to tree height

If hydraulic properties of wood did not change with tree size, the hydraulic conductivity of the stem would be in inverse proportion to its height. This could have two possible consequences. One would be that tall trees would have much reduced rates of transpiration per unit of leaf area. The other would be a requirement for large reductions in *LA:SA* with height, to compensate for the increased resistance to water transport – in direct contradiction to the pipe model. Neither of these effects is observed, because of the phenomenon of basipetal tapering of conducting tissues (Tyree and Ewers 1991; Olson and Rosell 2013). Olson et al. (2014) have shown that this is universal in the angiosperms. Taller plants are associated with larger vessel diameters but lower vessel densities (Olson et al. 2014). Increasing vessel diameter is a highly effective means of maintaining hydraulic conductivity, because of the fourth-power dependence of conductivity on vessel diameter, whereas hydraulic path length scales in the linear dimension according to Poiseuille's law (Tyree and Ewers 1991; Sellin and Kupper 2006). Olson and Rosell (2013) and Olson et al. (2014) demonstrated that vessel diameter is strongly predicted by stem diameter and that species in drier environments tend to have narrower vessels simply because they are shorter. Olson et al. (2014) further demonstrated that direct climate controls on vessel diameter are very weak, compared with the pure effect of size.

Low irradiances may favor height growth over an increase in sapwood area in plants not adapted to low light, where competition for light is intense (Calvo-Alvarado et al. 2008). For many tree species, height growth is an important process to outcompete neighbors for sunlight. Increased water transport through wider vessels with increasing height would provide a selective advantage when water is not limiting. There will always be some individual trees with small vessel density and some with large vessel density, and when conditions are favorable, trees may just increase the proportion of large-diameter

vessels. Even if vessel density related to height and not to climate, height should correlate with moisture availability; thus, the apparent trade-off between vessel density and climatic moisture is important for modeling purposes.

Tree height was positively correlated with *LA:SA* (Fig. 3) in contrast to several other studies in angiosperms (Schäfer et al. 2000; Sellin and Kupper 2006) and conifers (Magnani et al. 2000; McDowell et al. 2002; Delzon et al. 2004) where the correlation was found to be negative. All those studies were conducted in temperate climates. Other studies have shown *LA:SA* increasing with size for angiosperms in warm moist environments (Gerrish 1990; Vertessy et al. 1995; Mokany et al. 2003; Calvo-Alvarado et al. 2008), for conifers generally (McDowell et al. 2002), and for angiosperms in seasonal climates (Phillips et al., 2003). For exceptions in angiosperms, see Calvo-Alvarado et al. (2008) where one species of five showed a decrease in *LA:SA* with height in a wet environment, and for gymnosperms, see Hubbard et al. (1999) and Long and Smith (1988) where *LA:SA* increased with height in a dry environment. Considering the results in the present study and the generally similar results in the literature, it may be that the relation between tree height and *LA:SA* will be directly or indirectly influenced by environmental conditions: Warm moist environments should thus show positive correlations, and cold enviroments should show negative correlations. A more systematic global survey would be needed to test this.

Relationships of LA:SA to climatic moisture and the role of xylem hydraulic conductivity

There is evidence for acclimation of *LA:SA* across sites within *Pinus* species (Mencuccini and Grace 1995; Delucia et al. 2000; Schäfer et al. 2000; Warton et al. 2006). In contrast, relatively little has been published about how *LA:SA* among angiosperm species is affected by climatic characteristics of contrasting environments. Yet this information is required when modeling carbon and plant trait trade-offs in ecosystems.

Every growing season provides an opportunity for trees to modify *LA:SA*. The dimensions of xylem elements are one of the most important traits to determine a conservative or profligate strategy of water use, and this underpins the potential carbon gain attainable over the season (Magnani et al. 2000). The narrow tracheids of gymnosperms imply a low hydraulic conductivity, but this is accompanied by a reduced risk of embolism and thus the capacity to adapt to dry environments and also to environments subject to freezing (Tyree and Ewers 1991; Delucia et al. 2000). The low conductivity of gymnosperm wood is compensated for by larger sapwood area and generally smaller *LA:SA* in order to maintain rates of water transport. Variation in diameter of xylem-conducting elements between angiosperm species is much wider than between gymnosperm species (Sperry et al., 2006), and this fact may well have contributed to the large variation in *LA:SA* that we observed. Contrasts between low *LA:SA*, usually accompanied by narrow crowns in gymnosperm trees and high *LA:SA*, accompanied by more widely spreading crowns in many angiosperm trees, is an important aspect of the morphological difference between these phyla which may ultimately be controlled by differences in hydraulic capacity.

We could not confirm any universal relationship between *LA:SA* and moisture availability (Fig. 4). Non-*Pinus*-conifers showed a similar lack of relationship across environments at a global scale (Delucia et al. 2000). Nevertheless, quantile regression revealed a systematic increase in both the upper and lower bounds of *LA:SA* with increasing climatic moisture, as indexed by α or *MI*. Moreover, because of the slight departure from isometry in the relationship between *LA* and *SA*, the upper bound is formed by whole trees and the lower bound by branches. But the importance of these bounds is dwarfed by the large variation in *LA:SA* found within both tree and branch measurement sets. This variation may be related to plant hydraulic conductivity, which also shows large variations among species and which has frequently been mentioned as a key trait coordinated with leaf area and sapwood area to achieve convergence in water use (Mencuccini and Grace 1995; Zeppel and Eamus 2008; Choat et al. 2012; Gleason et al. 2012). Higher ranges of *LA:SA* in Australian angiosperm trees could indeed be predicted by xylem-specific hydraulic conductivity, and this relationship was stronger when considering climatic moisture. However, the dataset available for this study could not confirm a more general correlation in all ranges of *LA:SA* (Fig. 5). Improved understanding of the spectrum of plant hydraulic function would be promoted by studies specifically orienteded to coordinated measurements of *LA:SA* and hydraulic traits across species and environments.

Acknowledgments

This research was funded by the Terrestrial Ecosystem Research Network (TERN) and Macquarie University. Owen Atkin (ANU) provided logistical support for fieldwork. H.F. Togashi is supported by a Macquarie University International Research Scholarship (iMQRES). We are grateful to Amy Zanne (George Washington University) and Ian Wright (Macquarie University) for contributing trait data. We thank Craig Macfarlane (CSIRO-WA), Rhys Whitley, Daniel Falster and Sean

Gleason (Macquarie University), and two anonymous contributors for constructive comments on earlier drafts. This research is a contribution to the AXA Chair Programme on Biosphere and Climate Impacts and the Imperial College initiative on Grand Challenges in Ecosystems and the Environment.

Conflict of Interest

None declared.

References

Allen, R. G., L. S. Pereira, D. Raes, and M. Smith. 1998. Crop evapotranspiration-Guidelines for computing crop water requirements-FAO Irrigation and drainage paper 56. FAO, Rome, 300, 6541.

Cade, B. S., and B. R. Noon. 2003. A gentle introduction to quantile regression for ecologists. Front. Ecol. Environ. 1:412–420.

Calvo-Alvarado, J. C., N. G. McDowell, and R. H. Waring. 2008. Allometric relationships predicting foliar biomass and leaf area: sapwood area ratio from tree height in five Costa Rican rain forest species. Tree Physiol. 28:1601–1608.

Choat, B., S. Jansen, T. J. Brodribb, H. Cochard, S. Delzon, R. Bhaskar, et al. 2012. Global convergence in the vulnerability of forests to drought. Nature, 491:752–755.

Delucia, E. H., H. Maherali, and E. V. Carey. 2000. Climate-driven changes in biomass allocation in pines. Glob. Change Biol. 6:587–593.

Delzon, S., M. Sartore, R. Burlett, R. Dewar, and D. Loustau. 2004. Hydraulic responses to height growth in maritime pine trees. Plant, Cell Environ. 27:1077–1087.

Gerrish, G. 1990. Relating carbon allocation patterns to tree senescence in Metrosideros forests. Ecology 71:1176–1184.

Gleason, S. M., D. W. Butler, K. Ziemińska, P. Waryszak, and M. Westoby. 2012. Stem xylem conductivity is key to plant water balance across Australian angiosperm species. Funct. Ecol. 26:343–352.

Hubbard, R. M., B. J. Bond, and M. G. Ryan. 1999. Evidence that hydraulic conductance limits photosynthesis in old *Pinus ponderosa* trees. Tree Physiol. 19:165–172.

Koenker, R. 2004. Quantreg: an R package for quantile regression and related methods. http://cran.r-project.org.

Koenker, R., and G. Bassett Jr. 1978. Regression quantiles. Econometrica 46:33–50.

Koenker, R., and J. A. F. Machado. 1999. Goodness of fit and related inference processes for quantile regression. J. Am. Stat. Assoc. 94:1296–1310.

Long, J. N., and F. W. Smith. 1988. Leaf area - sapwood area relations of lodgepole pine as influenced by stand density and site index. Can. J. For. Res. 18:247–250.

Magnani, F., M. Mencuccini, and J. Grace. 2000. Age-related decline in stand productivity: the role of structural acclimation under hydraulic constraints. Plant, Cell Environ. 23:251–263.

McDowell, N., H. Barnard, B. Bond, T. Hinckley, R. Hubbard, H. Ishii, et al. 2002. The relationship between tree height and leaf area: sapwood area ratio. Oecologia 132:12–20.

Mencuccini, M., and L. Bonosi. 2001. Leaf/sapwood area ratios in Scots pine show acclimation across Europe. Can. J. For. Res., 31:442–456.

Mencuccini, M., and J. Grace. 1995. Climate influences the leaf area/sapwood area ratio in Scots pine. Tree Physiol. 15:1–10.

Mokany, K., R. E. McMurtrie, B. J. Atwell, and H. Keith. 2003. Interaction between sapwood and foliage area in alpine ash (*Eucalyptus delegatensis*) trees of different heights. Tree Physiol. 23:949–958.

Olson, M. E., and J. A. Rosell. 2013. Vessel diameter–stem diameter scaling across woody angiosperms and the ecological causes of xylem vessel diameter variation. New Phytol. 197:1204–1213.

Olson, M. E., T. Anfodillo, J. Rosell, S. Isnard, C. León-Gómez, G. Alvarado-Cárdenas, et al. 2014. Universal hydraulics of the flowering plants: vessel diameter scales with stem length across angiosperm lineages, habits and climates. Ecol. Lett. 17:988–997.

Phillips, N. G., M. G. Ryan, B. J. Bond, N. G. McDowell, T. M. Hinckley, and J. Čermák. 2003. Reliance on stored water increases with tree size in three species in the Pacific Northwest. Tree Physiol., 23:237–245.

Prentice, I. C., T. Meng, H. Wang, S. P. Harrison, J. Ni, and G. Wang. 2011. Evidence of a universal scaling relationship for leaf CO_2 drawdown along an aridity gradient. New Phytol. 190:169–180.

Prentice, I. C., N. Dong, S. M. Gleason, V. Maire, and I. J. Wright. 2014. Balancing the costs of carbon gain and water transport: testing a new theoretical framework for plant functional ecology. Ecol. Lett. 17:82–91.

R Core Team 2012. R: a language and environment for statistical computing. R Foundation for Statistical Computing, Vienna, Austria. Avilable via http://www.R-project.org/.

Running, S. W., and J. C. Coughlan. 1988. A general model of forest ecosystem processes for regional applications I. Hydrologic balance, canopy gas exchange and primary production processes. Ecol. Model. 42:125–154.

Schäfer, K. V. R., R. Oren, and J. D. Tenhunen. 2000. The effect of tree height on crown level stomatal conductance. Plant, Cell Environ. 23:365–375.

Sellin, A., and P. Kupper. 2006. Spatial variation in sapwood area to leaf area ratio and specific leaf area within a crown of silver birch. Trees-Struct. Funct. 20:311–319.

Shinozaki, K., K. Yoda, K. Hozumi, and T. Kira. 1964. A quantitative analysis of plant form;the pipe model theory,1. Japanese J. Ecol. 14:97–105.

Sperry, J. S., U. G. Hacke, and J. Pittermann. 2006. Size and function in conifer tracheids and angiosperm vessels. Am. J. Bot., 93:1490–1500.

Tyree, M. T., and F. W. Ewers. 1991. The hydraulic architecture of trees and other woody plants. New Phytol. 119:345–360.

Vertessy, R. A., R. G. Benyon, S. K. O'sullivan, and P. R. Gribben. 1995. Relationships between stem diameter, sapwood area, leaf area and transpiration in a young mountain ash forest. Tree Physiol. 15: 559–567.

Wang, E., C. J. Smith, W. J. Bond, and K. Verburg. 2004. Estimations of vapour pressure deficit and crop water demand in APSIM and their implications for prediction of crop yield, water use, and deep drainage. Aust. J. Agric. Res. 55:1227–1240.

Warton, D. I., I. J. Wright, D. S. Falster, and M. Westoby. 2006. Bivariate line-fitting methods for allometry. Biol. Rev. 81:259–291.

Westoby, M., W. K. Cornwell, and D. S. Falster. 2012. An evolutionary attractor model for sapwood cross section in relation to leaf area. J. Theor. Biol. 303:98–109.

Wright, I. J., P. B. Reich, M. Westoby, D. D. Ackerly, Z. Baruch, F. Bongers, et al. 2004. The worldwide leaf economics spectrum. Nature 428:821–827.

Zeppel, M., and D. Eamus. 2008. Coordination of leaf area, sapwood area and canopy conductance leads to species convergence of tree water use in a remnant evergreen woodland. Aust. J. Bot. 56:97–108.

Supporting Information

Additional Supporting Information may be found in the online version of this article:

Data S1. Togashi et al. Moisture availability constraints on LA:SA dataset.

Data S2. List of published literature for data compilation.

Supporting information

Data S1. Togashi *et al.* Moisture availability constraints on LA:SA dataset

Units ⇒ LA:SA (log10 transformed); Height (m); Alpha (annual unitless); MI (annual unitless)

As a condition for use of the dataset, we request that users agree:

(1) To notify the main author (Henrique Furstenau Togashi) if the dataset is to be used in any publication;

(2) To recognise that the researchers who gathered these data with formal recognition that may include co-authorship or acknowledgements on publications

Zanne *et al.* dataset is not included. The dataset can be requested to the main author (Henrique Furstenau Togashi).

Specie	Long	Lat	LA:SA	Sample	Height	Alpha	MI	References
Ceratopetalum apetalum	150.03	−35.58	2.79	trunk		0.57	0.99	Barrett et al. 1996
Doryphora sassafras	150.03	−35.58	2.77	trunk		0.57	0.99	Barrett et al. 1996
Eucalyptus maculata	150.03	−35.58	3.22	trunk		0.57	0.99	Barrett et al. 1996
Eucalyptus camaldulensis	149.03	−32.70	3.46	trunk		0.34	0.28	Benyon et al. 1999
Eucalyptus camaldulensis	149.03	−32.70	3.57	trunk		0.34	0.28	Benyon et al. 1999
Eucalyptus camaldulensis	149.03	−32.70	3.50	trunk	6.70	0.46	0.54	Benyon et al. 1999
Eucalyptus camaldulensis	149.03	−32.70	3.48	trunk	4.80	0.46	0.54	Benyon et al. 1999
Eucalyptus occidentalis	149.03	−32.70	3.51	trunk		0.34	0.28	Benyon et al. 1999
Eucalyptus occidentalis	149.03	−32.70	3.48	trunk	6.90	0.46	0.54	Benyon et al. 1999
Eucalyptus marginata	116.02	−32.65	3.43	branch		0.42	0.49	Bleby et al.2009
Eucalyptus marginata	116.02	−32.65	3.58	branch		0.42	0.49	Bleby et al.2009
Eucalyptus marginata	116.02	−32.65	3.57	branch		0.42	0.49	Bleby et al.2009
Eucalyptus coccifera	146.58	−42.68	3.54	branch		0.89	2.30	Brodribb and Felid 2000
Atherosperma moschatum	146.58	−42.68	3.46	branch		0.89	2.30	Brodribb and Felid 2000
Diselma archeri	146.58	−42.68	2.86	branch		0.89	2.30	Brodribb and Felid 2000
Leptospermum rupestre	146.58	−42.68	3.02	branch		0.89	2.30	Brodribb and Felid 2000
Nothofagus cunninghamii	146.58	−42.68	3.12	branch		0.89	2.30	Brodribb and Felid 2000
Phyllocladus aspleniifolius	146.58	−42.68	3.52	branch		0.89	2.30	Brodribb and Felid 2000
Podocarpus lawrencei	146.58	−42.68	3.03	branch		0.89	2.30	Brodribb and Felid 2000
Richea scoparium	146.58	−42.68	2.68	branch		0.89	2.30	Brodribb and Felid 2000
Tasmannia lanceolata	146.58	−42.68	3.17	branch		0.89	2.30	Brodribb and Felid 2000
Eucalyptus kochii	116.22	−30.04	3.51	trunk		0.17	0.19	Brooksbank et al. 2011
Eucalyptus kochii	116.22	−30.04	3.49	trunk		0.17	0.19	Brooksbank et al. 2011
Eucalyptus kochii	116.22	−30.04	3.50	trunk		0.17	0.19	Brooksbank et al. 2011
Eucalyptus kochii	116.22	−30.04	3.39	trunk		0.17	0.19	Brooksbank et al. 2011
Eucalyptus kochii	116.22	−30.04	3.39	trunk		0.17	0.19	Brooksbank et al. 2011
Eucalyptus kochii	116.22	−30.04	3.39	trunk		0.17	0.19	Brooksbank et al. 2011
Eucalyptus kochii	116.22	−30.04	3.34	trunk		0.17	0.19	Brooksbank et al. 2011
Eucalyptus kochii	116.22	−30.04	3.34	trunk		0.17	0.19	Brooksbank et al. 2011
Eucalyptus kochii	116.22	−30.04	3.35	trunk		0.17	0.19	Brooksbank et al. 2011
Banksia attenuata	115.95	−31.75	3.05	branch		0.38	0.33	Canham et al. 2009
Banksia attenuata	115.95	−31.75	3.15	branch		0.38	0.33	Canham et al. 2009
Banksia ilicifolia	115.95	−31.75	3.10	branch		0.38	0.33	Canham et al. 2009
Banksia ilicifolia	115.95	−31.75	3.22	branch		0.38	0.33	Canham et al. 2009
Banksia littoralis	115.95	−31.75	3.52	branch		0.38	0.33	Canham et al. 2009
Banksia menziesii	115.95	−31.75	3.15	branch		0.38	0.33	Canham et al. 2009
Banksia menziesii	115.95	−31.75	3.10	branch		0.38	0.33	Canham et al. 2009
Eucalyptus kochii	116.21	−30.04	3.47	trunk		0.18	0.20	Carter and White 2009
Eucalyptus kochii	116.21	−30.04	3.37	trunk		0.18	0.20	Carter and White 2009

continued on next page

continued from previous page

Specie	Long	Lat	LA:SA	Sample	Height	Alpha	MI	References
Eucalyptus miniata	131.15	−12.49	3.65	branch		0.53	0.52	Cernusak et al. 2006
Eucalyptus tetrodonta	131.15	−12.49	3.75	branch		0.53	0.52	Cernusak et al. 2006
Alphitonia excelsa	145.75	−19.18	3.67	branch		0.50	0.69	Choat et al. 2005
Austromyrtus bidwillii	145.75	−19.18	3.80	branch		0.50	0.69	Choat et al. 2005
Brachychiton australis	145.75	−19.18	3.50	branch		0.50	0.69	Choat et al. 2005
Cochlospermum gillivraei	145.75	−19.18	3.24	branch		0.50	0.69	Choat et al. 2005
Argyrodendron trifoliolatum	145.54	−17.38	3.46	branch		0.77	0.90	Drake and Franks 2003
Argyrodendron trifoliolatum	145.54	−17.38	3.30	branch		0.77	0.90	Drake and Franks 2003
Calamus australis	145.54	−17.38	4.00	branch		0.77	0.90	Drake and Franks 2003
Calamus australis	145.54	−17.38	3.82	branch		0.77	0.90	Drake and Franks 2003
Calamus caryotoides	145.54	−17.38	3.64	branch		0.77	0.90	Drake and Franks 2003
Calamus caryotoides	145.54	−17.38	3.36	branch		0.77	0.90	Drake and Franks 2003
Castanospora alphandii	145.54	−17.38	3.89	branch		0.77	0.90	Drake and Franks 2003
Castanospora alphandii	145.54	−17.38	3.70	branch		0.77	0.90	Drake and Franks 2003
Doryphora aromatica	145.54	−17.38	3.85	branch		0.77	0.90	Drake and Franks 2003
Doryphora aromatica	145.54	−17.38	3.46	branch		0.77	0.90	Drake and Franks 2003
Eucalyptus gomphocelia	116.15	−32.15	3.84	branch		0.48	0.52	Drake et al. 2011
Eucalyptus gomphocelia	116.15	−32.15	3.88	branch		0.48	0.52	Drake et al. 2011
Eucalyptus gomphocelia	116.15	−32.15	3.91	branch		0.48	0.52	Drake et al. 2011
Eucalyptus gomphocelia	116.15	−32.15	3.87	branch		0.48	0.52	Drake et al. 2011
Eucalyptus gomphocelia	116.15	−32.15	3.72	branch		0.48	0.52	Drake et al. 2011
Eucalyptus gomphocelia	116.15	−32.15	3.82	branch		0.48	0.52	Drake et al. 2011
Eucalyptus gomphocelia	116.15	−32.15	3.71	branch		0.48	0.52	Drake et al. 2011
Eucalyptus gomphocelia	116.15	−32.15	3.74	branch		0.48	0.52	Drake et al. 2011
Eucalyptus gomphocelia	116.15	−32.15	3.85	branch		0.48	0.52	Drake et al. 2011
Eucalyptus gomphocelia	116.15	−32.15	3.74	branch		0.48	0.52	Drake et al. 2011
Eucalyptus gomphocelia	116.15	−32.15	3.92	branch		0.48	0.52	Drake et al. 2011
Eucalyptus gomphocelia	116.15	−32.15	3.71	branch		0.48	0.52	Drake et al. 2011
Eucalyptus gomphocelia	116.15	−32.15	3.92	branch		0.48	0.52	Drake et al. 2011
Eucalyptus gomphocelia	116.15	−32.15	3.69	branch		0.48	0.52	Drake et al. 2011
Eucalyptus gomphocelia	116.15	−32.15	3.84	branch		0.48	0.52	Drake et al. 2011
Eucalyptus gomphocelia	116.15	−32.15	3.90	branch		0.48	0.52	Drake et al. 2011
Eucalyptus gomphocelia	116.15	−32.15	3.87	branch		0.48	0.52	Drake et al. 2011
Eucalyptus gomphocelia	116.15	−32.15	3.77	branch		0.48	0.52	Drake et al. 2011
Eucalyptus gomphocelia	116.15	−32.15	3.95	branch		0.48	0.52	Drake et al. 2011
Eucalyptus gomphocelia	116.15	−32.15	3.76	branch		0.48	0.52	Drake et al. 2011
Eucalyptus gomphocelia	116.15	−32.15	3.92	branch		0.48	0.52	Drake et al. 2011
Eucalyptus gomphocelia	116.15	−32.15	3.73	branch		0.48	0.52	Drake et al. 2011
Eucalyptus gomphocelia	116.15	−32.15	3.90	branch		0.48	0.52	Drake et al. 2011
Eucalyptus gomphocelia	116.15	−32.15	3.85	branch		0.48	0.52	Drake et al. 2011
Eucalyptus gomphocelia	116.15	−32.15	3.69	branch		0.48	0.52	Drake et al. 2011
Eucalyptus gomphocelia	116.15	−32.15	3.72	branch		0.48	0.52	Drake et al. 2011
Eucalyptus gomphocelia	116.15	−32.15	3.50	branch		0.48	0.52	Drake et al. 2011
Eucalyptus gomphocelia	116.15	−32.15	3.84	branch		0.48	0.52	Drake et al. 2011
Eucalyptus gomphocelia	116.15	−32.15	3.86	branch		0.48	0.52	Drake et al. 2011
Eucalyptus gomphocelia	116.15	−32.15	3.83	branch		0.48	0.52	Drake et al. 2011
Eucalyptus gomphocelia	116.15	−32.15	3.51	branch		0.48	0.52	Drake et al. 2011
Eucalyptus gomphocelia	116.15	−32.15	3.97	branch		0.48	0.52	Drake et al. 2011
Eucalyptus gomphocelia	116.15	−32.15	3.77	branch		0.48	0.52	Drake et al. 2011
Eucalyptus gomphocelia	116.15	−32.15	3.85	branch		0.48	0.52	Drake et al. 2011
Eucalyptus gomphocelia	116.15	−32.15	3.84	branch		0.48	0.52	Drake et al. 2011
Eucalyptus gomphocelia	116.15	−32.15	3.82	branch		0.48	0.52	Drake et al. 2011
Eucalyptus camaldulensis	140.87	−33.98	3.66	trunk	28.55	0.24	0.30	Eldridge et al. 1993
Eucalyptus largiflorens	140.87	−33.98	3.59	trunk	7.56	0.24	0.30	Eldridge et al. 1993
Eucalyptus largiflorens	140.87	−33.98	3.56	trunk	9.68	0.24	0.30	Eldridge et al. 1993
Eucalyptus largiflorens	140.87	−33.98	3.49	trunk	11.20	0.24	0.30	Eldridge et al. 1993
Eucalyptus largiflorens	140.87	−33.98	3.39	trunk	8.88	0.24	0.30	Eldridge et al. 1993
Eucalyptus largiflorens	140.87	−33.98	3.48	trunk	6.52	0.24	0.30	Eldridge et al. 1993
Eucalyptus globulus	143.79	−37.69	3.83	trunk		0.55	0.69	Forrester et al. 2010a
Eucalyptus globulus	143.79	−37.69	3.83	trunk		0.55	0.69	Forrester et al. 2010a
Eucalyptus globulus	143.79	−37.69	3.86	trunk		0.55	0.69	Forrester et al. 2010a
Eucalyptus globulus	143.79	−37.69	3.84	trunk		0.55	0.69	Forrester et al. 2010a
Eucalyptus globulus	143.79	−37.69	3.86	trunk		0.55	0.69	Forrester et al. 2010a
Eucalyptus globulus	143.64	−37.61	3.62	trunk		0.54	0.67	Forrester et al. 2010a
Eucalyptus globulus	143.64	−37.61	3.63	trunk		0.54	0.67	Forrester et al. 2010a

continued on next page

continued from previous page

Specie	Long	Lat	LA:SA	Sample	Height	Alpha	MI	References
Eucalyptus globulus	143.64	−37.61	3.59	trunk		0.54	0.67	Forrester et al. 2010a
Eucalyptus globulus	143.79	−37.69	3.49	trunk		0.55	0.69	Forrester et al. 2010a
Eucalyptus globulus	143.79	−37.69	3.54	trunk		0.55	0.69	Forrester et al. 2010a
Eucalyptus globulus	143.79	−37.69	3.56	trunk		0.55	0.69	Forrester et al. 2010a
Eucalyptus globulus	143.79	−37.69	3.58	trunk		0.55	0.69	Forrester et al. 2010a
Eucalyptus globulus	143.79	−37.69	3.57	trunk		0.55	0.69	Forrester et al. 2010a
Eucalyptus globulus	143.64	−37.61	3.44	trunk		0.54	0.67	Forrester et al. 2010a
Eucalyptus globulus	143.64	−37.61	3.50	trunk		0.54	0.67	Forrester et al. 2010a
Eucalyptus globulus	143.64	−37.61	3.53	trunk		0.54	0.67	Forrester et al. 2010a
Eucalyptus globulus	143.79	−37.69	3.50	trunk		0.55	0.69	Forrester et al. 2010a
Eucalyptus globulus	143.79	−37.69	3.49	trunk		0.55	0.69	Forrester et al. 2010a
Eucalyptus globulus	143.79	−37.69	3.59	trunk		0.55	0.69	Forrester et al. 2010a
Eucalyptus globulus	143.79	−37.69	3.54	trunk		0.55	0.69	Forrester et al. 2010a
Eucalyptus globulus	143.79	−37.69	3.46	trunk		0.55	0.69	Forrester et al. 2010a
Eucalyptus globulus	144.03	−37.61	3.52	trunk		0.59	0.76	Forrester et al. 2010a
Eucalyptus globulus	144.03	−37.61	3.47	trunk		0.59	0.76	Forrester et al. 2010a
Eucalyptus globulus	144.03	−37.61	3.48	trunk		0.59	0.76	Forrester et al. 2010a
Acacia mearnsii	149.02	−37.58	3.40	trunk		0.69	0.68	Forrester et al. 2010b
Acacia mearnsii	149.02	−37.58	3.29	trunk		0.69	0.68	Forrester et al. 2010b
Acacia mearnsii	149.02	−37.58	3.38	trunk		0.69	0.68	Forrester et al. 2010b
Acacia mearnsii	149.02	−37.58	3.40	trunk		0.71	0.94	Forrester et al. 2010b
Acacia mearnsii	149.02	−37.58	3.34	trunk		0.71	0.94	Forrester et al. 2010b
Acacia mearnsii	149.02	−37.58	3.35	trunk		0.71	0.94	Forrester et al. 2010b
Acacia mearnsii	149.02	−37.58	3.41	trunk		0.69	0.68	Forrester et al. 2010b
Acacia mearnsii	149.02	−37.58	3.57	trunk		0.69	0.68	Forrester et al. 2010b
Acacia mearnsii	149.02	−37.58	3.45	trunk		0.69	0.68	Forrester et al. 2010b
Acacia mearnsii	149.02	−37.58	3.37	trunk		0.71	0.94	Forrester et al. 2010b
Acacia mearnsii	149.02	−37.58	3.34	trunk		0.71	0.94	Forrester et al. 2010b
Acacia mearnsii	149.02	−37.58	3.36	trunk		0.71	0.94	Forrester et al. 2010b
Eucalyptus globulus	149.02	−37.58	3.28	trunk		0.69	0.68	Forrester et al. 2010b
Eucalyptus globulus	149.02	−37.58	3.59	trunk		0.69	0.68	Forrester et al. 2010b
Eucalyptus globulus	149.02	−37.58	3.35	trunk		0.69	0.68	Forrester et al. 2010b
Eucalyptus globulus	149.02	−37.58	3.16	trunk		0.71	0.94	Forrester et al. 2010b
Eucalyptus globulus	149.02	−37.58	3.34	trunk		0.71	0.94	Forrester et al. 2010b
Eucalyptus globulus	149.02	−37.58	3.36	trunk		0.71	0.94	Forrester et al. 2010b
Eucalyptus globulus	149.02	−37.58	3.31	trunk		0.69	0.68	Forrester et al. 2010b
Eucalyptus globulus	149.02	−37.58	3.25	trunk		0.69	0.68	Forrester et al. 2010b
Eucalyptus globulus	149.02	−37.58	3.27	trunk		0.69	0.68	Forrester et al. 2010b
Eucalyptus globulus	149.02	−37.58	3.28	trunk		0.71	0.94	Forrester et al. 2010b
Eucalyptus globulus	149.02	−37.58	3.28	trunk		0.71	0.94	Forrester et al. 2010b
Eucalyptus globulus	149.02	−37.58	3.28	trunk		0.71	0.94	Forrester et al. 2010b
Eucalyptus grandis	152.60	−27.08	4.33	trunk	4.40	0.43	0.44	Kalma et al. 1998
Eucalyptus grandis	152.08	−26.00	4.44	trunk	11.93	0.35	0.33	Kalma et al. 1998
Aegiceras corniculatum	151.02	−33.07	2.99	branch		0.61	0.63	McClenahan et al. 2004
Aegiceras corniculatum	151.02	−33.07	3.20	branch		0.47	0.45	McClenahan et al. 2004
Angophora hispida	151.02	−33.07	2.86	branch		0.61	0.63	McClenahan et al. 2004
Angophora hispida	151.02	−33.07	3.60	branch		0.47	0.45	McClenahan et al. 2004
Angophora hispida	151.02	−34.02	3.19	branch		0.61	0.71	McClenahan et al. 2004
Angophora hispida	151.02	−34.02	3.69	branch		0.49	0.52	McClenahan et al. 2004
Avicennia marina	151.02	−33.07	2.97	branch		0.61	0.63	McClenahan et al. 2004
Avicennia marina	151.02	−33.07	3.21	branch		0.47	0.45	McClenahan et al. 2004
Banksia integrifolia	151.02	−33.07	3.09	branch		0.61	0.63	McClenahan et al. 2004
Banksia integrifolia	151.02	−33.07	3.29	branch		0.47	0.45	McClenahan et al. 2004
Banksia oblongifolia	151.02	−33.07	2.85	branch		0.61	0.63	McClenahan et al. 2004
Banksia oblongifolia	151.02	−33.07	3.22	branch		0.47	0.45	McClenahan et al. 2004
Banksia oblongifolia	151.02	−34.02	3.00	branch		0.61	0.71	McClenahan et al. 2004
Banksia oblongifolia	151.02	−34.02	3.14	branch		0.49	0.52	McClenahan et al. 2004
Cissus hypoglauca	151.02	−33.07	3.00	branch		0.61	0.63	McClenahan et al. 2004
Cissus hypoglauca	151.02	−33.07	3.41	branch		0.47	0.45	McClenahan et al. 2004
Eucalyptus haemostoma	151.02	−33.07	2.69	branch		0.61	0.63	McClenahan et al. 2004
Eucalyptus haemostoma	151.02	−33.07	3.49	branch		0.47	0.45	McClenahan et al. 2004
Glochidion ferdinandi	151.02	−33.07	3.46	branch		0.61	0.63	McClenahan et al. 2004
Glochidion ferdinandi	151.02	−33.07	3.46	branch		0.47	0.45	McClenahan et al. 2004
Persoonia lanceolata	151.02	−34.02	2.82	branch		0.61	0.71	McClenahan et al. 2004
Persoonia lanceolata	151.02	−34.02	3.27	branch		0.49	0.52	McClenahan et al. 2004

continued on next page

continued from previous page

Specie	Long	Lat	LA:SA	Sample	Height	Alpha	MI	References
Eucalyptus nitens	147.02	−43.30	4.37	trunk		0.88	1.49	Medhurst et al. 1999
Eucalyptus nitens	147.28	−41.02	4.76	trunk		0.65	0.85	Medhurst et al. 1999
Eucalyptus nitens	146.90	−43.35	4.40	trunk		0.92	1.92	Medhurst et al. 1999
Eucalyptus nitens	146.90	−43.35	4.31	trunk		0.92	1.92	Medhurst et al. 1999
Eucalyptus nitens	146.90	−43.35	4.66	trunk		0.92	1.92	Medhurst et al. 1999
Eucalyptus nitens	146.90	−43.35	4.42	trunk		0.92	1.92	Medhurst et al. 1999
Eucalyptus nitens	147.27	−41.20	4.55	trunk		0.77	1.30	Medhurst et al. 1999
Eucalyptus nitens	147.27	−41.20	4.46	trunk		0.73	1.10	Medhurst et al. 1999
Eucalyptus nitens	147.28	−41.02	3.54	trunk		0.65	0.85	Medhurst et al. 1999
Eucalyptus nitens	147.28	−41.02	3.69	trunk		0.65	0.85	Medhurst et al. 1999
Eucalyptus nitens	147.60	−42.82	4.11	trunk				Medhurst et al. 1999
Eucalyptus nitens	147.60	−42.82	3.66	trunk				Medhurst et al. 1999
Eucalyptus nitens	147.60	−42.82	4.39	trunk				Medhurst et al. 1999
Eucalyptus nitens	147.60	−42.82	3.86	trunk				Medhurst et al. 1999
Eucalyptus nitens	148.10	−41.08	3.69	trunk		0.72	0.74	Medhust and Beadle 2002
Eucalyptus nitens	148.10	−41.08	3.53	trunk		0.72	0.74	Medhust and Beadle 2002
Eucalyptus nitens	148.10	−41.08	3.59	branch		0.72	0.74	Medhust and Beadle 2002
Eucalyptus nitens	148.10	−41.08	3.74	branch		0.72	0.74	Medhust and Beadle 2002
Eucalyptus nitens	148.10	−41.08	3.77	branch		0.72	0.74	Medhust and Beadle 2002
Eucalyptus delegatensis	148.05	−35.70	3.60	trunk	20.57	0.70	0.96	Mokany et al. 2003
Eucalyptus delegatensis	148.05	−35.70	3.58	trunk	15.74	0.70	0.96	Mokany et al. 2003
Eucalyptus camaldulensis	145.00	−36.42	3.52	trunk		0.29	0.26	Morris and Collopy 1999
Eucalyptus camaldulensis	145.00	−36.42	3.58	trunk		0.29	0.26	Morris and Collopy 1999
Acacia aneura	133.85	−21.90	3.19	branch		0.12	0.16	O'Grady et al. 2009
Acacia aneura	133.85	−21.90	2.84	branch		0.12	0.16	O'Grady et al. 2009
Acacia aneura	133.32	−22.03	3.23	branch		0.16	0.20	O'Grady et al. 2009
Acacia aneura	133.32	−22.03	3.01	branch		0.16	0.20	O'Grady et al. 2009
Corymbia opaca	133.85	−21.90	3.92	branch		0.12	0.16	O'Grady et al. 2009
Corymbia opaca	133.85	−21.90	3.46	branch		0.12	0.16	O'Grady et al. 2009
Eucalyptus camaldulensis	133.32	−22.03	3.66	branch		0.16	0.20	O'Grady et al. 2009
Eucalyptus camaldulensis	133.32	−22.03	3.54	branch		0.16	0.20	O'Grady et al. 2009
Eucalyptus victrix	133.85	−21.90	3.72	branch		0.12	0.16	O'Grady et al. 2009
Eucalyptus victrix	133.85	−21.90	3.59	branch		0.12	0.16	O'Grady et al. 2009
Eucalyptus nitens	146.12	−41.30	3.56	trunk		0.83	1.12	Pinkard and Neilsen 2003
Eucalyptus nitens	146.12	−41.30	3.41	trunk		0.83	1.12	Pinkard and Neilsen 2003
Eucalyptus miniata	130.88	−12.42	3.53	branch		0.52	1.15	Prior and Eamus 2000
Eucalyptus miniata	130.88	−12.42	3.46	branch		0.52	1.15	Prior and Eamus 2000
Eucalyptus tetrodonta	130.88	−12.42	3.77	branch		0.51	0.80	Prior and Eamus 2000
Eucalyptus tetrodonta	130.88	−12.42	3.76	branch		0.52	1.15	Prior and Eamus 2000
Eucalyptus tetrodonta	130.88	−12.42	3.79	branch		0.52	1.15	Prior and Eamus 2000
Eucalyptus sieberi	149.58	−37.48	4.02	trunk		0.61	0.64	Roberts et al. 2001
Eucalyptus sieberi	149.58	−37.48	3.68	trunk		0.61	0.64	Roberts et al. 2001
Eucalyptus sieberi	149.58	−37.48	3.57	trunk		0.61	0.64	Roberts et al. 2001
Eucalyptus sieberi	149.58	−37.48	3.14	trunk		0.61	0.64	Roberts et al. 2001
Eucalyptus sieberi	149.58	−37.48	4.15	trunk		0.61	0.64	Roberts et al. 2001
Eucalyptus sieberi	149.58	−37.48	3.90	trunk		0.61	0.64	Roberts et al. 2001
Eucalyptus sieberi	149.58	−37.48	3.51	trunk		0.61	0.64	Roberts et al. 2001
Angophora bakeri	150.78	−33.66	3.66	branch		0.38	0.37	Taylor and Eamus 2008
Angophora costata	151.32	−33.19	3.68	branch		0.61	0.64	Taylor and Eamus 2008
Angophora hispida	151.06	−34.10	3.90	branch		0.48	0.56	Taylor and Eamus 2008
Callitris glaucophylla	146.93	−32.81	3.27	branch		0.16	0.15	Taylor and Eamus 2008
Eucalyptus haemostoma	151.06	−34.10	3.82	branch		0.48	0.56	Taylor and Eamus 2008
Eucalyptus haemostoma	151.32	−33.19	3.82	branch		0.61	0.64	Taylor and Eamus 2008
Eucalyptus populnea	146.93	−32.81	3.62	branch		0.16	0.15	Taylor and Eamus 2008
Eucalyptus sclerophylla	150.78	−33.66	3.76	branch		0.38	0.37	Taylor and Eamus 2008
Pinus radiata	145.43	−37.78	3.38	trunk	23.98	0.77	0.82	Teskey and Sheriff 1996
Acacia dealbata	145.63	−37.57	3.26	trunk		0.85	1.68	Vertessy et al. 1995
Eucalyptus regnans	145.63	−37.57	3.43	trunk		0.85	1.68	Vertessy et al. 1995
Eucalyptus regnans	145.63	−37.57	3.61	trunk	65.00	0.78	1.50	Vertessy et al. 1997
Eucalyptus regnans	145.63	−37.57	3.58	trunk	55.23	0.78	1.50	Vertessy et al. 1997
Eucalyptus regnans	145.63	−37.57	3.29	trunk		0.69	0.74	Vertessy et al. 2001
Pomaderris aspera	145.63	−37.57	3.57	trunk		0.69	0.74	Vertessy et al. 2001
Acacia colletioides	146.15	−32.97	2.15	branch		0.33	0.38	Westoby and Wright 2003
Acacia havilandii	146.15	−32.97	2.43	branch		0.33	0.38	Westoby and Wright 2003
Acacia wilhelmiana	146.15	−32.97	2.48	branch		0.33	0.38	Westoby and Wright 2003

continued on next page

continued from previous page

Specie	Long	Lat	LA:SA	Sample	Height	Alpha	MI	References
Bertya cunninghamii	146.15	−32.97	2.22	branch		0.33	0.38	Westoby and Wright 2003
Beyeria opaca	146.15	−32.97	2.54	branch		0.33	0.38	Westoby and Wright 2003
Cassinia laevis	146.15	−32.97	2.85	branch		0.33	0.38	Westoby and Wright 2003
Eremophila deserti	146.15	−32.97	3.10	branch		0.33	0.38	Westoby and Wright 2003
Eucalyptus dumosa	146.15	−32.97	3.25	branch		0.33	0.38	Westoby and Wright 2003
Eucalyptus socialis	146.15	−32.97	3.22	branch		0.33	0.38	Westoby and Wright 2003
Eutaxia microphylla	146.15	−32.97	2.42	branch		0.33	0.38	Westoby and Wright 2003
Olearia oswaldii	146.15	−32.97	2.59	branch		0.33	0.38	Westoby and Wright 2003
Olearia pimelioides	146.15	−32.97	2.56	branch		0.33	0.38	Westoby and Wright 2003
Philotheca difformis	146.15	−32.97	2.09	branch		0.33	0.38	Westoby and Wright 2003
Santalum acuminatum	146.15	−32.97	2.88	branch		0.33	0.38	Westoby and Wright 2003
Acacia myrtifolia	151.14	−33.69	3.02	branch		0.75	1.09	Westoby and Wright 2003
Acacia suaveolens	151.14	−33.69	3.06	branch		0.75	1.09	Westoby and Wright 2003
Angophora hispida	151.14	−33.69	3.30	branch		0.75	1.09	Westoby and Wright 2003
Baeckea brevifolia	151.14	−33.69	2.30	branch		0.75	1.09	Westoby and Wright 2003
Banksia oblongifolia	151.14	−33.69	3.20	branch		0.75	1.09	Westoby and Wright 2003
Banksia spinulosa	151.14	−33.69	3.21	branch		0.75	1.09	Westoby and Wright 2003
Boronia pinnata	151.14	−33.69	3.12	branch		0.75	1.09	Westoby and Wright 2003
Bossiaea obcordata	151.14	−33.69	2.70	branch		0.75	1.09	Westoby and Wright 2003
Corymbia gummifera	151.14	−33.69	3.26	branch		0.75	1.09	Westoby and Wright 2003
Dillwynia retorta	151.14	−33.69	3.02	branch		0.75	1.09	Westoby and Wright 2003
Epacris microphylla	151.14	−33.69	3.06	branch		0.75	1.09	Westoby and Wright 2003
Epacris pulchella	151.14	−33.69	2.74	branch		0.75	1.09	Westoby and Wright 2003
Eucalyptus capitellata	151.14	−33.69	3.42	branch		0.75	1.09	Westoby and Wright 2003
Eucalyptus haemostoma	151.14	−33.69	3.31	branch		0.75	1.09	Westoby and Wright 2003
Gompholobium glabratum	151.14	−33.69	2.72	branch		0.75	1.09	Westoby and Wright 2003
Grevillea speciosa	151.14	−33.69	2.95	branch		0.75	1.09	Westoby and Wright 2003
Hakea dactyloides	151.14	−33.69	3.26	branch		0.75	1.09	Westoby and Wright 2003
Hakea teretifolia	151.14	−33.69	2.84	branch		0.75	1.09	Westoby and Wright 2003
Hibbertia bracteata	151.14	−33.69	3.09	branch		0.75	1.09	Westoby and Wright 2003
Isopogon anemonifolius	151.14	−33.69	3.02	branch		0.75	1.09	Westoby and Wright 2003
Lambertia formosa	151.14	−33.69	2.89	branch		0.75	1.09	Westoby and Wright 2003
Leptospermum squarrosum	151.14	−33.69	3.00	branch		0.75	1.09	Westoby and Wright 2003
Leptospermum trinervium	151.14	−33.69	3.00	branch		0.75	1.09	Westoby and Wright 2003
Leucopogon esquamatus	151.14	−33.69	2.89	branch		0.75	1.09	Westoby and Wright 2003
Leucopogon microphyllus	151.14	−33.69	2.38	branch		0.75	1.09	Westoby and Wright 2003
Micrantheum ericoides	151.14	−33.69	3.06	branch		0.75	1.09	Westoby and Wright 2003
Persoonia levis	151.14	−33.69	3.42	branch		0.75	1.09	Westoby and Wright 2003
Persoonia pinifolia	151.14	−33.69	3.40	branch		0.75	1.09	Westoby and Wright 2003
Petrophile pulchella	151.14	−33.69	3.28	branch		0.75	1.09	Westoby and Wright 2003
Phyllanthus hirtellus	151.14	−33.69	2.48	branch		0.75	1.09	Westoby and Wright 2003
Phyllota phylicoides	151.14	−33.69	2.94	branch		0.75	1.09	Westoby and Wright 2003
Pultenaea elliptica	151.14	−33.69	3.36	branch		0.75	1.09	Westoby and Wright 2003
Pultenaea stipularis	151.14	−33.69	3.08	branch		0.75	1.09	Westoby and Wright 2003
Acacia doratoxylon	146.15	−32.97	3.60	branch		0.33	0.38	Westoby and Wright 2003
Brachychiton populneus	146.15	−32.97	3.18	branch		0.33	0.38	Westoby and Wright 2003
Dodonaea viscosa	146.15	−32.97	3.32	branch		0.33	0.38	Westoby and Wright 2003
Eremophila glabra	146.15	−32.97	2.89	branch		0.33	0.38	Westoby and Wright 2003
Eremophila longifolia	146.15	−32.97	3.21	branch		0.33	0.38	Westoby and Wright 2003
Eucalyptus intertexta	146.15	−32.97	3.24	branch		0.33	0.38	Westoby and Wright 2003
Geijera parviflora	146.15	−32.97	3.36	branch		0.33	0.38	Westoby and Wright 2003
Melaleuca uncinata	146.15	−32.97	2.63	branch		0.33	0.38	Westoby and Wright 2003
Philotheca difformis	146.15	−32.97	2.28	branch		0.33	0.38	Westoby and Wright 2003
Pimelea microcephala	146.15	−32.97	2.98	branch		0.33	0.38	Westoby and Wright 2003
Senna artemisioides	146.15	−32.97	2.93	branch		0.33	0.38	Westoby and Wright 2003
Eucalyptus globulus	147.60	−42.82	3.77	trunk				White et al. 1998
Eucalyptus globulus	147.60	−42.82	3.77	trunk				White et al. 1998
Eucalyptus globulus	147.60	−42.82	3.87	trunk				White et al. 1998
Eucalyptus globulus	147.60	−42.82	3.76	trunk				White et al. 1998
Eucalyptus globulus	147.60	−42.82	3.92	trunk				White et al. 1998
Eucalyptus globulus	147.60	−42.82	3.70	trunk				White et al. 1998
Eucalyptus nitens	147.60	−42.82	3.63	trunk				White et al. 1998
Eucalyptus nitens	147.60	−42.82	3.68	trunk				White et al. 1998
Eucalyptus nitens	147.60	−42.82	3.72	trunk				White et al. 1998
Eucalyptus nitens	147.60	−42.82	3.65	trunk				White et al. 1998

continued on next page

continued from previous page

Specie	Long	Lat	LA:SA	Sample	Height	Alpha	MI	References
Eucalyptus nitens	147.60	−42.82	3.86	trunk				White et al. 1998
Eucalyptus nitens	147.60	−42.82	3.65	trunk				White et al. 1998
Eucalyptus camaldulensis	145.93	−36.60	3.70	trunk		0.25	0.18	Yunusa et al. 2010
Eucalyptus camaldulensis	145.93	−36.60	4.20	trunk		0.25	0.18	Yunusa et al. 2010
Eucalyptus camaldulensis	145.93	−36.60	3.74	trunk		0.35	0.42	Yunusa et al. 2010
Eucalyptus camaldulensis	145.93	−36.60	4.12	trunk		0.35	0.42	Yunusa et al. 2010
Eucalyptus crebra	150.12	−31.08	3.22	trunk		0.24	0.18	Zeppel and Eamus 2008
Eucalyptus crebra	150.12	−31.08	3.22	trunk		0.33	0.35	Zeppel and Eamus 2008
Eucalyptus crebra	150.12	−31.08	3.40	trunk		0.39	0.48	Zeppel and Eamus 2008
Eucalyptus crebra	150.12	−31.08	2.94	trunk		0.24	0.18	Zeppel and Eamus 2008
Eucalyptus crebra	150.12	−31.08	3.15	trunk		0.33	0.35	Zeppel and Eamus 2008
Eucalyptus crebra	150.12	−31.08	3.35	trunk		0.39	0.48	Zeppel and Eamus 2008
Alphitonia whitei	145.63	−17.12	3.80	branch		0.76	1.36	This study
Alstonia muelleriana	145.63	−17.12	4.00	branch	19.00	0.76	1.36	This study
Argyrodedron trifoliolatum	145.63	−17.12	4.02	branch	19.00	0.76	1.36	This study
Cardwellia sublimis	145.63	−17.12	3.86	branch		0.76	1.36	This study
Ceratopelatum sucirubrum	145.63	−17.12	3.82	branch	14.00	0.76	1.36	This study
Cryptocarya mackinnoniana	145.63	−17.12	3.87	branch		0.76	1.36	This study
Doryphora aromatica	145.63	−17.12	3.54	branch	19.00	0.76	1.36	This study
Flindersia brayleyana	145.63	−17.12	3.83	branch		0.76	1.36	This study
Gillbeea adenopetala	145.63	−17.12	3.86	branch		0.76	1.36	This study
Syzygium johnsonii	145.63	−17.12	3.65	branch	13.00	0.76	1.36	This study
Eucalyptus globulus	147.50	−42.82	3.67	trunk				O'Glady et al. 2006
Eucalyptus globulus	147.50	−42.82	3.75	trunk				O'Glady et al. 2006
Eucalyptus globulus	147.50	−42.82	3.73	trunk				O'Glady et al. 2006
Eucalyptus globulus	147.50	−42.82	3.93	trunk				O'Glady et al. 2006
Eucalyptus nitens	146.68	−38.38	3.50	trunk		0.76	1.45	Forrester et al. 2012
Eucalyptus nitens	146.68	−38.38	3.54	trunk		0.76	1.45	Forrester et al. 2012
Eucalyptus nitens	146.68	−38.38	3.60	trunk		0.71	0.99	Forrester et al. 2012
Eucalyptus nitens	146.68	−38.38	3.58	trunk		0.71	0.99	Forrester et al. 2012
Eucalyptus nitens	146.68	−38.38	3.61	trunk		0.71	0.99	Forrester et al. 2012
Eucalyptus nitens	146.68	−38.38	3.61	trunk		0.71	0.99	Forrester et al. 2012
Eucalyptus nitens	146.68	−38.38	3.57	trunk		0.76	1.45	Forrester et al. 2012
Eucalyptus nitens	146.68	−38.38	3.63	trunk		0.76	1.45	Forrester et al. 2012
Eucalyptus nitens	146.68	−38.38	3.73	trunk		0.71	0.99	Forrester et al. 2012
Eucalyptus nitens	146.68	−38.38	3.71	trunk		0.71	0.99	Forrester et al. 2012
Eucalyptus nitens	146.68	−38.38	3.71	trunk		0.71	0.99	Forrester et al. 2012
Eucalyptus nitens	146.68	−38.38	3.69	trunk		0.71	0.99	Forrester et al. 2012
Eucalyptus nitens	146.68	−38.38	3.74	trunk		0.71	0.99	Forrester et al. 2012
Eucalyptus nitens	146.68	−38.38	3.72	trunk		0.71	0.99	Forrester et al. 2012
Eucalyptus nitens	146.68	−38.38	3.71	trunk		0.71	0.99	Forrester et al. 2012
Eucalyptus kochii	118.09	−34.60	3.27	trunk	2.23	0.82	0.82	Brooksbank et al. (submitted)
Eucalyptus loxophleba	118.09	−34.60	3.55	trunk	3.94	0.82	0.82	Brooksbank et al. (submitted)
Eucalyptus polybractea	118.09	−34.60	3.47	trunk	4.28	0.82	0.82	Brooksbank et al. (submitted)
Acacia colletioides	151.15	−33.38	2.15	branch	2.60	0.44	0.50	Pickup et al. 2005
Acacia havilandiorum	151.15	−33.38	2.43	branch	4.00	0.44	0.50	Pickup et al. 2005
Acacia wilhelmiana	151.15	−33.38	2.48	branch	2.30	0.44	0.50	Pickup et al. 2005
Bertya cunninghamii	151.15	−33.38	2.22	branch	2.10	0.44	0.50	Pickup et al. 2005
Beyeria opaca	151.15	−33.38	2.47	branch	0.70	0.44	0.50	Pickup et al. 2005
Cassinia laevis	151.15	−33.38	2.85	branch	2.40	0.44	0.50	Pickup et al. 2005
Eremophila deserti	151.15	−33.38	3.11	branch	1.20	0.44	0.50	Pickup et al. 2005
Eucalyptus dumosa	151.15	−33.38	3.25	branch	6.00	0.44	0.50	Pickup et al. 2005
Eucalyptus socialis	151.15	−33.38	3.22	branch	8.30	0.44	0.50	Pickup et al. 2005
Eutaxia microphylla	151.15	−33.38	2.33	branch	0.70	0.44	0.50	Pickup et al. 2005
Olearia decurrens	151.15	−33.38	2.61	branch	1.80	0.44	0.50	Pickup et al. 2005
Olearia pimelioides	151.15	−33.38	2.54	branch	1.20	0.44	0.50	Pickup et al. 2005
Philotheca difformis	151.15	−33.38	2.13	branch	1.80	0.44	0.50	Pickup et al. 2005
Santalum acuminatum	151.15	−33.38	2.87	branch	6.00	0.44	0.50	Pickup et al. 2005
Acacia doratoxylon	151.32	−33.38	3.59	branch	12.00	0.72	0.87	Pickup et al. 2005
Brachychiton populneus	151.32	−33.38	3.19	branch	8.30	0.72	0.87	Pickup et al. 2005
Dodonaea viscosa	151.32	−33.38	3.30	branch	4.00	0.72	0.87	Pickup et al. 2005
Eremophila glabra	151.32	−33.38	2.90	branch	1.90	0.72	0.87	Pickup et al. 2005
Eremophila longifolia	151.32	−33.38	3.21	branch	3.50	0.72	0.87	Pickup et al. 2005
Eucalyptus intertexta	151.32	−33.38	3.24	branch	16.90	0.72	0.87	Pickup et al. 2005
Geijera parviflora	151.32	−33.38	3.36	branch	10.30	0.72	0.87	Pickup et al. 2005

continued on next page

continued from previous page

Specie	Long	Lat	LA:SA	Sample	Height	Alpha	MI	References
Melaleuca uncinata	151.32	−33.38	2.62	branch	6.50	0.72	0.87	Pickup et al. 2005
Philotheca difformis	151.32	−33.38	2.26	branch	2.00	0.72	0.87	Pickup et al. 2005
Pimelea microcephala	151.32	−33.38	2.97	branch	3.00	0.72	0.87	Pickup et al. 2005
Senna artemisioides	151.32	−33.38	2.94	branch	2.70	0.72	0.87	Pickup et al. 2005
Acacia floribunda	151.29	−33.58	3.96	branch		0.59	0.56	Zanne (2007, unpublished)
Astrotricha floccosa	151.29	−33.58	3.78	branch		0.59	0.56	Zanne (2007, unpublished)
Lasiopetalum ferrugineum	151.29	−33.58	3.39	branch		0.59	0.56	Zanne (2007, unpublished)
Lomatia silaifolia	151.29	−33.58	3.63	branch		0.59	0.56	Zanne (2007, unpublished)
Persoonia linearis	151.29	−33.58	3.73	branch		0.59	0.56	Zanne (2007, unpublished)
Pultenea flexilis	151.29	−33.58	3.74	branch		0.59	0.56	Zanne (2007, unpublished)
Synoum glandulosum	151.29	−33.58	3.56	branch		0.59	0.56	Zanne (2007, unpublished)
Syncarpia glomulifera	151.29	−33.58	3.80	branch		0.59	0.56	Zanne (2007, unpublished)
Acacia suaveolens	151.14	−33.69	3.25	branch		0.59	0.62	Zanne (2007, unpublished)
Boronia ledifolia	151.14	−33.69	3.07	branch		0.59	0.62	Zanne (2007, unpublished)
Eriostemon australasius	151.14	−33.69	3.36	branch		0.59	0.62	Zanne (2007, unpublished)
Hakea dactyloides	151.14	−33.69	3.51	branch		0.59	0.62	Zanne (2007, unpublished)
Lambertia formosa	151.14	−33.69	3.63	branch		0.59	0.62	Zanne (2007, unpublished)
Leptospermum trinervium	151.14	−33.69	3.73	branch		0.59	0.62	Zanne (2007, unpublished)
Persoonia levis	151.14	−33.69	3.60	branch		0.59	0.62	Zanne (2007, unpublished)
Phyllota phylicoides	151.14	−33.69	3.12	branch		0.59	0.62	Zanne (2007, unpublished)
Acacia havilandiorum	146.15	−32.97	2.76	branch		0.18	0.22	Zanne (2007, unpublished)
Brachychiton populneus	146.15	−32.97	3.95	branch		0.18	0.22	Zanne (2007, unpublished)
Dodonaea viscosa	146.15	−32.97	3.45	branch		0.18	0.22	Zanne (2007, unpublished)
Eremophila longifolia	146.15	−32.97	3.55	branch		0.18	0.22	Zanne (2007, unpublished)
Geijera parviflora	146.15	−32.97	3.32	branch		0.18	0.22	Zanne (2007, unpublished)
Hakea tephrosperma	146.15	−32.97	3.28	branch		0.18	0.22	Zanne (2007, unpublished)
Philotheca difformis	146.15	−32.97	3.39	branch		0.18	0.22	Zanne (2007, unpublished)
Senna artemisioides	146.15	−32.97	3.27	branch		0.18	0.22	Zanne (2007, unpublished)
Acacia doratoxylon	146.15	−32.98	3.62	branch		0.18	0.22	Zanne (2007, unpublished)
Bertya cunninghamii	146.15	−32.98	3.28	branch		0.18	0.22	Zanne (2007, unpublished)
Beyeria opaca	146.15	−32.98	3.10	branch		0.18	0.22	Zanne (2007, unpublished)
Cassinia laevis	146.15	−32.98	3.19	branch		0.18	0.22	Zanne (2007, unpublished)
Eremophila glabra	146.15	−32.98	3.04	branch		0.18	0.22	Zanne (2007, unpublished)
Eucalyptus socialis	146.15	−32.98	3.47	branch		0.18	0.22	Zanne (2007, unpublished)
Melaleuca uncinata	146.15	−32.98	3.11	branch		0.18	0.22	Zanne (2007, unpublished)
Olearia pimelioides	146.15	−32.98	3.06	branch		0.18	0.22	Zanne (2007, unpublished)
Eucalyptus globulus	147.68	−41.78	3.29	trunk		0.50	0.47	Feikema et al. 2010
Eucalyptus globulus	147.68	−41.78	3.25	trunk		0.56	0.77	Feikema et al. 2010
Eucalyptus globulus	143.58	−38.87	3.43	trunk				Feikema et al. 2010
Eucalyptus globulus	144.60	−38.58	3.54	trunk				Feikema et al. 2010
Eucalyptus globulus	148.32	−38.30	3.39	trunk				Feikema et al. 2010
Eucalyptus globulus	147.12	−37.28	3.43	trunk		0.70	1.00	Feikema et al. 2010
Eucalyptus globulus	144.48	−37.57	3.59	trunk				Feikema et al. 2010
Eucalyptus nitens	147.68	−41.78	3.23	trunk		0.50	0.47	Feikema et al. 2010
Eucalyptus nitens	147.68	−41.78	3.24	trunk		0.56	0.77	Feikema et al. 2010
Eucalyptus nitens	143.58	−38.87	3.37	trunk				Feikema et al. 2010
Eucalyptus nitens	148.32	−38.30	3.35	trunk				Feikema et al. 2010
Eucalyptus nitens	149.38	−37.38	3.51	trunk		0.63	0.62	Feikema et al. 2010
Eucalyptus nitens	147.12	−37.28	3.44	trunk		0.70	1.00	Feikema et al. 2010

Data S2. List of published literature for data compilation

Barrett, D. J, Hatton, T. J, Ash, J. E, and Ball, M. C. Transpiration by trees from contrasting forest types. *Australian Journal of Botany*, 44(3):249–263, 1996.

Benyon, R. G, Marcar, N. E, Crawford, D. F, and Nicholson, A. T. Growth and water use of eucalyptus camaldulensis and e. occidentalis on a saline discharge site near wellington, nsw, australia. *Agricultural Water Management*, 39(2–3):229–244, 1999.

Bleby, T. M, Colquhoun, I. J, and Adams, M. A. Architectural plasticity in young eucalyptus marginata on restored bauxite mines and adjacent natural forest in south-western australia. *Tree Physiology*, 29(8):1033–1045, 2009.

Brodribb, T. J and Feild, T. S. Stem hydraulic supply is linked to leaf photosynthetic capacity: evidence from new caledonian and tasmanian rainforests. *Plant Cell & Environment*, 23(12):1381–1388, 2000.

Brooksbank, K, Veneklaas, E. J, White, D. A, and Carter, J. L. Water availability determines hydrological impact of tree belts in dryland cropping systems. *Agricultural Water Management*, 100(1):76–83, 2011.

Canham, C. A, Froend, R. H, and Stock, W. D. Water stress vulnerability of four banksia species in contrasting ecohydrological habitats on the gnangara mound, western australia. *Plant Cell & Environment*, 32(1):64–72, 2009. Canham, Caroline A Froend, Raymond H Stock, William D Plant Cell Environ. 2009 Jan;32(1):64-72. Epub 2008 Nov 10.

Carter, J. L and White, D. A. Plasticity in the huber value contributes to homeostasis in leaf water relations of a mallee eucalypt with variation to groundwater depth. *Tree Physiology*, 29(11):1407–18, 2009. Carter, Jennifer L White, Donald A Canada Tree Physiol. 2009 Nov;29(11):1407-18. Epub 2009 Sep 28.

Cernusak, L. A, Hutley, L. B, Beringer, J, and Tapper, N. J. Stem and leaf gas exchange and their responses to fire in a north australian tropical savanna. *Plant Cell & Environment*, 29(4):632–646, 2006.

Choat, B, Ball, M. C, Luly, J. G, and Holtum, J. A. M. Hydraulic architecture of deciduous and evergreen dry rainforest tree species from north-eastern australia. *Trees - Structure and Function*, 19(3):305–311, 2005.

Drake, P. L and Franks, P. J. Water resource partitioning, stem xylem hydraulic properties, and plant water use strategies in a seasonally dry riparian tropical rainforest. *Oecologia*, 137(3):321–329, 2003.

Drake, P. L, Froend, R. H, and Franks, P. J. Linking hydraulic conductivity and photosynthesis to water-source partitioning in trees versus seedlings. *Tree Physiology*, 31(7):763–773, 2011.

Eldridge, S, Thorburn, P, McEwan, K, and T.J., H. Health and structure of eucalyptus communities on chowilla and monoman islands of the river murray floodplain, south australia. *Divisional report (CSIRO. Division of Water Resources)*: 20–21, 1993.

Feikema, P. M, Morris, J. D, Beverly, C. R, Collopy, J. J, Baker, T. G, and Lane, P. N. J. Validation of plantation transpiration in south-eastern australia estimated

using the 3pg+ forest growth model. *Forest Ecology and Management*, 260(5):663–678, 2010.

Forrester, D. I, Collopy, J. J, and Morris, J. D. Transpiration along an age series of eucalyptus globulus plantations in southeastern australia. *Forest Ecology and Management*, 259(9):1754–1760, 2010a.

Forrester, D. I, Theiveyanathan, S, Collopy, J. J, and Marcar, N. E. Enhanced water use efficiency in a mixed eucalyptus globulus and acacia mearnsii plantation. *Forest Ecology and Management*, 259(9):1761–1770, 2010b.

Forrester, D. I, Collopy, J. J, Beadle, C. L, and Baker, T. G. Interactive effects of simultaneously applied thinning, pruning and fertiliser application treatments on growth, biomass production and crown architecture in a young eucalyptus nitens plantation. *Forest Ecology and Management*, 267(0):104–116, 2012.

Kalma, S. J, Thorburn, P. J, and Dunn, G. M. A comparison of heat pulse and deuterium tracing techniques for estimating sap flow in eucalyptus grandis trees. *Tree Physiology*, 18(10):697–705, 1998.

McClenahan, K, Macinnis-Ng, C, and Eamus, D. Hydraulic architecture and water relations of several species at diverse sites around sydney. *Australian Journal of Botany*, 52(4):509–518, 2004.

Medhurst, J. L, Battaglia, M, Cherry, M. L, Hunt, M. A, White, D. A, and Beadle, C. L. Allometric relationships for eucalyptus nitens (deane and maiden) maiden plantations. *Trees - Structure and Function*, 14(2):91–101, 1999.

Medhurst, J. L, Battaglia, M, and Beadle, C. L. Measured and predicted changes in tree and stand water use following high-intensity thinning of an 8-year-old eucalyptus nitens plantation. *Tree Physiology*, 22(11):775–784, 2002.

Mokany, K, McMurtrie, R. E, Atwell, B. J, and Keith, H. Interaction between sapwood and foliage area in alpine ash (eucalyptus delegatensis) trees of different heights. *Tree Physiology*, 23(14):949–958, 2003.

Morris, J. D and Collopy, J. J. Water use and salt accumulation by eucalyptus camaldulensis and casuarina cunninghamiana on a site with shallow saline groundwater. *Agricultural Water Management*, 39(2–3):205–227, 1999.

O'Grady, A, Cook, P, Eamus, D, Duguid, A, Wischusen, J, Fass, T, and Worldege, D. Convergence of tree water use within an arid-zone woodland. *Oecologia*, 160(4): 643–655, 2009.

O'Grady, A. P, Worledge, D, and Battaglia, M. Above- and below-ground relationships, with particular reference to fine roots, in a young eucalyptus globulus (labill.) stand in southern tasmania. *Trees*, 20(5):531–538, 2006.

Pickup, M, Westoby, M, and Basden, A. Dry mass costs of deploying leaf area in relation to leaf size. *Functional Ecology*, 19(1):88–97, 2005.

Pinkard, E. A and Neilsen, W. A. Crown and stand characteristics of eucalyptus nitens in response to initial spacing: implications for thinning. *Forest Ecology and Management*, 172(2–3):215–227, 2003.

Prior, L. D and Eamus, D. Seasonal changes in hydraulic conductance, xylem embolism and leaf area in eucalyptus tetrodonta and eucalyptus miniata saplings in a north australian savanna. *Plant Cell & Environment*, 23(9):955–965, 2000.

Roberts, S, Vertessy, R, and Grayson, R. Transpiration from eucalyptus sieberi (l. johnson) forests of different age. *Forest Ecology and Management*, 143(1–3):153–161, 2001.

Taylor, D and Eamus, D. Coordinating leaf functional traits with branch hydraulic conductivity: resource substitution and implications for carbon gain. *Tree Physiology*, 28(8):1169–1177, 2008.

Teskey, R. O and Sheriff, D. W. Water use by pinus radiata trees in a plantation. *Tree Physiology*, 16(1-2):273–279, 1996.

Vertessy, R. A, Benyon, R. G, O'Sullivan, S. K, and Gribben, P. R. Relationships between stem diameter, sapwood area, leaf area and transpiration in a young mountain ash forest. *Tree Physiology*, 15(9):559–567, 1995.

Vertessy, R. A, Hatton, T. J, Reece, P, O'Sullivan, S. K, and Benyon, R. G. Estimating stand water use of large mountain ash trees and validation of the sap flow measurement technique. *Tree Physiology*, 17(12):747–756, 1997.

Vertessy, R. A, Watson, F. G. R, and OSullivan, S. K. Factors determining relations between stand age and catchment water balance in mountain ash forests. *Forest Ecology and Management*, 143(1–3):13–26, 2001.

Westoby, M and Wright, I. J. The leaf size - twig size spectrum and its relationship to other important spectra of variation among species. *Oecologia*, 135(4):621–628, 2003.

White, D, Beadle, C, Worledge, D, Honeysett, J, and Cherry, M. The influence of drought on the relationship between leaf and conducting sapwood area in *eucalyptus globulus* and *eucalyptus nitens*. *Trees - Structure and Function*, 12(7):406–414, 1998.

Yunusa, I. A. M, Aumann, C. D, Rab, M. A, Merrick, N, Fisher, P. D, Eberbach, P. L, and Eamus, D. Topographical and seasonal trends in transpiration by two co-occurring eucalyptus species during two contrasting years in a low rainfall environment. *Agricultural and Forest Meteorology*, 150(9):1234–1244, 2010.

Zeppel, M and Eamus, D. Coordination of leaf area, sapwood area and canopy conductance leads to species convergence of tree water use in a remnant evergreen woodland. *Australian Journal of Botany*, 56(2):97–108, 2008.

3

Thermal acclimation of leaf photosynthetic traits in an evergreen woodland, consistent with the coordination hypothesis

Henrique Furstenau Togashi[1,2,7], Iain Colin Prentice[1,2,3], Owen K. Atkin[4,5], Craig Macfarlane[6], Suzanne M. Prober[6], Keith J. Bloomfield[4], Bradley John Evans[1,2]

[1]Department of Biological Sciences, Macquarie University 2109, Sydney, NSW, Australia
[2]Terrestrial Ecosystem Research Network Ecosystem Modelling and Scaling Infrastructure, Macquarie University 2109 and University of Sydney 2006, NSW, Australia
[3]AXA Chair of Biosphere and Climate Impacts, Grand Challenges in Ecosystems and the Environment and Grantham Institute, Climate Change and the Environment, Department of Life Sciences, Imperial College London, Silwood Park Campus, Buckhurst Road, Ascot SL5 7PY, UK
[4]Division of Plant Sciences, Research School of Biology, Australian National University, Canberra, Australia
[5]ARC Centre of Excellence in Plant Energy Biology, Research School of Biology, Australian National University, Canberra, Australia
[6]CSIRO Land and Water Flagship, Private Bag 5, Wembley WA 6913, Australia

This chapter has been submitted to *Functional Plant Ecology*

3.1 Summary

Ecosystem models commonly assume that key photosynthetic traits, such as carboxylation capacity measured at a standard temperature, are constant in time. The temperature responses of modelled photosynthetic/respiratory rates then depend entirely on enzyme kinetics. Optimality considerations suggest this assumption may be incorrect. The 'coordination hypothesis' (that Rubisco- and electron-transport limited rates of photosynthesis are co-limiting under typical daytime conditions) predicts instead that carboxylation (V_{cmax}) and light-harvesting (J_{max}) capacities, and mitochondrial respiration in the dark (R_{dark}), should acclimate so that they increase with growth temperature - but less steeply than their instantaneous response rates. To explore this hypothesis, photosynthetic measurements were carried out on woody species during the warm and the cool seasons in the semi-arid Great Western Woodlands, Australia, under broadly similar light environments. A consistent linear relationship between V_{cmax} and J_{max} was found across species. V_{cmax}, J_{max} and R_{dark} increased with temperature, but values standardized to 25°C declined. The c_i:c_a ratio increased slightly with temperature. The leaf N:P ratio was lower in the warm season. The slopes of the relationships of log-transformed V_{cmax} and J_{max} to temperature were close to values predicted by the coordination hypothesis, but shallower than those predicted by enzyme kinetics.

3.2 Introduction

Net photosynthetic CO_2 uptake (A_{net}) depends on temperature in all vegetation models, but models commonly disregard possible acclimation of the parameters determining A_{net} to temporal variations in the growth environment. There are plentiful data on the instantaneous (minutes to hours) temperature responses of photosynthetic uptake (Hikosaka *et al.*, 2006; Sage and Kubien, 2007; Way and Sage, 2008), but data on the responses of photosynthetic traits on ecologically relevant time scales (days to years) are scarce (Lin *et al.*, 2013). Nonetheless there is evidence that temperature responses of biochemical processes are a function of plant growth temperature, and not just instantaneous temperature: from studies comparing species (Miyazawa and Kikuzawa, 2006; Kattge *et al.*, 2007) and experiments or serial measurements on single species (Medlyn *et al.*, 2002a; Onoda *et al.*, 2005). Neglecting acclimation to the growth temperature could lead to incorrect model estimates of the responses of primary production and ecosystem carbon budgets to climate change.

Farquhar *et al.* (1980) provided the standard model to predict photosynthetic responses to environment in C3 plants. The model describes photosynthesis as instantaneously determined by the slower of two biochemical rates: the carboxylation of RuBP (ribulose-1,5-bisphosphate), dependent on Rubisco (ribulose-1,5-bisphosphate carboxylase/oxygenase) activity (V_{cmax}); and electron transport for RuBP regeneration in the Calvin cycle, dependent on light intensity and the capacity of the electron transport chain (J_{max}). Both rates are influenced by intercellular CO_2 concentration (c_i), which in turn is partially regulated by stomatal conductance (g_s). Unlimited mesophyll conductance (Miyazawa and Kikuzawa, 2006; Lin *et al.*, 2013) remains the standard implementation of the Farquhar model although it is recognized to be an approximation that results in an overestimation of V_{cmax} and J_{max}, hence the values estimated are 'apparent' V_{cmax} and J_{max}. These are highly variable both within and between species (Wullschleger, 1993), ranging through two to three orders of magnitude. Despite acceptance of the importance of these parameters for predicting rates of net CO_2 exchange in natural ecosystems, a full understanding of how seasonal changes in the environment affect these parameters remains elusive.

The 'coordination hypothesis' (Field and Mooney, 1986; Chen *et al.*, 1993; Maire *et al.*, 2012) predicts that values of V_{cmax} and J_{max} should acclimate, in time as well as in space, in such a way that carboxylation and RuBP regeneration are co-limiting under typical daytime conditions. This hypothesis makes a number of testable predictions regarding photosynthetic properties of trees experiencing large seasonal variations in growth temperature, including an increase in V_{cmax} with rising growth temperature - because at higher daily temperatures, greater Rubisco activity is required to match any given rate of photosynthesis. On the other hand, the hypothesis predicts that values of V_{cmax} and J_{max} normalized to 25°C - and also the leaf N per unit area (Maire *et al.*, 2012) - should decline with increasing daily average temperature, as the quantities of proteins needed to maintain a given level of photosynthetic activity decline more steeply with temperature than the predicted increases in V_{cmax} and J_{max}. R_{dark} is also expected to acclimate to temperature, and this can take place on a daily time scale (Atkin *et al.*, 2000). A recent data synthesis (Atkin *et al.*, 2015) showed that geographic variation in R_{dark} at growth temperature from the tropics to the tundra is much smaller than would be expected on the basis of enzyme kinetics.

Many models assume optimality criteria for stomatal behaviour, in which carbon assimilation is traded off against water loss. Prentice *et al.* (2014) provided field evidence supporting the 'least-cost' hypothesis, which states that plants adopt an optimal c_i:c_a ratio that minimizes the combined costs per unit carbon assimilation of main-

taining the capacities for carboxylation (V_{cmax}) and water transport. This hypothesis predicts, *inter alia*, that the c_i:c_a ratio should increase with the Michaelis-Menten coefficient for Rubisco-limited photosynthesis (K) and decrease with vapour pressure deficit (D). The c_i:c_a ratio is expected to increase with temperature, due to lower water viscosity (reducing water costs) and higher photorespiration (increasing carboxylation costs) (Prentice *et al.*, 2014), while declining with D (Prentice *et al.*, 2011) .

We present leaf-level measurements carried out during the warm and the cool seasons in the semi-arid environment of the Great Western Woodlands of southwestern Australia. By sampling towards the end of both seasons, we were able to compare observations under broadly overlapping light conditions but spanning a range of temperatures. We are not aware of any previous study that has tested whether seasonal temperature acclimation is consistent with the coordination hypothesis. We explore the idea by comparing the field-observed relationships of each trait to temperature with the theoretical acclimation of photosynthetic traits (as predicted by the coordination hypothesis) and with the alternative, i.e. the relationship of each trait to temperature to be expected if it were controlled only by enzyme kinetics (i.e. no acclimation).

3.3 Materials and methods

3.3.1 Site

Eight representative woody species were studied at the Great Western Woodlands SuperSite flux station (17°07' S, 145 °37' E) approximately 70 km north-west of Kalgoorlie. The area has a semi-arid climate and the vegetation is an intact mosaic of temperate woodland, shrubland and mallee. The mean annual rainfall (MAP) for 1970-2013 was 380 mm (Hutchinson, 2014c). The average rainfall is slightly higher during summer months, but this rain often falls during short periods as intense storms. Mean annual temperature (MAT) is 20°C Hutchinson (2014a,b). Mean monthly daily temperature minima range between 6°C and 18°C and maxima between 17°C and 35°C. Data for daily temperature and shortwave radiation were obtained from the flux tower (Australian and New Zealand Flux Research and Monitoring, www.ozflux.org.au). All trees were sampled within a 5 km radius from the tower. The species studied were the evergreen angiosperm trees *Eucalyptus clelandii*, *E. salmonophloia*, *E. salubris* and *E. transcontinentalis* and the shrub *Eremophila scoparia*; the nitrogen-fixing leguminous tree *Acacia aneura* and shrub *A. hemiteles*; and one gymnosperm tree (*Callitris columellaris*).

3.3.2 Gas exchange measurements

We measured 109 A-c_i curves altogether during the warm season (late March/early April) and the cool season (late August/early September). The same individual plants were sampled in both seasons. A portable infrared gas analyser (IRGA) system (LI-6400; Li-Cor, Inc., Lincoln, NB, USA) was used. Sunlit terminal branches from the top one-third of the canopy were collected and immediately re-cut under water (Domingues *et al.*, 2010). One of the youngest fully expanded leaves, attached to the branch, was sealed in the leaf chamber. Measurements in the field were taken with the chamber block temperature close to the air ambient temperature. The CO_2 mixing ratios for the A-c_i curves proceeded stepwise down from 400 to 35 and up to 2000 µmol mol^{-1}. Prior to the measurements, we tested plants to determine appropriate light-saturation levels. The photosynthetic photon flux density (PPFD) adopted for measurement ranged between 1500 and 1800 µmol m^{-2} s^{-1}. After measuring the A-c_i curves over about 35 minutes, light was set to zero for five minutes before measuring R_{dark}. Following Domingues *et al.* (2010), we discarded 23 A-c_i curves in which g_s declined to very low levels (i.e. resulting in 86 curves being used in further analyses), adversely affecting the calculation of V_{cmax}. TPU (triose phosphate utilization) limitation (Sharkey *et al.*, 2007) was not considered, as it would be unlikely to occur at our field temperatures of above 17°C. Data is published in Togashi *et al.* (2015). Reported ratios of c_i:c_a relate to chamber conditions of ambient $CO_2 \approx 400$ µmol mol^{-1}.

3.3.3 Photosynthetic parameters and their temperature responses

Apparent values of V_{cmax} and J_{max} were fitted using the Farquhar *et al.* (1980) model. Values were standardized to 25°C (V_{cmax25} and J_{max25}) using the in vivo temperature dependencies given in Bernacchi *et al.* (2001) and Bernacchi *et al.* (2003). Following Bernacchi *et al.* (2009), we used the Arrhenius equation to describe the temperature responses of V_{cmax}, and J_{max}:

$$parameter = parameter_{25}\, exp\left[\frac{(T_k - 298.15)\,\Delta H_a}{R'\,T_k\,298.15}\right] \quad (1)$$

where ΔH_a is the activation energy (J mol-1), R' is the universal gas constant (8.314 J mol^{-1} K^{-1}) and T_k is leaf temperature (K).

To derive R_{dark25} we applied a temperature-dependent Q_{10} (fractional change in respiration with a 10°C increase in temperature) equation in which Q_{10} declines with

increasing leaf temperature (Atkin and Tjoelker, 2003):

$$R_{dark25} = R_{dark}\left[3.09 - 0.043\left(\frac{T_2 + T_1}{2}\right)\right]^{\frac{T_2 - T_1}{10}} \quad (2)$$

where 3.09 and 0.04 are empirical values, T_2 (25°C) and T_1 are leaf temperatures (°C) for R_{dark25} and R_{dark} respectively.

3.3.4 Nutrient analyses

After completion of each A-c_i curve, leaves were retained to determine leaf area, dry mass, and mass-based nitrogen (N) and phosphorus (P) concentrations (mg g^{-1}). Leaves were sealed in plastic bags containing moist tissue paper to prevent wilting. Leaf area was determined using a 600 dots/inch flatbed top-illuminated optical scanner and Image J software (http://imagej.nih.gov/ij/). Leaves were dried in a portable desiccator for 48 hours, to be preserved until the end of the campaign. Subsequently, in the laboratory, leaves were oven-dried for 24 hours at 70°C and the dry weight determined (Mettler-Toledo Ltd, Port Melbourne, Victoria, Australia). Leaf mass per unit area (LMA; g m^{-2}) was calculated from leaf area and dry mass. N_{mass} and P_{mass} were obtained by Kjeldahl acid digestion of the same leaves (Allen *et al.*, 1974). The leaf material was digested using sulphuric acid 98% and hydrogen peroxide 30%. Digested material was analyzed for N and P using a flow injection analyser system (LaChat QuikChem 8500 Series 2, Lachat Instruments, Milwaukee, WI, USA). Area-based N and P values (mg m^{-2}) were calculated as products of LMA and N_{mass} or P_{mass}.

3.3.5 Statistical analyses

All statistics were performed in R (Team R Core, 2012). For graphing we used the ggplot2 package (Wickham, 2010). V_{cmax}, V_{cmax25}, J_{max}, J_{max25}, R_{dark}, R_{dark25}, N_{area} and P_{area} data were $\log_{10}$-transformed, unless otherwise indicated, to approximate a normal distribution of values. The ratio c_i:c_a was not transformed because of its small variance and approximately normal distribution in this study. Linear regression (*lm*) was used to test dependencies among parameters. Slopes and elevations of regressions were compared using standardized major axis regression with the smatr package (Warton *et al.*, 2006). The Welch two-sample *t-test* was used to test pairwise differences in traits (e.g. differences between the warm season and the cool season measurements). Generalized linear models (*glm*) were used to test acclimation to temperature across species, using species and temperature as predictors.

3.3.6 Predicted responses to temperature

Natural log-transformed V_{cmax}, J_{max} and R_{dark} were regressed against leaf temperature measured in field. All regressions were fitted across species, with species identity included as a predictor (*glm*) to control for species effects on parameter values at a given temperature. We compared the slopes of these regressions with theoretically derived values based on alternative hypotheses: (1) based on enzyme kinetics (without acclimation), and (2) based on the coordination hypothesis for V_{cmax}, J_{max} and R_{dark} and the least-cost hypothesis for c_i:c_a. The derivations are summarized in Appendix A. Although enzyme activation energy (ΔH_a) can vary among species and with temperature (Von Caemmerer, 2000), for simplicity we adopted the same ΔH_a for all species and temperatures. This approximation could affect interspecies comparisons of ΔH_a-dependent parameters but should not substantially interfere with the comparison of theoretical and fitted slopes.

3.4 Results

3.4.1 Relationships among photosynthetic parameters

When measured at near ambient air temperature, species-average V_{cmax} values ranged across seasons from 44.4 to 105 µmol m^{-2} s^{-1}, J_{max} from 77.4 to 160 µmol m^{-2} s^{-1}, R_{dark} from 1.16 to 3.14 µmol m^{-2} s^{-1} and c_i:c_a from 0.39 to 0.60 (at ambient $CO_2 \approx$ 400 µmol mol^{-1}). At the prevailing air temperatures, V_{cmax}, J_{max} and R_{dark} were systematically higher in the warm season, while their values normalised to 25°C were higher in the cool season (figure 3.1). The c_i:c_a ratio also exhibited significantly higher average values in the warm season in six out of eight species (not shown).

V_{cmax} and J_{max} were closely correlated across species within and across seasons (figure 3.2). The warm and the cool seasons equations relating V_{cmax} and J_{max} were statistically indistinguishable. The warm and the cool seasons slopes of regressions forced through the origin are shown in figure 3.2. Regressions between V_{cmax} and J_{max} for the warm and the cool seasons together yielded $J_{max} = 0.84\ V_{cmax} + 55.2$ ($p < 0.05$, slope standard error = 0.2). There were negative correlations between species-average of c_i:c_a ratios and R_{dark} *versus* both V_{cmax} and J_{max} across seasons (figure 3.3): $\log_{10} V_{cmax} = 0.26 \log_{10} R_{dark} + 1.70$ ($p < 0.05$, slope standard error = 0.08, R^2 = 0.18) and $\log_{10} J_{max} = 0.27 \log_{10} R_{dark} + 1.94$ ($p < 0.05$, slope standard error = 0.06, R^2 = 0.2); $\log_{10} V_{cmax} = -0.75\ c_i{:}c_a + 2.17$ ($p < 0.05$, slope standard error = 0.21, R^2

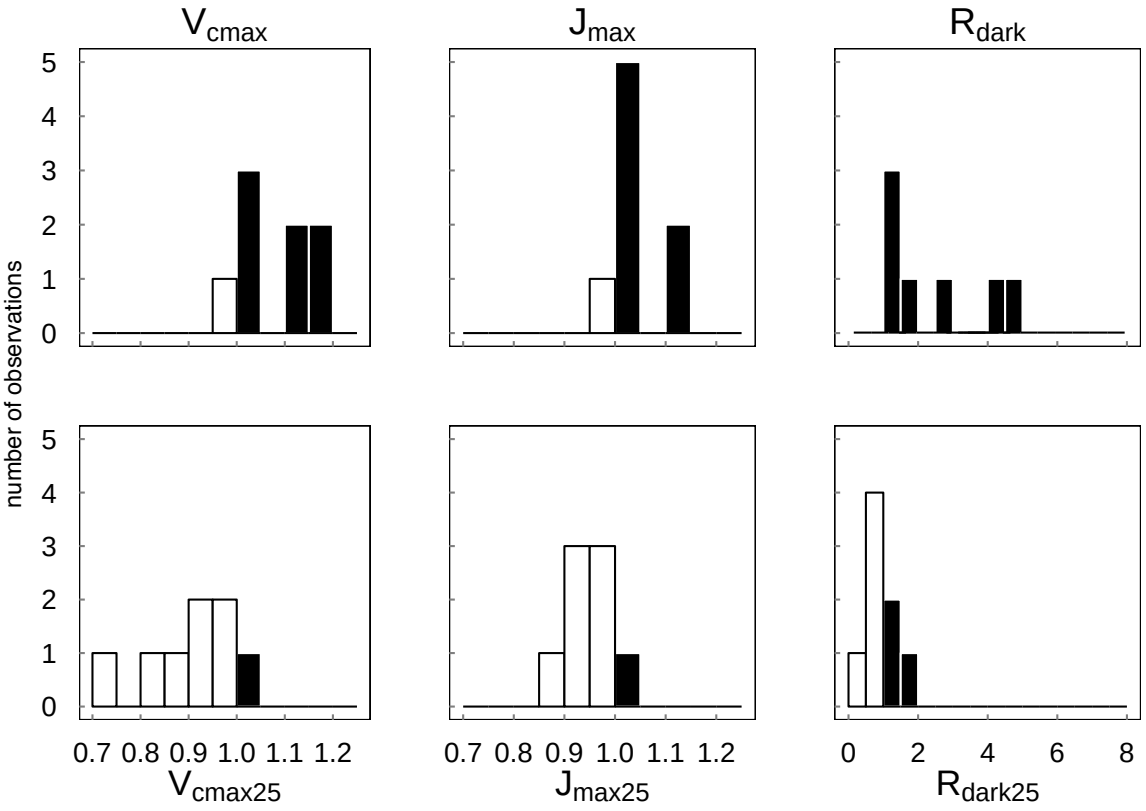

FIGURE 3.1: Species distribution warm:cool seasons ratios of $\log_{10}$-transformed V_{cmax}, J_{max} and R_{dark} as measured at ambient temperature (top panel) and standardized to 25°C (bottom panel). Ratios > 1 are shown as black bars, ratios < 1 as white bars (n = 8).

= 0.12) and $\log_{10} J_{max} = -0.31\ c_i{:}c_a + 2.18$ ($p < 0.05$, slope standard error = 0.16, R^2 = 0.13) For individual species, $\log_{10} V_{cmax}$ and $\log_{10} J_{max}$ were significantly related to $\log_{10} R_{dark}$ ($p < 0.05$) in *E. salmonophloia* and *C. columellaris*.

3.4.2 Photosynthetic trait responses to temperature

Based on data from all species together, V_{cmax}, J_{max} and R_{dark} all increased with leaf temperature, while the corresponding normalized (to 25 °C) values declined with leaf temperature ($p < 0.05$, figure 3.4). The $c_i{:}c_a$ ratio also increased slightly but significantly with leaf temperature, ($p < 0.05$, $R^2 = 0.05$; figure 3.5 left). The ratio $J_{max}{:}V_{cmax}$ did not correlate with temperature based on the data from all species together, but it was negatively correlated with temperature for *E. salmonophloia*, *E. scoparia* and *C. columellaris* (not shown). Excluding the two *N*-fixing species, and/or

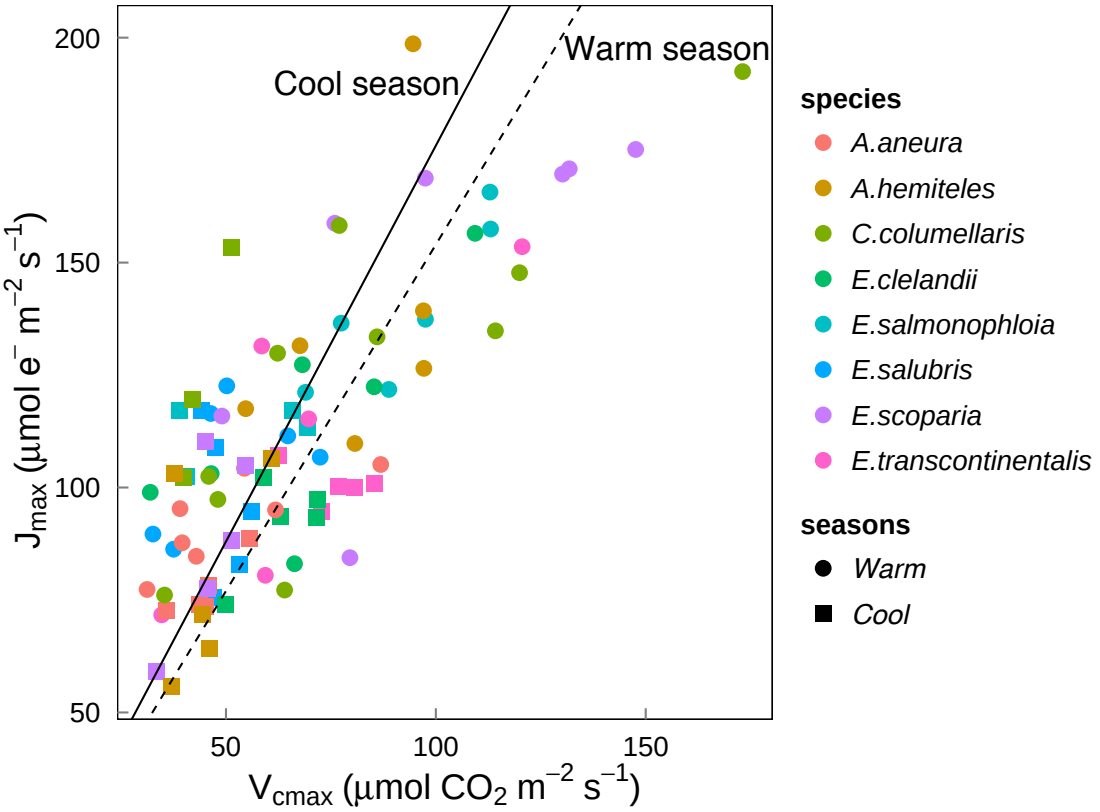

Figure 3.2: Linear regressions forced through the origin between J_{max} (µmol m^{-2} s^{-1}) and V_{cmax} (µmol m^{-2} s^{-1}) for individual trees of eight species in the warm season (circles, solid line, slope = 1.58, df = 51, R^2 = 0.65) and the cool season (squares, dashed line, slope = 1.79, df = 31, R^2 = 0.59). Both regressions are significant (p<0.05). Each point represents one A-c_i curve (n=86).

the one gymnosperm, from the dataset had no effect on these results.

The relationship between air temperature and leaf temperature was $T_{leaf} = 1.01\ T_{air}$ + 0.35 ($p < 0.05$, R2 = 0.96). Regression slopes between photosynthetic parameters and T_{air} showed no significant differences from those calculated using T_{leaf}, but the goodness of fit was weaker with T_{air} than with T_{leaf}. We also fitted regressions using T_{day} (the daily mean temperature). Again the slopes did not change, but the goodness of fit was further reduced. The factor 'season' (included as a predictor in a *glm*, in addition to T_{leaf}) did not improve model fit.

Within individual species, we also found positive responses of V_{cmax} and J_{max} to temperature, and negative responses when the parameters were corrected to 25°C (figure 3.6). The response of the c_i:c_a ratio to leaf temperature was similar in most species

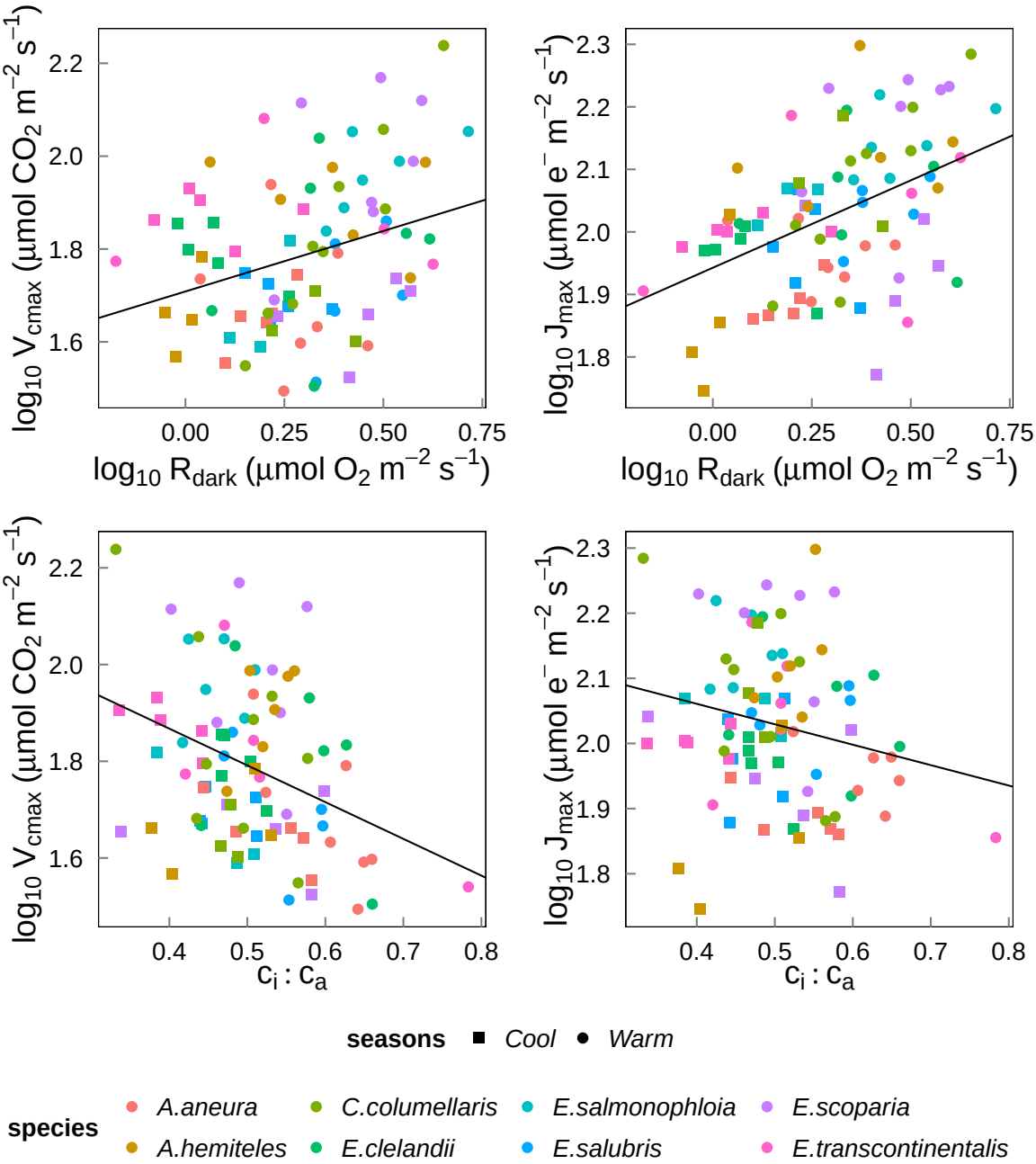

FIGURE 3.3: Linear regressions of individual trees by season (n=16) and species (n=8) for photosynthetic capacity, V_{cmax} and J_{max} with R_{dark} (µmol m^{-2} s^{-1}) and the c_i:c_a ratio at ambient $CO_2 \approx 400$ µmol mol^{-1} ($p < 0.05$). V_{cmax}, J_{max} and R_{dark} were $\log_{10}$ transformed; c_i:c_a was not. Each point represents one A-c_i curve (n=86).

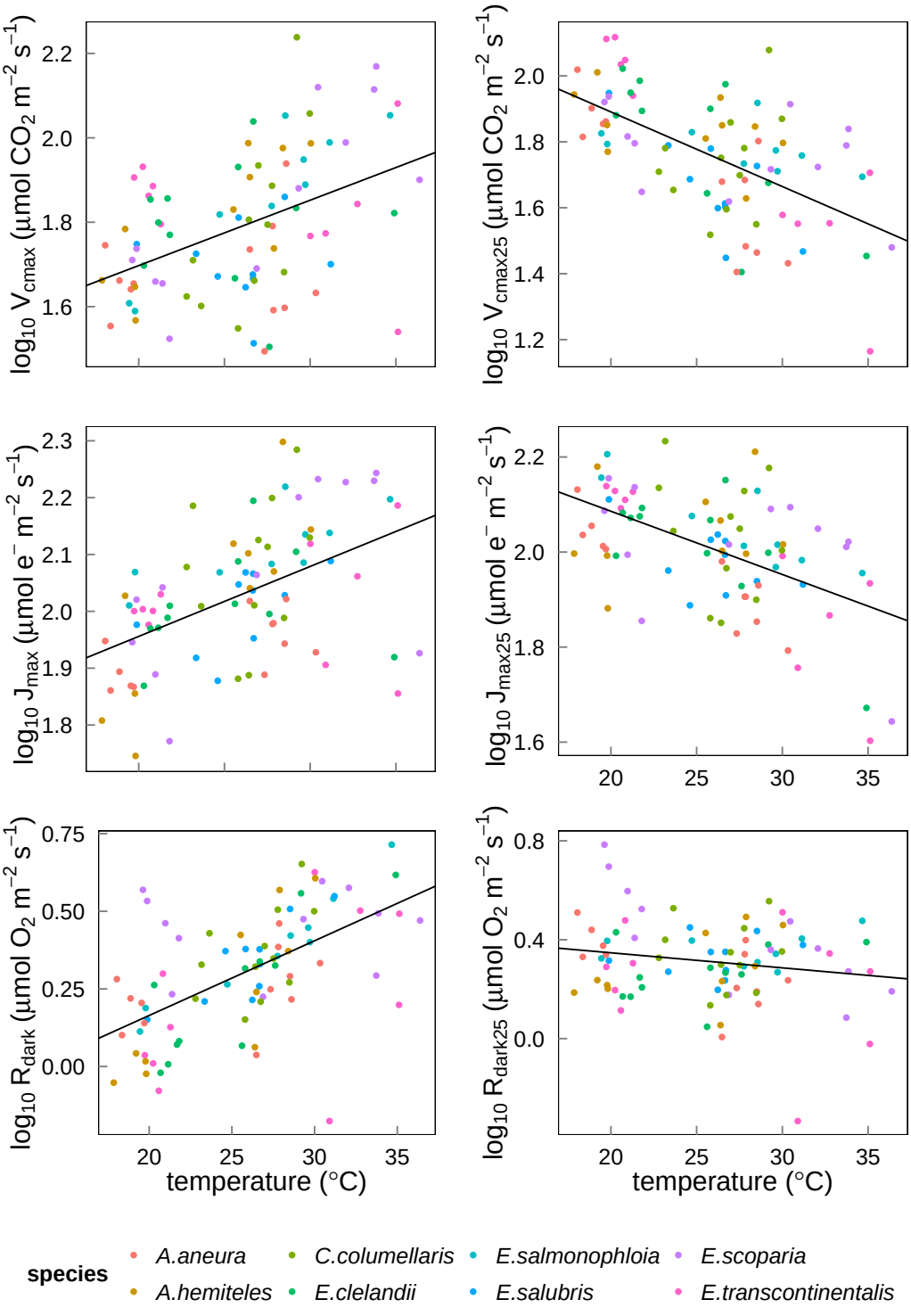

Figure 3.4: Bivariate linear regressions ($p < 0.05$) of $\log_{10}$ transformed V_{cmax}, V_{cmax25}, J_{max}, J_{max25}, R_{dark} and R_{dark25} (µmol m^{-2} s^{-1}) versus leaf temperature (T_{leaf}, °C). R^2 were respectively 0.18, 0.33, 0.23, 0.26, 0.33 and 0.12. Each point represents one A-c_i curve (n=86).

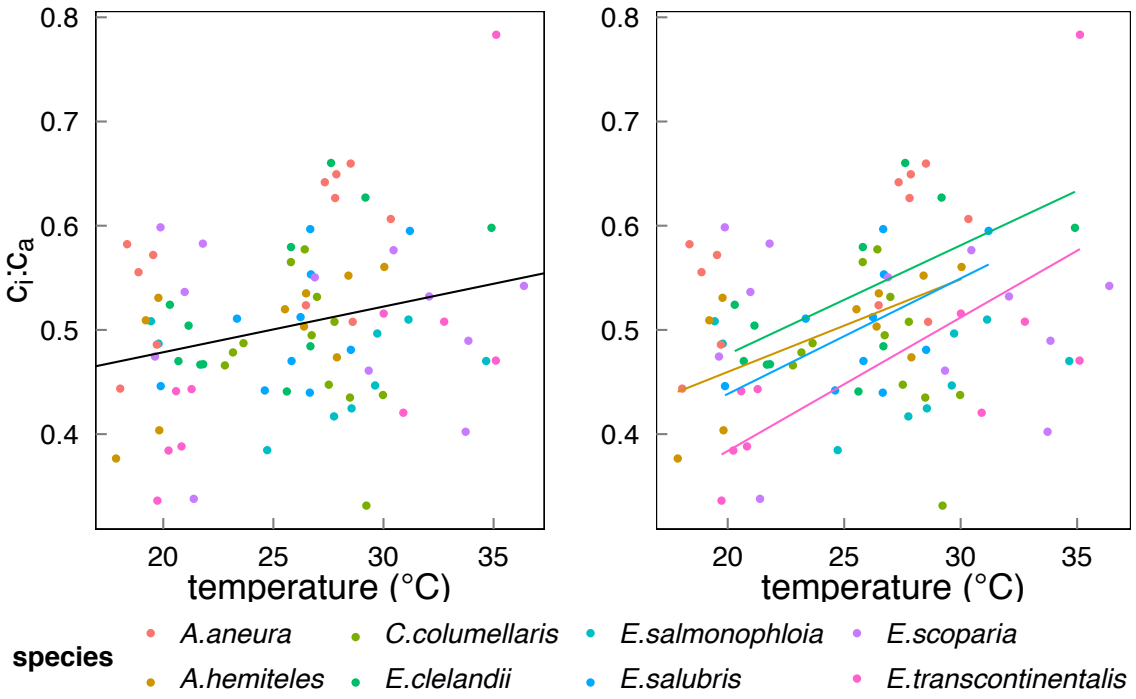

FIGURE 3.5: Bivariate linear regressions of the c_i:c_a ratio (at ambient $CO_2 \approx 400$ µmol mol^{-1}) versus temperature (T_{leaf}, °C) for individual trees considering all data (left plot) and within species (right plot). Only significant regressions ($p < 0.05$) are shown. Each point represents one A-c_i curve (n=86).

(figure 3.5 right). Within-species responses of R_{dark} to leaf temperature were weaker and less consistent (figure 3.6), suggesting that respiration had acclimated to a greater extent than was the case for V_{cmax} and J_{max}.

Incoming shortwave radiation at the surface is used here as a proxy for PPFD. Daily values ranged from 90 to 256 W m^{-2} and averaged 193 W m^{-2}. Averages for the warm and the cool seasons sampling periods were not significantly different. None of the photosynthetic parameters showed any relationship with shortwave radiation.

3.4.3 Leaf *N* and *P* relationships to photosynthetic traits and temperature

Photosynthetic parameters were not systematically related to N_{area} or P_{area} (data not shown). There was a positive relationship between N and P (by mass) across species, and within three of the species ($p < 0.05$; figure 3.7). High values of the foliar N:P ratio (> 16) in seven out of eight species (figure 3.8) suggests that P in this ecosystem

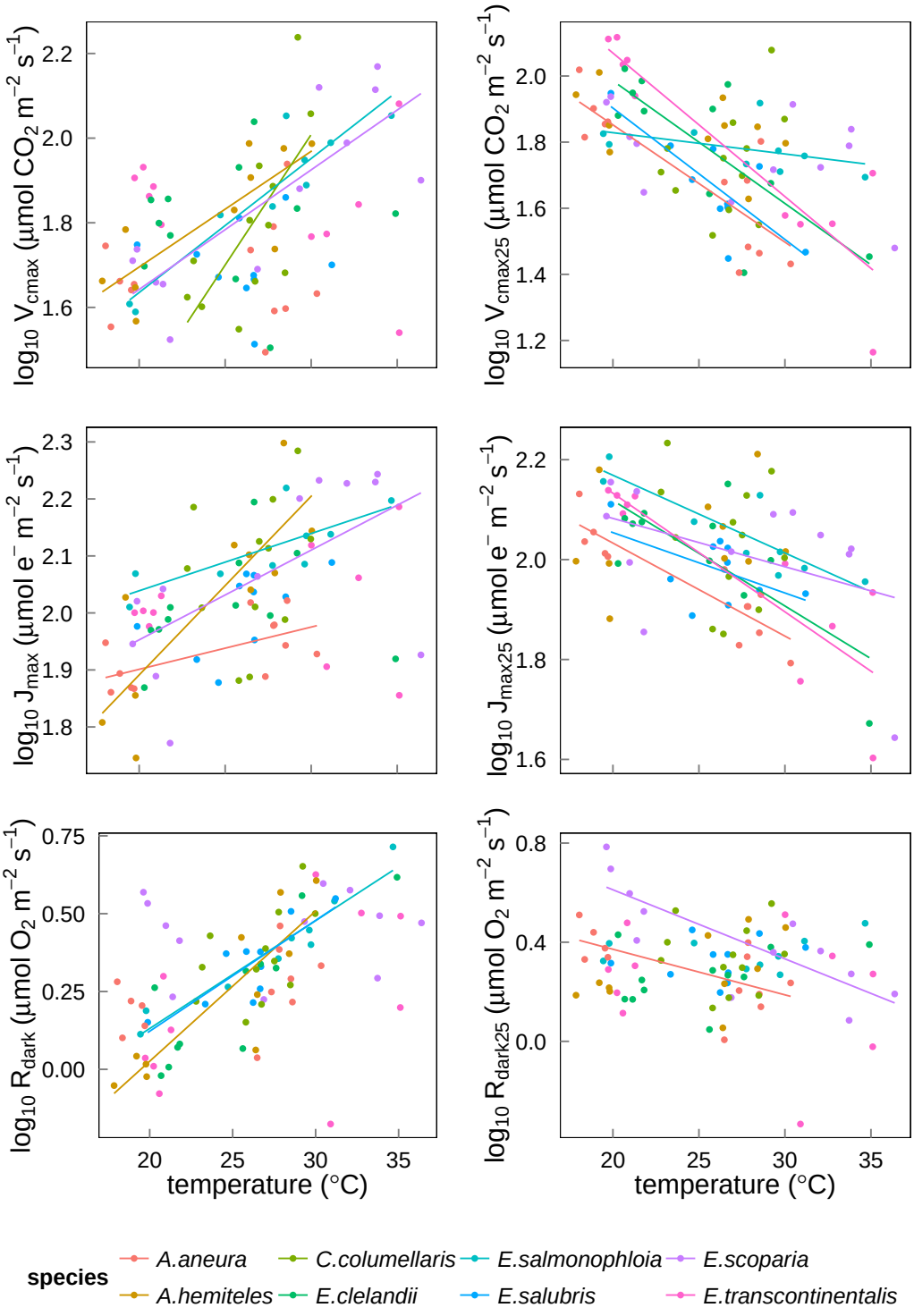

Figure 3.6: Bivariate linear regressions of $\log_{10}$ transformed V_{cmax}, V_{cmax25}, J_{max}, J_{max25}, R_{dark} and R_{dark25} (µmol m^{-2} s^{-1}) versus leaf temperature (T_{leaf}, °C) within species ($p < 0.05$). Only significant regressions ($p < 0.05$) are shown. Each point represents one A-c_i curve (n=86).

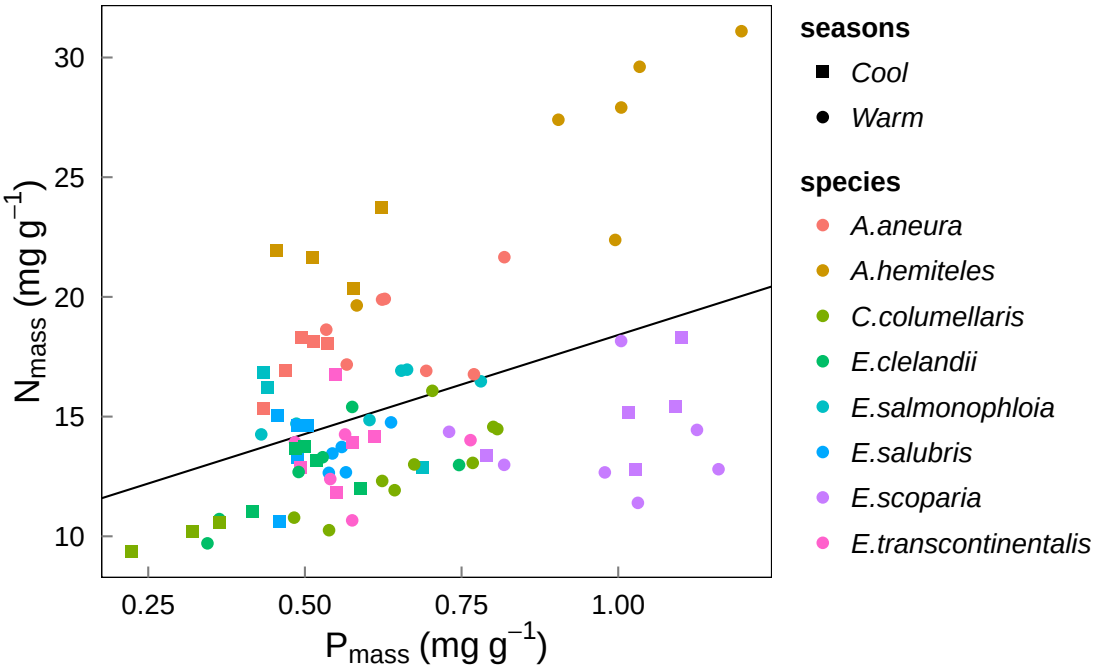

FIGURE 3.7: Bivariate linear regression of N_{mass} (mg g^{-1}) versus P_{mass} (mg g^{-1}) for all data (black line, slope = 0.33, R^2 = 0.17). Each point represents one leaf (n=86).

is more limiting to growth than N (Westoby and Wright 2006). N:P ratios declined with increasing temperature ($p < 0.05$). *A. aneura* and *A. hemiteles* presented the highest N:P as expected for N-fixing species.

3.4.4 Quantitative temperature responses

For V_{cmax} and J_{max}, the fitted slopes with leaf temperature were shallower than the predicted 'kinetic' slopes by a margin that greatly exceeded their 95% confidence limits (Table 3.1). The 'kinetic' values are what would be expected if the activities of the relevant enzyme complexes remained constant with changing growth temperature. The coordination hypothesis, however, predicts shallower rate $\leftrightarrow$ temperature slopes. The theoretical 'acclimated' slope for V_{cmax} falls just marginally above the 95% confidence interval for the fitted slope. The acclimated slope of J_{max} falls well within the 95% confidence interval for the fitted slope. For R_{dark} the acclimated and kinetic slopes are closer together and both fall within the 95% confidence interval of the fitted slope.

There is no 'kinetic' response of c_i:c_a, but the least-cost hypothesis predicts a pos-

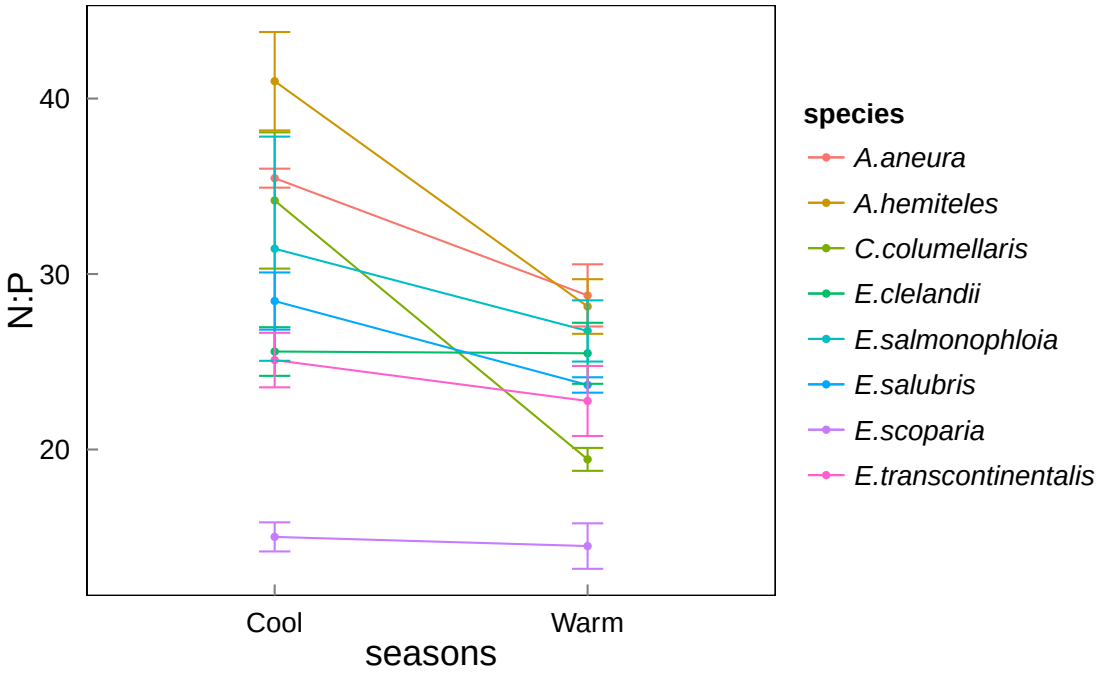

Figure 3.8: Changes in the average foliar N:P ratio for each species between the cool and the warm seasons. Standard errors shown.

itive response to temperature. This was observed, although the fitted slope of the response to temperature is shallower than predicted. The observed response of c_i:c_a to temperature is taken into account as a small correction to the acclimated slope of V_{cmax} against temperature (Appendix A).

3.5 Discussion

3.5.1 Quantitative ranges of photosynthesis traits

Values of V_{cmax}, J_{max}, R_{dark} and c_i:c_a for the eight species measured here were within ranges commonly reported. V_{cmax} and J_{max} were generally lower than expected for desert species, but higher than typical values for mesic perennial species (Wullschleger, 1993). The values were also high compared with trees from savannas with twice the annual rainfall (Domingues *et al.*, 2010). The c_i:c_a ratios fall within the range typical for dry environments (Prentice *et al.*, 2014).

TABLE 3.1: Linear regression slopes (K^1) and their 95% confidence intervals for natural log-transformed photosynthetic traits, with species included as a factor. The values are compared to 'kinetic' slopes (as expected in the absence of acclimation) and 'acclimated' slopes, as predicted by the coordination hypothesis for V_{cmax}, J_{max} and R_{dark} and the least-cost hypothesis for c_i:c_a. See Appendix A for the calculation of kinetic and acclimated slopes.

	V_{cmax}	J_{max}	R_{dark}	c_i:c_a
Fitted	0.0328	0.0251	0.0514	0.0060
	(±0.0158)	(±0.0108)	(±0.0164)	(±0.0033)
Kinetic	0.0885	0.0628	0.0675	n/a
Acclimated	0.0498	0.0236	0.0494	0.0131

3.5.2 Comparison between seasons

Our results were consistent with acclimation of photosynthetic traits to temperature as predicted by the coordination hypothesis. When measured at the prevailing ambient temperature, V_{cmax}, J_{max} and R_{dark} were all generally higher in the warm season than in the cool season, whereas values standardised to 25°C were generally lower in the warm season than in the cool season (figure 3.1). This is *prima facie* evidence for active seasonal acclimation, as the coordination hypothesis predicts lower allocation of N to Rubisco and other photosynthetic enzymes at higher temperatures, offsetting the increase in enzyme activity with elevated temperature.

Levels of leaf N and P have been reported to change seasonally (Medlyn *et al.*, 2002b, and figure 3.8). We found a reduction in the N:P ratio in the warm season, consistent with a reduced allocation of N to photosynthetic functions (Way and Sage, 2008). A reduction in total leaf N does not necessarily indicate changes in N allocation; however, a strong coupling between N and photosynthesis has been widely observed, even though Rubisco accounts for only 10-30% of the total leaf N (Evans, 1989). Furthermore, a reduction of leaf N in the warm season is unlikely to be caused by general growth dilution during an actively growing part of the year because: a) this is an environment with a year-round growing season; b) PAR levels during the periods of the field campaigns were similar; and c) the measured V_{cmax} values were shown to be consistent with the coordination hypothesis, implying similar assimilation rates in the two seasons. We did not find significant relationships of photosynthetic traits to foliar N or P but the study area is extremely limited in supplies of both nutrients (Prober *et al.*, 2012).

The comparison of fitted and theoretically predicted slopes (Table 3.1) reveals not only that the responses of V_{cmax}, J_{max} and R_{dark} to ambient temperature were smaller

than would be predicted from enzyme kinetics alone, but also that the observed responses were close to, or (in the case of J_{max}) statistically indistinguishable from the responses predicted by the coordination hypothesis. The response of c_i:c_a is in the same direction (positive) as the response predicted by the least-cost hypothesis, but only about half as large, probably due to the opposing effect (reduction in c_i:c_a) of greater vapour pressure deficits in the warm season than in the cool season (Prentice *et al.*, 2014).

V_{cmax} and J_{max} were strongly and positively correlated across species (figure 3.2), and the relationship did not shift significantly between seasons. Some studies have reported a lower J_{max}:V_{cmax} ratio in warmer seasons compared to cooler seasons (Medlyn *et al.*, 2002b; Lin *et al.*, 2013). Our data show a tendency in this direction, but not enough to be significant (figure 3.2). V_{cmax} and J_{max} have previously been reported to increase seasonally with leaf temperature. In one recent study on six *Eucalyptus* species, measurements were taken at six temperature levels in winter, spring and summer; there was an increase in V_{cmax} and J_{max} with air temperature in seasons with overlapping temperatures, and V_{cmax25} was significantly higher in the winter than in the summer (Lin *et al.*, 2013). Miyazawa and Kikuzawa (2006) obtained similar results in five evergreen broadleaved species. Our measurements yielded similar results (figure 3.4 and 3.6).

3.5.3 Links between photosynthetic activity, R_{dark} and c_i:c_a

V_{cmax}, J_{max} and R_{dark} were positively correlated with leaf temperature across a wide range (cool season 17 to 27°C; warm season 26 to 37°C), both for the dataset as a whole and within individual species (figure 3.4 and 3.6). Photosynthetic capacity and respiratory flux are linked via the ATP (adenosine triphosphate) demand of sucrose synthesis and transport, leading to the interdependence of chloroplast and mitochondrial metabolism (Krömer, 1995; Ghashghaie *et al.*, 2003). The parallel temperature acclimation of R_{dark} and V_{cmax} illustrates this close relationship.

Across all species, there was a strong negative relationship between c_i:c_a and photosynthetic capacity. This is to be expected from the coordination hypothesis as the lower the c_i:c_a ratio, the greater photosynthetic capacity (V_{cmax} and J_{max}) required to achieve a given assimilation rate. c_i:c_a ratios increased with temperature as predicted by the least-cost hypothesis, but the slope of 0.006 (figure 3.5) based on all data is shallower than the predicted slope of 0.0131. This difference may reflect higher vapour pressure deficits in the warm season, which would be expected to close stomata and

therefore act in the opposite way to the effect of temperature alone (Prentice *et al.*, 2014).

3.5.4 Implications for modelling

One dynamic global vegetation model, the Lund-Potsdam-Jena (LPJ) model (Sitch *et al.*, 2003) together with later models based on LPJ, formally assumes the coordination hypothesis (as well as the coupling between R_{dark} and V_{cmax}) and thus implicitly allows photosynthetic parameters and leaf respiration to acclimate, on a daily to monthly time scale, to the seasonal course of climate. The same assumption is implicit in the simple primary production models developed by Wang *et al.* (2013, 2014), but there are few data available to test this model assumption. Our study has presented field evidence supporting predictions of the coordination hypothesis regarding the seasonal acclimation of V_{cmax}, J_{max} and the allocation of N in leaves. Models that do not allow such acclimation may incorrectly represent the seasonal time course of carbon exchange at the plant and ecosystem levels.

Appendix A: Derivation of theoretical responses of photosynthetic traits to temperature

Kinetic responses

Temperature responses of many biological reaction rates are accurately described (within normal physiological ranges) by the Arrhenius equation, which can be written as:

$$ln\,parameter(T) - ln\,parameter(T_{ref}) = \frac{\Delta H_a}{R}\left(\frac{1}{T_{ref}} - \frac{1}{T}\right) \qquad \text{(A1)}$$

where T is the measurement temperature and T_{ref} is a reference temperature (K), ΔH_a is the activation energy of the reaction (J mol^{-1} K^{-1}) and R is the universal gas constant (8.314 J mol^{-1} K^{-1}). This expression can be approximated by a simple exponential function as follows, by linearizing around T_{ref}:

$$ln\,parameter(T) - ln\,parameter(T_{ref}) \approx \frac{\Delta H_a}{R}\left(\frac{1}{{T_{ref}}^2}\right)\Delta T \qquad \text{(A2)}$$

where $\Delta T = T - T_{ref}$. Thus, the slope of $ln\,param(T)$ versus T can be predicted from equation (A2), when ΔH_a is known. We set $T_{ref} = 298$ K (which is both conventional, and close to the median measurement temperature in our data set). We used the ΔH_a

values based on in vivo measurements at 25°C by Bernacchi et al. (2001) for V_{cmax} (65 330 J mol^{-1} K^{-1}). For J_{max}, we used the ΔH_a value based on in vivo measurements by Bernacchi et al. (2003) on plants that had been grown at 25°C (43 900 J mol^{-1} K^{-1}). For R_{dark}, we used ΔH_a (50230 J mol^{-1} K^{-1}) calculated from equation 2.

Acclimated responses

The 'acclimated' response of V_{cmax} according to the coordination hypothesis is obtained by setting the Rubisco- and electron-transport limited rates of photosynthesis to be equal. To simplify matters, we disregarded the curvature of the response of electron transport to PPFD, giving:

$$V_{cmax} = \varphi_0 I_{abs} \left[\frac{c_i + K}{c_i + 2\Gamma^*} \right] \tag{A3}$$

where φ_0 is the intrinsic quantum efficiency of photosynthesis, I_{abs} is the absorbed PPFD, K is the effective Michaelis-Menten coefficient for carbon fixation and Γ^* is the photorespiratory compensation point. The sensitivity of V_{cmax} to temperature can then be calculated from the derivative of (A3):

$$\begin{aligned} \frac{\partial ln\, V_{cmax}}{\partial T} = \frac{1}{V_{cmax}} \frac{\partial V_{cmax}}{\partial T} = \frac{\partial c_i}{\partial T} \left(\frac{1}{c_i + K} - \frac{1}{c_i + 2\Gamma^*} \right) + \\ \frac{\partial K}{\partial T} \left(\frac{1}{c_i + K} \right) - 2 \frac{\partial \Gamma^*}{\partial T} \left(\frac{1}{c_i + 2\Gamma^*} \right) \end{aligned} \tag{A4}$$

We evaluated equation (A4) at 25°C and ci = 200 µmol mol^{-1} (approximately the median of our observed values of c_i), using the temperature dependencies of K and Γ^* from Bernacchi *et al.* (2001). The temperature dependency of K was determined from those of the constituent terms K_c and K_o (the Michaelis-Menten coefficients for carboxylation and oxygenation, respectively) as given by Bernacchi et al. (2001), using similar methods.

Again for simplicity, we assumed an approximation of the theoretical acclimated slope for J_{max} that is simply the acclimated slope of V_{cmax}, minus the difference between the 'kinetic' slopes of V_{cmax} and J_{max}. We assumed that R_{dark} (on acclimation) should simply be equal to a constant fraction of V_{cmax}, implying the same acclimated temperature response for R_{dark} as for V_{cmax}.

The least-cost hypothesis (Prentice *et al.*, 2014) provides an optimal value for c_i:c_a,

denoted by χ^*, such that:

$$\chi^* = \frac{\chi_0}{1-\chi_0} = \sqrt{\frac{b\,K}{1.6\,a\,D}} \tag{A5}$$

where b is the (assumed constant) ratio of R_{dark} to V_{cmax} and a is the cost of maintaining the transpiration pathway. Both K and a are temperature-dependent; a because it is proportional to the viscosity of water, η. Holding vapour pressure deficit (D) constant, we can obtain an expression for $\partial\chi^*/\partial T$:

$$\frac{\partial\chi^*}{\partial T} = \frac{\chi^*}{2}\left(\frac{\partial ln\,K}{\partial T} - \frac{\partial a}{\partial T}\right) \tag{A6}$$

and from equations (A5) and (A6), with the help of the chain rule,

$$\frac{\partial\chi_0}{\partial T} = \frac{\chi_0}{2}(1-\chi_0)\left(\frac{\partial ln\,K}{\partial T} - \frac{\partial a}{\partial T}\right) \tag{A7}$$

We evaluated equation (A7) at T = 25°C, $\chi_0 = 0.5$ and $c_a = 400$ ppm using known temperature dependencies of K and η.

Appendix B: Species list, average and standard error of key photosynthetic traits (µmol m^{-2} s^{-1})

Specie	Season	n	V_{cmax}	J_{max}	R_{dark}	V_{cmax25}	J_{max25}	R_{dark25}
Acacia aneura	Warm	7	50.83	92.78	1.99	38.78	77.51	1.71
			(±7.15)	(±3.86)	(±0.22)	(±5.48)	(±4.31)	(±0.19)
Acacia hemiteles	Warm	6	81.97	137.21	2.61	66.11	118.35	2.24
			(±7.23)	(±12.99)	(±0.45)	(±5.79)	(±9.90)	(±0.31)
Callitris columellaris	Warm	10	78.42	122.45	2.50	60.08	103.52	2.14
			(±14.24)	(±12.77)	(±0.32)	(±8.97)	(±9.26)	(±0.24)
Eucalyptus clelandii	Warm	6	67.93	115.21	2.55	53.17	98.21	1.93
			(±11.22)	(±10.56)	(±0.45)	(±11.38)	(±12.96)	(±0.20)
Eucalyptus salmonophloia	Warm	6	93.11	140.01	3.15	59.08	103.43	2.26
			(±7.43)	(±7.46)	(±0.44)	(±4.97)	(±6.58)	(±0.18)
Eucalyptus salubris	Warm	6	53.27	109.39	2.73	42.18	93.00	2.30
			(±7.01)	(±5.59)	(±0.27)	(±6.39)	(±5.32)	(±0.13)
Eucalyptus transcontinentalis	Warm	5	68.57	110.48	2.55	34.93	70.95	1.75
			(±14.21)	(±15.36)	(±0.63)	(±5.81)	(±10.28)	(±0.49)
Eremophila scoparia	Warm	7	101.65	149.07	2.92	55.62	102.11	1.96
			(±13.60)	(±13.22)	(±0.32)	(±6.51)	(±10.26)	(±0.23)
Acacia aneura	Cool	5	45.26	77.43	1.56	78.75	112.37	2.54
			(±3.16)	(±2.97)	(±0.11)	(±6.82)	(±6.13)	(±0.21)
Acacia hemiteles	Cool	5	47.02	74.52	0.99	80.04	106.24	1.62
			(±5.00)	(±11.15)	(±0.05)	(±9.56)	(±15.93)	(±0.04)
Callitris columellaris	Cool	3	44.44	125.03	2.16	52.22	139.45	2.67
			(±3.47)	(±15.02)	(±0.30)	(±4.45)	(±17.49)	(±0.37)
Eucalyptus clelandii	Cool	5	62.99	92.09	1.24	89.00	115.97	1.81
			(±4.12)	(±4.82)	(±0.16)	(±5.50)	(±4.55)	(±0.23)
Eucalyptus salmonophloia	Cool	4	48.41	112.25	1.56	65.50	141.03	2.36

continued on next page

continued from previous page

Specie	Season	n	V_{cmax}	J_{max}	R_{dark}	V_{cmax25}	J_{max25}	R_{dark25}
			(±8.72)	(±4.91)	(±0.16)	(±5.50)	(±4.55)	(±0.23)
Eucalyptus salubris	Cool	5	49.55	95.79	1.77	55.91	101.05	2.01
			(±2.16)	(±7.76)	(±0.16)	(±9.07)	(±8.68)	(±0.22)
Eucalyptus transcontinentalis	Cool	5	75.62	100.59	1.25	113.48	131.68	1.97
			(±3.89)	(±1.98)	(±0.20)	(±8.02)	(±2.47)	(±0.29)
Eremophila scoparia	Cool	5	46.04	87.96	2.86	68.46	114.46	4.18
			(±3.62)	(±9.28)	(±0.35)	(±7.65)	(±13.14)	(±0.62)

3.6 Acknowledgments

This research was funded by the Terrestrial Ecosystem Research Network (TERN), Macquarie University and the Australian National University. H.F. Togashi is supported by an international Macquarie University International Research Scholarship (iMQRES). Prentice, Evans, and Togashi are funded by the Ecosystem Modelling and Scaling Infrastructure (eMAST, part of TERN). TERN and eMAST are supported by the Australian Government through the National Collaborative Research Infrastructure Strategy (NCRIS). Owen Atkin acknowledges the support of the Australian Research Council (DP130101252 and CE140100008). The Australian SuperSites Network and OzFlux (part of TERN), the CSIRO Land and Water Flagship, and the Western Australia Department of Environment and Conservation support the Great Western Woodlands Supersite. N and P were analysed in the Department of Forestry, ANU. We are grateful to Jack Egerton (ANU), Li Guangqi (Macquarie), Lingling Zhu (ANU), Danielle Creek (University of Western Sydney), Lasantha Weerasinghe (ANU), Lucy Hayes (ANU) and Stephanie McCaffery (ANU) for help with fieldwork and/or N and P digestions. We thank Santi Sabat (Universitat Autnoma de Barcelona) and Maurizio Mencuccini (University of Edinburgh) for comments that helped to improve this paper. This paper is a contribution to the AXA Chair Programme in Biosphere and Climate Impacts and the Imperial College initiative on Grand Challenges in Ecosystems and the Environment.

3.7 References

Allen, S. E, Grimshaw, H, Parkinson, J. A, and Quarmby, C. L. *Chemical analysis of ecological materials*. Blackwell Scientific Publications, 1974.

Atkin, O. K, Holly, C, and Ball, M. C. Acclimation of snow gum (*Eucalyptus pauciflora*) leaf respiration to seasonal and diurnal variations in temperature: the importance of changes in the capacity and temperature sensitivity of respiration. *Plant, Cell & Environment*, 23(1):15–26, 2000.

Atkin, O. K and Tjoelker, M. G. Thermal acclimation and the dynamic response of plant respiration to temperature. *Trends in Plant Science*, 8(7):343–351, 2003.

Atkin, O. K, Bloomfield, K. J, Reich, P. B, Tjoelker, M. G, Asner, G. P, Bonal, D, Bönisch, G, Bradford, M. G, Cernusak, L. A, Cosio, E. G, Creek, D, Crous, K. Y, Domingues, T. F, Dukes, J. S, Egerton, J. J. G, Evans, J. R, Farquhar, G. D, Fyllas, N. M, Gauthier, P. P. G, Gloor, E, Gimeno, T. E, Griffin, K. L, Guerrieri, R, Heskel, M. A, Huntingford, C, Ishida, F. Y, Kattge, J, Lambers, H, Liddell, M. J, Lloyd, J, Lusk, C. H, Martin, R. E, Maksimov, A. P, Maximov, T. C, Malhi, Y, Medlyn, B. E, Meir, P, Mercado, L. M, Mirotchnick, N, Ng, D, Niinemets, Ü, O'Sullivan, O. S, Phillips, O. L, Poorter, L, Poot, P, Prentice, I. C, Salinas, N, Rowland, L. M, Ryan, M. G, Sitch, S, Slot, M, Smith, N. G, Turnbull, M. H, VanderWel, M. C, Valladares, F, Veneklaas, E. J, Weerasinghe, L. K, Wirth, C, Wright, I. J, Wythers, K. R, Xiang, J, Xiang, S, and Zaragoza-Castells, J. Global variability in leaf respiration in relation to climate, plant functional types and leaf traits. *New Phytologist*, 206(2):614–636, 2015.

Bernacchi, C. J, Singsaas, E. L, Pimentel, C, Portis Jr, A. R, and Long, S. P. Improved temperature response functions for models of rubisco-limited photosynthesis. *Plant, Cell & Environment*, 24(2):253–259, 2001.

Bernacchi, C. J, Pimentel, C, and Long, S. P. *In vivo* temperature response functions of parameters required to model RuBP-limited photosynthesis. *Plant, Cell & Environment*, 26(9):1419–1430, 2003.

Bernacchi, C, Rosenthal, D, Pimentel, C, Long, S, and Farquhar, G. *Modeling the Temperature Dependence of C_3 Photosynthesis*, volume 29 of *Advances in Photosynthesis and Respiration*, book section 10, pages 231–246. Springer Netherlands, 2009.

Chen, J-L, Reynolds, J, Harley, P, and Tenhunen, J. Coordination theory of leaf nitrogen distribution in a canopy. *Oecologia*, 93(1):63–69, 1993.

Domingues, T. F, Meir, P, Feldpausch, T. R, Saiz, G, Veenendaal, E. M, Schrodt, F, Bird, M, Djagbletey, G, Hien, F, Compaore, H, Diallo, A, Grace, J, and Lloyd, J. O. N. Co-limitation of photosynthetic capacity by nitrogen and phosphorus in west Africa woodlands. *Plant, Cell & Environment*, 33(6):959–980, 2010.

Evans, J. Photosynthesis and nitrogen relationships in leaves of C_3 plants. *Oecologia*, 78(1):9–19, 1989.

Farquhar, G. D, von Caemmerer, S, and Berry, J. A. A biochemical model of photosynthetic CO_2 assimilation in leaves of C_3 species. *Planta*, 149(1):78–90, 1980.

Field, C. H, and Mooney, H. A. The photosynthesis-nitrogen relationship in wild plants. Givinsh TJ. In: *On the economy of form and function*, pages 22–55. *Cambridge University Press*, Cambridge, 1986.

Ghashghaie, J, Badeck, F-W, Lanigan, G, Nogués, S, Tcherkez, G, Deléens, E, Cornic, G, and Griffiths, H. Carbon isotope fractionation during dark respiration and photorespiration in C_3 plants. *Phytochemistry Reviews*, 2(1-2):145–161, 2003.

Hikosaka, K, Ishikawa, K, Borjigidai, A, Muller, O, and Onoda, Y. Temperature acclimation of photosynthesis: mechanisms involved in the changes in temperature dependence of photosynthetic rate. *Journal of Experimental Botany*, 57(2):291–302, 2006.

Hutchinson, M. Daily maximum temperature: Anuclimate 1.0, 0.01 degree, Australian coverage, 1970-2012, 2014a. http://www.emast.org.au/

Hutchinson, M. Daily minimum temperature: Anuclimate 1.0, 0.01 degree, Australian coverage, 1970-2012, 2014b. http://www.emast.org.au/

Hutchinson, M. Daily precipitation: Anuclimate 1.0, 0.01 degree, Australian coverage, 1970-2012, 2014c. http://www.emast.org.au/

Kattge, J and Knorr, W. Temperature acclimation in a biochemical model of photosynthesis: a reanalysis of data from 36 species. *Plant, Cell & Environment*, 30(9): 1176–1190, 2007.

Krömer, S. Respiration during photosynthesis. *Annual review of plant biology*, 46(1): 45–70, 1995.

Lin, Y-S, Medlyn, B. E, De Kauwe, M. G, and Ellsworth, D. S. Biochemical photosynthetic responses to temperature: how do interspecific differences compare with seasonal shifts? *Tree Physiology*, 33(8):793–806, 2013.

Maire, V, Martre, P, Kattge, J, Gastal, F, Esser, G, Fontaine, S, and Soussana, J-F. The coordination of leaf photosynthesis links C and N fluxes in C_3 plant species. *PLoS ONE*, 7(6):e38345, 2012.

Medlyn, B. E, Dreyer, E, Ellsworth, D, Forstreuter, M, Harley, P. C, Kirschbaum, M. U. F, Le Roux, X, Montpied, P, Strassemeyer, J, Walcroft, A, Wang, K, and Loustau, D. Temperature response of parameters of a biochemically based model of photosynthesis. II. A review of experimental data. *Plant, Cell & Environment*, 25 (9):1167–1179, 2002a.

Medlyn, B. E, Loustau, D, and Delzon, S. Temperature response of parameters of a biochemically based model of photosynthesis. I. Seasonal changes in mature maritime pine (*Pinus pinaster* ait.). *Plant, Cell & Environment*, 25(9):1155–1165, 2002b.

Miyazawa, Y and Kikuzawa, K. Physiological basis of seasonal trend in leaf photosynthesis of five evergreen broad-leaved species in a temperate deciduous forest. *Tree Physiology*, 26(2):249–256, 2006.

Onoda, Y, Hikosaka, K, and Hirose, T. Seasonal change in the balance between capacities of RuBP carboxylation and RuBP regeneration affects CO_2 response of photosynthesis in *Polygonum cuspidatum*. *Journal of Experimental Botany*, 56(412): 755–763, 2005.

Prentice, I. C, Meng, T, Wang, H, Harrison, S. P, Ni, J, and Wang, G. Evidence of a universal scaling relationship for leaf CO_2 drawdown along an aridity gradient. *New Phytologist*, 190(1):169–180, 2011.

Prentice, I. C, Dong, N, Gleason, S. M, Maire, V, and Wright, I. J. Balancing the costs of carbon gain and water transport: testing a new theoretical framework for plant functional ecology. *Ecology Letters*, 17(1):82–91, 2014.

Prober, S, Thiele, K, Rundel, P, Yates, C, Berry, S, Byrne, M, Christidis, L, Gosper, C, Grierson, P, Lemson, K, Lyons, T, Macfarlane, C, O'Connor, M, Scott, J, Standish, R, Stock, W, van Etten, E. B, Wardell-Johnson, G, and Watson, A. Facilitating adaptation of biodiversity to climate change: a conceptual framework applied to the world's largest mediterranean-climate woodland. *Climatic Change*, 110(1-2): 227–248, 2012.

Sage, R. F and Kubien, D. S. The temperature response of C_3 and C_4 photosynthesis. *Plant, Cell & Environment*, 30(9):1086–1106, 2007.

Sharkey, T. D, Bernacchi, C. J, Farquhar, G. D, and Singsaas, E. L. Fitting photosynthetic carbon dioxide response curves for C_3 leaves. *Plant, Cell & Environment*, 30 (9):1035–1040, 2007.

Sitch, S, Smith, B, Prentice, I. C, Arneth, A, Bondeau, A, Cramer, W, Kaplan, J. O, Levis, S, Lucht, W, Sykes, M. T, Thonicke, K, and Venevsky, S. Evaluation of ecosystem dynamics, plant geography and terrestrial carbon cycling in the LPJ dynamic global vegetation model. *Global Change Biology*, 9(2):161–185, 2003.

Team R Core. R: A language and environment for statistical computing. R foundation for statistical computing, Vienna, Austria. http://www.r-project.org/. 2012.

Togashi, H. F, Bloomfield, K. J, Prentice, I. C, Atkin, O. K, Macfarlane, C, Prober, S, and Evans, B. J. *Leaf level physiology, chemistry and structural traits, Great Western Woodlands TERN - supersite, 2014, 2015.* AEKOS [DATASET], 2015. http://www.supersites.net.au/knb/metacat/supersite.302.2/html

Von Caemmerer, S. *Biochemical models of leaf photosynthesis.* CSIRO publishing, 2000.

Wang, H, Prentice, I. C, and Ni, J. Data-based modelling and environmental sensitivity of vegetation in China. *Biogeosciences*, 10(9):5817–5830, 2013.

Wang, H, Prentice, I. C, and Davis, T. W. Biophysical constraints on gross primary production by the terrestrial biosphere. *Biogeosciences Discussions*, 11:3209–3240, 2014.

Warton, D, Wright, I, Falster, D, and Westoby, M. Bivariate line-fitting methods for allometry. *Biological Reviews*, 81(2):259–291, 2006.

Way, D. A and Sage, R. F. Thermal acclimation of photosynthesis in black spruce. *Picea mariana. Plant, Cell & Environment*, 31(9):1250–1262, 2008.

Wickham, H. *ggplot2: Elegant Graphics for Data Analysis.* Springer, 2010.

Wullschleger, S. D. Biochemical limitations to carbon assimilation in C_3 plants—a retrospective analysis of the A-c_i curves from 109 species. *Journal of Experimental Botany*, 44(5):907–920, 1993.

4

Functional trait variation related to gap dynamics in tropical moist forests: a perspective for vegetation modelling

Henrique Furstenau Togashi[1,2], Iain Colin Prentice[1,2,3,4], Owen K. Atkin[5,6], Keith J. Bloomfield[5], Matt Bradford[7], Lasantha K. Weerasinghe[5,8], Sandy P. Harrison[1,9], Bradley John Evans[1,2], Michael J. Liddell[10], Han Wang[1,4], Kun-Fang Cao[11], Ze-xin Fan[12]

[1]Department of Biological Sciences, Macquarie University 2109, Sydney, NSW, Australia
[2]Terrestrial Ecosystem Research Network Ecosystem Modelling and Scaling Infrastructure, Macquarie University 2109 and University of Sydney 2006, NSW, Australia
[3]AXA Chair of Biosphere and Climate Impacts, Grand Challenges in Ecosystems and the Environment and Grantham Institute, Climate Change and the Environment, Department of Life Sciences, Imperial College London, Silwood Park Campus, Buckhurst Road, Ascot SL5 7PY, UK
[4]College of Forestry, Northwest A&F University, Yangling 712100, China
[5]Division of Plant Sciences, Research School of Biology, Australian National University, Canberra, Australia
[6]ARC Centre of Excellence in Plant Energy Biology, Research School of Biology, Australian National University, Canberra, Australia
[7]CSIRO Land and Water, Tropical Forest Research Centre, P.O. Box 780, Atherton, Q, 4883, Australia
[8]Faculty of Agriculture, University of Peradeniya, Peradeniya 20400, Sri Lanka
[9]Geography & Environmental Sciences, School of Archaeology, Geography and Environmental Sciences, University of Reading, Whiteknights, Reading, RG6 6AH, UK
[10]Discipline of Chemistry & Centre for Tropical Environmental and Sustainable Sciences, James Cook University, Cairns, Qld, Australia

[11]State Key Laboratory for Conservation and Utilization of Subtropical Agrobioresources, and College of Forestry, Guangxi University, Nanning 530004, Guangxi, China
[12]Key Laboratory of Tropical Forest Ecology, Xishuangbanna Tropical Botanical Garden, Chinese Academy of Sciences, Menla 666303, China.

This chapter will be submitted to *Perspectives in Plant Ecology, Evolution and Systematics*

4.1 Summary

The representation of Plant Functional Types (PFTs) in the current generation of Dynamic Global Vegetation Models (DGVMs) is simplistic and has limited predictive power. Key ecophysiological traits, including photosynthetic parameters, are typically assigned single values for each, broadly defined PFT. Trait variation within PFTs - which may represent continuous variation in response to environmental factors, and/or differences linked to spatial and temporal niche differentiation within communities - is thus neglected. A stronger empirical basis for the treatment of plant functional trait variation in DGVMs is greatly needed. We present and analyse 431 sets of measurements of leaf and whole-plant traits, including photoynthesis measurements, on evergreen angiosperm trees in tropical moist forests of Australia and China. By confining attention to a relatively narrow range of climate, our analysis highlights trait differences linked to vegetation dynamic roles. Certain predictions of coordination theory (that Rubisco- and electron-transport limited rates of photosynthesis are co-limiting under field conditions) and the least-cost hypothesis (that air-to-leaf CO_2 drawdown minimizes the combined costs per unit carbon assimilation of maintaining carboxylation and transpiration capacities) are supported for within-community trait variation linked to canopy position, just as they are for variation along spatial environmental gradients. Trait differences among plant species occupying different structural and temporal niches provide an initial basis for the ecophysiological representation of vegetation dynamics in next-generation DGVMs.

4.2 Introduction

The development of Dynamic Global Vegetation Models (DGVMs) from the earliest stages has emphasized the role of the distribution of different types of plants and vegetation in predicting the exchanges of carbon between the atmosphere and the land biota (Prentice and Cowling, 2013). Plant Functional Type (PFT) classifications can be traced back to Raunkiær's (1934) 'life form' classification, based on plant traits that ensure persistence through seasons unfavourable for growth (Harrison *et al.*, 2010). After several decades when plant functional geography was neglected, new PFT classifications appeared during the 1980's (Box, 1981; Woodward, 1987) with a view to the development of DGVMs - which began in earnest during the late 1980's (Leemans and Prentice, 1989). The PFT concept has received significant attention since then (Prentice *et al.*, 1992; Díaz and Cabido, 1997; Lavorel and Garnier, 2002; Wright *et al.*, 2004; Prentice *et al.*, 2007; Harrison *et al.*, 2010; Fyllas *et al.*, 2012). It has become widely accepted that PFT classifications for modelling purposes ideally should reflect aspects of trait diversity that can predict plant responses to the physical environment and land management.

Many PFT schemes have been developed since Raunkiær's (1934) pioneering work. PFTs adopted in DGVMs today are most commonly defined in terms of up to five qualitative traits: (a) life form (using various definitions), (b) leaf type (usually just broad- or needle-leaf), (c) phenological type (usually just deciduous or evergreen), (d) photosynthetic pathway (C3, C4 or CAM) (Calvin and Benson, 1948; Ranson and Thomas, 1960; Kortschak *et al.*, 1965), and (e) climatic range defined in terms of broad climatic classes such as boreal, tropical, desert (Köppen, 1931). This conventional approach to PFT classification has numerous limitations (Prentice and Cowling, 2013). For example, life-form definitions are often incompletely defined, as informal and potentially ambiguous terms such as 'shrub' have been used in place of Raunkiær's explicitly specified categories. Leaf-type definitions usually ignore the huge variations in leaf size among 'broad-leaved' plants, and even the distinction between broad and needle-leaved trees is often effectively an (imperfect) surrogate for the important distinction in hydraulic architecture between angiosperms and gymnosperms - the latter, in fact, including many species with broad leaves. The physiological distinction between C3 and C4 herbaceous plants is usually made, but CAM has usually been disregarded in models. Thermal climate categories make sense if it is recognized that they are a surrogate for different cold-tolerance mechanisms in phanerophytes (Prentice *et al.* 1992; see Harrison *et al.* 2010 for a compilation of experimental data on cold tolerance),

but they are often used without clear definitions and in effect they may often stand in for a continuum of physiological differences between plants adapted or acclimated to different seasonal temperature regimes, rather than representing qualitative differences among types of plant.

Another key aspect of plant functional classification that is ignored by the majority of DGVMs pertains to species' distinct 'roles' in vegetation dynamics. Classifications of tree species according to shade tolerance (Whitmore, 1982), growth characteristics (maximum height and growth rate) (Shugart, 1984; Swaine and Whitmore, 1988) and successional stage (pioneer versus climax) (Swaine and Whitmore, 1988) have been a mainstay of regionally specific 'gap models' designed to predict forest dynamics under constant or changing environmental conditions (Botkin et al., 1972; Shugart, 1984; Denslow, 1987; Prentice and Leemans, 1990; Prentice et al., 1993, Turner, 2001). But these aspects are not treated by most DGVMs. Exceptions are those models with individual-based dynamical cores, such as LPJ-GUESS (Smith *et al.*, 2001) and Hybrid (Friend *et al.*, 1993), and the ED model (Moorcroft *et al.*, 2001) which uses a mathematical short-cut to represent the essentials of forest dynamics without simulating individual trees explicitly.

A critique of the use of PFTs for modelling purposes has recently emerged with the initial development of models based on continuous traits variation (Pavlick *et al.*, 2013; Scheiter *et al.*, 2013; Verheijen *et al.*, 2013). The jury is out on whether next-generation DGVMs should include PFT classifications at all; and if so, at what level. For example, there is a clear case to be made for retaining well-understood distinctions among photosynthetic pathways, and there may be good reasons also to retain life-form distinctions at least at the highest level of Raunkiær's classification. At the same time, most quantitative traits show continuous adaptive variation along environmental gradients (Meng *et al.*, 2015), indicating that the conventional approach in most models of assigning fixed values of leaf-level traits such as carboxylation capacity (V_{cmax}) and nitrogen content per unit leaf area (N_{area}) to PFTs does not adequately describe the plasticity of such traits in the real world. Even the less plastic biophysical traits (Meng *et al.*, 2015), such as leaf mass per area (LMA) and leaf dry-matter content show systematic, quantitative variations along environmental gradients as a consequence of species turnover within PFTs, and thus not necessarily the replacement of one PFT by another. Faced with continuous trait variation, models can either treat it as continuous - as the LPJ model (Sitch *et al.*, 2003) does for photosynthetic traits, following the approach developed by Haxeltine and Prentice (1996) - or subdivide the continuum for convenience. But problems such as unrealistically abrupt modelled vegetation

transitions (as climatic limits of PFTs are reached) can arise if the subdivision is too coarse.

In this paper we focus principally on the neglected 'dynamical' aspect of PFT classification. We adopt the simple fourfold classification popularized by Shugart (1984) to define species' roles, while recognizing that this classification represents a convenient subdivision of two orthogonal continua of variation - shade tolerance (requiring, versus not requiring, a gap for regeneration) and size at maturity (producing, versus not producing, a gap upon mortality). We focus on functional trait variations within tropical moist forests, which harbour enormous tree species diversity and contain species that exhibit all combinations of these traits (Turner, 2001). We build on a previous analysis by Fyllas *et al.* (2012), who showed that quantitative traits including foliar δ13C discrimination, LMA and nutrients including N and P could be used to discriminate PFTs with distinct dynamical characteristics in Amazonian rain forests. Our analysis focuses on east Asian (SW China) and northern Australian tropical rain forests, and extends the approach of Fyllas *et al.* (2012) to include field photosynthetic measurements.

4.3 Background and principles of this study

Some recent work directed towards the development of 'next-generation' DGVMs has focused on the predictability of key quantitative traits as a function of environmental variation. The 'least-cost' (Prentice *et al.*, 2014) and 'coordination' (Maire *et al.*, 2012) hypotheses together suggest a degree of predictability (across environments and clades) for the air-to-leaf CO_2 drawdown (c_i:c_a ratio, the ratio of leaf-internal to ambient CO_2: Prentice *et al.*, 2014), V_{cmax} and the electron-transport capacity J_{max} (Togashi *et al.*, in revision), and N_{area} (Dong *et al.*, submitted). Both hypotheses have a much longer pedigree than indicated by the recent references cited here, but systematic testing of these hypotheses has only been undertaken quite recently.

The 'least-cost' hypothesis indicates that at the leaf level, plants should respond to differences in the relative costs (per unit of assimilation achieved) of maintaining the biochemical capacity for photosynthesis versus the structural capacity for transpiration by making an optimal investment 'decision' that minimizes the total carbon cost of maintaining both essential functions. This hypothesis can be shown to lead to an optimum value of the c_i:c_a ratio that depends predictably on temperature and vapour pressure deficit (Prentice *et al.*, 2014). Moreover, this optimum has the same mathematical form as that predicted approximately by the Cowan-Farquhar optimality criterion for electron-transport limited photosynthesis, and known to provide good

predictions of stomatal behaviour under a range of conditions (Medlyn *et al.*, 2011; Lin *et al.*, 2015). The least-cost hypothesis however is more explicit than the Cowan-Farquhar criterion in that it 'unpacks' water transport and biochemical costs, and its predictive ability is more general in that it does not only apply to electron-transport limited photosynthesis.

The coordination hypothesis indicates that under typical daytime conditions, the Rubisco-limited and electron transport-limited rates of photosynthesis should be approximately equal. This represents the optimal disposition of resources between light capture and carbon fixation. It leads to the prediction that top-of-canopy V_{cmax} (measured at the growth temperature) should be determined by the c_i:c_a ratio (higher values of one quantity being consistent with lower values of the other), temperature (as higher V_{cmax} is required to achieve a given assimilation rate at higher temperatures), and incident photosynthetically active radiation (PAR) (as productive investment in V_{cmax} is directly proportional to the available PAR). N_{area} is generally found to be roughly proportional to Rubisco content, and thus to V_{cmax} at standard temperature, although leaf N also has structural and defensive components that are roughly proportional to LMA and represent a largely independent source of variation in N_{area} (Dong *et al.*, submitted). So far, these predictions have been supported for seasonal variations within individual plants (Togashi *et al.*, in revision), and for spatial variations along environmental gradients (Prentice *et al.*, 2014; Dong *et al.*, submitted). Here we extend their application to biotically conditioned, microenvironmental variation within forest environments. The framework provided by the least-cost and coordination hypotheses suggest moreover that shade tolerance, and stem properties such as height and wood density, should also be related to leaf metabolic and structural traits, as proposed e.g. by Whitehead *et al.* (1984) and many later commentators.

The least-cost and coordination hypotheses are based on optimality concepts, whose rationale depends on the heuristic principle that natural selection has eliminated trait combinations that fall short of optimality according to various criteria. Another optimality concept lies behind the Leaf Economics Spectrum, LES (Wright *et al.*, 2004). Fundamentally, the LES simply represents a universal negative correlation between LMA and leaf life-span (Lloyd *et al.*, 2013), which can be considered to arise from a trade-off because (a) carbon available for investment in leaves is limited and (b) long-lived leaves need to be thicker and/or tougher than short-lived leaves in order to avoid high risks of predation by herbivores and other damages. Thus leaves can be short-lived and flimsy or long-lived and thick and/or tough, or somewhere in between. In contrast, short-lived leaves with high LMA would be uneconomic, while long-lived

leaves with low LMA would be unviable.

This study considers four groups of leaf and stem traits. The first group consists of leaf metabolic traits: V_{cmax}, J_{max} and leaf day respiration (R_{day}). This last one has been found to closely correlate with V_{cmax} (Atkin *et al.*, 2000; Weerasinghe *et al.*, 2014). The second group contains the leaf structural/chemical traits N_{area}, P_{area} and LMA, reflecting the LES; although as noted, N_{area} has a metabolic component as well as a structural component and the same may be true for P_{area} (Evans, 1989; Reich *et al.*, 1997; Fyllas *et al.*, 2009). The third group, represented principally by wood density (WD), stands in for plant hydraulics, as denser wood tends also to have lower permeability to water (Sperry, 2003; Lin *et al.*, 2015). Wood density also has an automatic impact on plant growth because height growth is necessarily slower, for a given photosynthetic output, in trees with dense wood. Although the correlation between WD and more directly instrumental traits for plant hydraulics, such as the Huber value (the ratio of cross-sectional sapwood area to subtended leaf area) (Togashi *et al.*, 2015b), vessel density and calibre, and permeability (Reid *et al.*, 2005) is far from perfect, these last traits are much more time-consuming to measure and thus comparatively under-represented in available data sets. We anticipate that plants with an aggressive water use strategy should present higher conductivity and lower average WD, while plants adapted to environments with long droughts, or vulnerable to water use competition, should tend to adopt a more conservative water-use strategy and to have high-density wood. The fourth group reflects the ability to compete with other species for light, expressed as potential maximum height (H_{max}): taller plants are able to harvest more light while shorter plants are often more shade-tolerant (Turner, 2001). This group also includes the c_i:c_a ratio, which has been reported to show a negative relationship with height (Koch *et al.*, 2015).

Leaf-level measurements were conducted in tropical forests of Queensland, Australia and Yunnan, China, and combined with (a) published and unpublished datasets on H_{max}, WD, and (b) expert information on the species' vegetation dynamical roles. Thus we are able to present what is (to our knowledge) the first study to analyse key biochemical rates in the context of tree species contrasting dynamical roles, and the first empirical trait-based analysis to include measured biochemical rates in a PFT classification. The objective of this work was to quantify trait variation within these forests that can be linked to dynamical roles. We also aimed specifically to test the following predictions: (i) within the same climate, photosynthetic capacity should be governed by incident PAR (a prediction of the coordination hypothesis); (ii) c_i:c_a should be lower at high H_{max} because water transport is more expensive with increasing height

(a prediction of the least-cost hypothesis); and (iii) pioneer species should tend to have low WD (an expectation from the theory of forest dynamics).

4.4 Materials and methods

4.4.1 Sites

Our analysis includes in total material from 232 evergreen angiosperm tree species (431 leaf samples, one leaf per each individual tree) from intact moist tropical forests of Queensland, northern Australia (from the inland Atherton Tablelands to Cape Tribulation near the Pacific coast) and Yunnan, southwestern China (the Xishuangbanna region in southern Yunnan, near the land borders with Myanmar, Thailand and Laos). Field campaigns conducted in Queensland (Robson Creek and Cape Tribulation) and Yunnan yielded data on 191 species. Data from these campaigns were combined with data on a further 41 Queensland species, from field studies carried out by the TROpical Biomes In Transition (TROBIT) network (Bloomfield *et al.*, 2014). Climates covered by the sampled areas range in mean annual precipitation (MAP) from 1427±443 to 3671±828 mm (Harris *et al.*, 2014; Hutchinson, 2014c) and in mean annual temperature (MAT) between 19.0±0.4 and 24.3±0.4°C (Harris *et al.*, 2014; Hutchinson, 2014a,b). Both Queensland and Yunnan have a marked wet season in summer and dry season in the winter. Gridded data at 0.01°resolution on MAP, MAT, the annual Moisture Index (MI, the ratio of precipitation to equilibrium evaporation) and mean monthly photosynthetic active radiation (mPAR) were acquired for the Australian sites at www.emast.org.au. The Chinese climatology data were derived from records at 1814 meteorological stations (740 stations have observations from 1971-2000, the rest from 1981-1990: China Meteorological Administration, unpublished data), interpolated to a 0.01°grid using a three dimensional thin-plate spline (ANUSPLIN version 4.36, Hancock and Hutchinson, 2006). Figure 4.1 and Table 4.1 provide further details on sites and climates.

4.4.2 Gas exchange measurements and photosynthetic variables

We used a portable infrared gas analyser (IRGA) system (LI-6400; Li-Cor, Inc., Lincoln, NB, USA) to perform leaf gas-exchange measurements. Sunlit terminal branches from

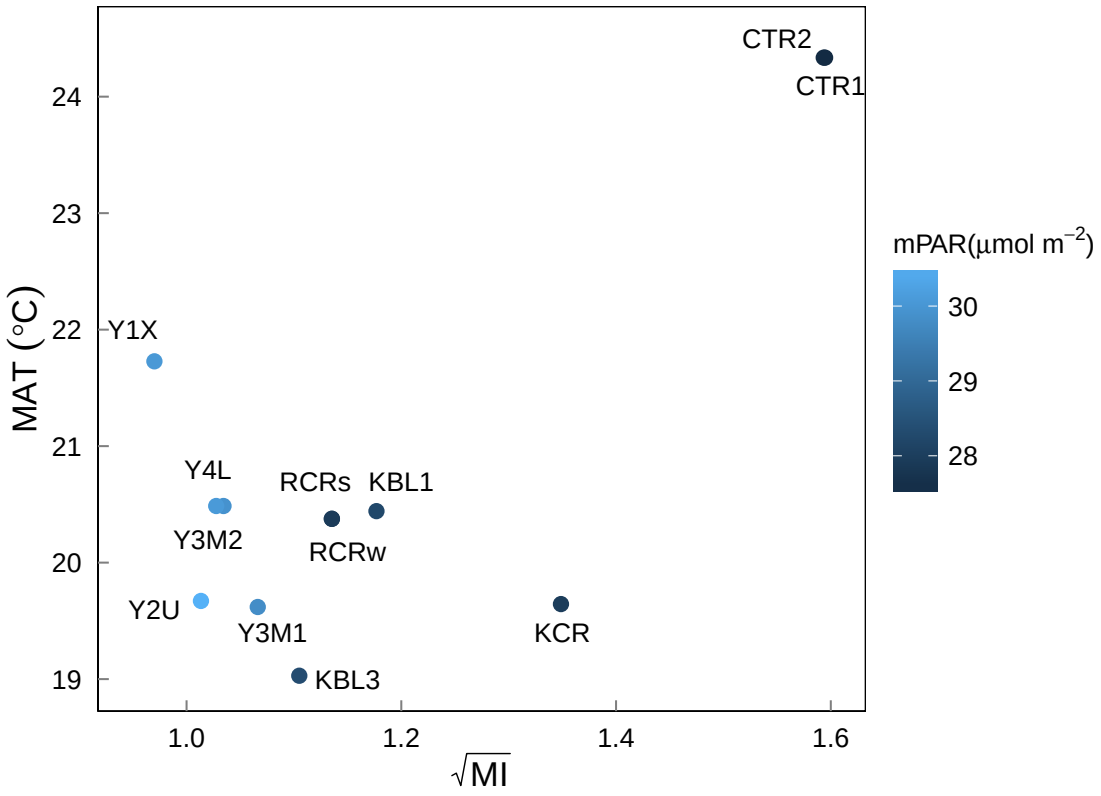

FIGURE 4.1: Mean annual temperature (MAT, °C), the square root of Moisture Index (MI, ratio of precipitation to potential evaporation) and mean monthly photosynthetic active radiation (mPAR, µmol m^{-2}) for in north-east Australia (CTR1, CTR2, KBL1, KBL3, KCR, RCRs, RCRw) and south-east China (Y1X, Y2U, Y3M1, Y3M2, Y4L).

the top one-third of the canopy were collected and immediately re-cut under water. One of the youngest fully expanded leaves, attached to the branch, was sealed in the leaf chamber. Measurements in the field were taken with relative humidity and chamber block temperature close to those of the ambient air at the time of measurement. The rate of airflow was held constant at 500 µmol s^{-1}, but exceptionally the flow was reduced (to a minimum of 250 µmol s^{-1}) under very low stomatal conductance.

We obtained 130 A-c_i curves from Robson Creek (RCRs and RCRw). The CO_2 mixing ratios for the A-c_i curves proceeded stepwise down from 400 to 35 and up to 2000 µmol s^{-1}. Prior to the measurements, we tested plants to determine appropriate light-saturation levels. The photosynthetic photon flux density (PPFD) adopted for measurement ranged between 1500 and 1800 µmol m^{-2} s^{-1}. After measuring the A-c_i curves over about 35 minutes, light was set to zero for five minutes before measuring mitochondrial respiration in the dark (R_{dark}). Following the protocol of Domingues

Table 4.1: Climate averages (MAT = mean annual temperature, MI = Moisture Index, mPAR = mean monthly photosynthetic active radiation), geographic location and soil properties (CEC = cation exchange capacity, TN = total soil nitrogen, TP = total soil phosphorus) of the study sites in north-east Australia (CTR1, CTR2, KBL1, KBL3, KCR, RCRs, RCRw) and south-east China (Y1X, Y2U, Y3M1, Y3M2, Y4L)

SITE	LON	LAT	Altitude (m)	MAT (°C)	MAP (mm)	mPAR (µmol m^{-2})	MI	CEC (cmol kg^{-1})	TN (%)	TP (%)
CTR1	145.45	−16.10	64	24.3	3671	27.5	2.54		0.02	0.01
CTR2	145.45	−16.10	90	24.3	3671	27.5	2.54		0.02	0.01
KBL1	145.54	−17.76	761	20.4	1976	28.2	1.39	10.83	0.08	0.03
KBL3	145.54	−17.69	1055	19.0	1726	28.3	1.22	11.11	0.08	0.03
KCR	145.60	−17.11	813	19.6	2541	27.9	1.82	9.81	0.01	0.01
RCRs	145.63	−17.12	700	20.4	1813	27.9	1.29	9.81	0.01	0.01
RCRw	145.63	−17.12	700	20.4	1813	27.9	1.29	9.81	0.01	0.01
Y1X	101.27	21.92	502	21.7	1427	30.1	0.94	8.68	0.08	0.04
Y2U	101.24	21.98	1075	19.7	1562	30.6	1.03	6.09	0.08	0.04
Y3M1	101.58	21.61	668	19.6	1662	29.8	1.14	10.21	0.08	0.05
Y3M2	101.58	21.62	828	20.5	1604	29.9	1.07	10.21	0.08	0.05
Y4L	101.58	21.62	1034	20.5	1604	30.1	1.06	10.21	0.08	0.05

et al. (2010), we discarded 37 of a total 167 A-c_i curves in which gs declined to very low levels, adversely affecting the calculation of V_{cmax}. These procedures were very similar to the ones applied to the 187 A-c_i curves obtained in the TROBIT sites (CTR2, KBL1, KBL3 and KCR) and are further described in Bloomfield *et al.* (2014).

We sampled 114 leaves in Yunnan (Y1X, Y2U, Y3M1, Y3M2, Y4L) and data for 62 leaves was obtained from Cape Tribulation (CTR1: Weerasinghe *et al.*, 2014). We repeated the same sampling methods for Yunnan and Cape tribulation. The PPFD was held constant at 1800 µmol m^{-2} s^{-1}. For each leaf, we first set the CO_2 mixing ratio to 400 µmol mol^{-1} to obtain the rate of photosynthesis under light saturation (A_{sat}) and related variables. Measurement was taken under stable conditions of gs (> 0.5 µmol m^{-2} s^{-1}), CO_2 and leaf-to-air vapour pressure deficit. The next step was to increase the CO_2 mixing ratio to 2000 µmol mol^{-1} in order to register the rate of photosynthesis under light and CO_2 saturation (A_{max}). R_{dark} was not measured in Yunnan. For R_{dark} in CTR1, the leaf was wrapped in foil sheets after A_{sat} and A_{max} measurements. There was a waiting period of at least 30 min of darkness before taking R_{dark} values. Triose phosphate utilization (Sharkey *et al.*, 2007) limitation was not considered, as it would be unlikely to occur at our field temperatures > 22°C.

Apparent values of V_{cmax}, J_{max} and mitochondrial respiration in presence of light (R_{day}) were fitted using the Farquhar *et al.* (1980) model. Unlimited mesophyll con-

ductance (Miyazawa and Kikuzawa, 2006; Lin *et al.*, 2013) remains the standard implementation of the Farquhar model although it is recognized to be an approximation that results in an overestimation of V_{cmax} and J_{max}, hence all of the values estimated are (as in most of the ecophysiological literature) 'apparent' V_{cmax} and J_{max} values. In cases where A-c_i curves and R_{dark} were not measured we estimated V_{cmax} from A_{sat} by the so-called one-point method, which simply inverts the equation for Rubisco-limited photosynthesis, taking into account the measured c_i and temperature by applying the temperature dependences of the Michaelis-Menten coefficients of Rubisco K_c, K_o and the photorespiratory compensation point, Γ^* from Bernacchi *et al.* (2001). This method relies on the assumption that light-saturated photosynthesis is Rubisco-limited, which has been found to be true in almost all cases (De Kauwe *et al.*, accepted). J_{max} was estimated from A_{max} in an analogous way (Bernacchi *et al.*, 2003) from A_{max} measurements.

4.4.3 Nutrient analyses

After completion of the leaf gas-exchange measurements, the leaf was retained to determine leaf area, dry mass, and mass-based N and P concentrations (mg g^{-1}). Leaves were sealed in plastic bags containing moist tissue paper to prevent wilting. Leaf area was determined using a 600 dots/inch flatbed top-illuminated optical scanner and Image J software (http://imagej.nih.gov/ij/). Leaves were dried in a portable desiccator for 48 hours, to be preserved until the end of the campaign. Subsequently, in the laboratory, leaves were oven-dried for 24 hours at 70°C and the dry weight determined (Mettler-Toledo Ltd, Port Melbourne, Victoria, Australia). LMA (g m^{-2}) was calculated from leaf area and dry mass. Nmass and Pmass were obtained by Kjeldahl acid digestion of the same leaves (Allen *et al.*, 1974). The leaf material was digested using sulphuric acid 98% and hydrogen peroxide 30%. Digested material was analyzed for N and P using a flow injection analyser system (LaChat QuikChem 8500 Series 2, Lachat Instruments, Milwaukee, WI, USA). Area-based N and P values (mg m^{-2}) were calculated as products of LMA and Nmass or Pmass. TROBIT nutrient analysis were performed using similar methods but different equipment, as described in Bloomfield et al. (2014).

4.4.4 Wood density and tree height

Twenty-year series of wood density (WD), tree height (H), and tree diameter at breast height (D) were obtained from (Bradford *et al.*, 2014) (n = 138). Maximum tree

height (H_{max}) was estimated using the derivative of the Mitscherlich function relating diameter and height (Li *et al.*, 2014):

$$\frac{dH}{dD} = a\, exp\left(\frac{-a\, D}{H_{max}}\right) = a\left(1 - \frac{H}{H_{max}}\right) \quad (1)$$

where a is the initial slope of the relationship between height and diameter.

4.4.5 Vegetation dynamical roles

Australian species ($n = 262$) were assigned to dynamical roles with the help of the database published by Bradford *et al.* (2014), which gives the authors' expert assessment based on over 20 years' experience in plant identification and rainforest dynamics research in tropical Australia, while Chinese species ($n = 85$) were assigned by a geobotanist and taxonomist from the Xishuangbanna Botanical Garden, Professor Zhu Hua (A1: Dynamic roles based on expert assessment). The classification was implemented accordingly to the Shugart (1984) framework, which can also be related to those of Denslow (1987), Turner (2001), and Fyllas *et al.* (2012):

(1) Requires a gap, and produces a gap. These are long-lived pioneers that reach the canopy.

(2) Doesn't require gap, but produces a gap. These are long-lived climax species that reach the canopy and grow large.

(3) Requires a gap, but doesn't produce a gap. These are short-lived pioneers that never grow large.

(4) Doesn't require a gap, and doesn't produce a gap. These are subcanopy species.

4.4.6 Statistical analyses

All statistics were performed in R (R Core Team, 2012). For graphing we used the ggplot2 package (Wickham, 2010). Moisture index was represented in Figure 4.1 as its square root, a transformation appropriate to precipitation values generally (M.F. Hutchinson, pers. comm. 2011) which approximately normalizes the distribution of values and thus contains the spread of values at the high end. V_{cmax}, J_{max}, R_{day}, LMA, N_{area}, P_{area}, H_{max} and WD data were all $\log_{10}$-transformed, unless otherwise indicated, to approximate a normal distribution of values. The ratio c_i:c_a was logit- rather than log-transformed as this variable is bounded between 0 and 1, and the logit transformation results in approximately linear relationships between the transformed ratio and environmental predictors including temperature (Prentice *et al.*, 2014). Or-

dinary least-squares linear regression (lm) was used to test relationships between plant traits and climate variables. Pairwise combinations of quantitative traits were tested for significant relationships across all data, and within groups corresponding to high and low MI, high and low mPAR, and high and low MAT. Slopes and elevations of regressions were compared using standardized major axis regression with the smatr package (Warton *et al.*, 2006). We used the package vegan (Oksanen *et al.*, 2015) to assess multivariate trait variation, using the following methods:

- Principal component analysis (PCA) of nine plant traits (V_{cmax}, J_{max}, R_{day}, LMA, N_{area}, P_{area}, H_{max} and WD);
- Redundancy analysis (RDA) of the same nine traits, constrained by three climate variables (MI, mPAR, and MAT);
- Redundancy analysis (RDA) of the same nine traits, constrained by dynamic roles (as factors); and
- Redundancy analysis (RDA) of the same nine traits, constrained simultaneously by both climate and dynamic roles.

PCA was used to identify patterns of covariation among traits irrespective of their dynamical or environmental correlates; RDA to analyse multivariate trait relationships to predictors. Note that PCA is an exploratory method with no associated formal test of significance. By contrast, the significance of trait-environment relationships identified by RDA can be assessed in a similar way to generalized linear models (see e.g. Ter Braak and Prentice, 1988). The K-means (R Core Team, 2012) clustering method was used to create four groups of species based on the nine plant traits (A2: Dynamic roles based on quantitative assessment). K-means clustering was performed with the number of iterations set to 100 and bootstrapped with 10,000 repetitions. RDA and bivariate correlations were used to compare A2 and A1. The dataset used for PCA and RDA analysis consist of 130 observations where data was available for all traits, climatologies and dynamic roles. All RDA visualizations here follow the response-variable focused 'Type 2 scaling' (Oksanen *et al.*, 2015), such that the angles between pairs of vectors as plotted approximate their pairwise correlations. For PCA and RDA input data where direct measurements of R_{dark} were not available, R_{day} ($n = 58$) was estimated from A_{sat} following (Prentice *et al.*, 2014) using the approximation $R_{day} \approx 0.01\ V_{cmax}$ (De Kauwe *et al.*, accepted).

4.5 Results

4.5.1 Trait values and dimensions of variation

Average values of the metabolic traits V_{cmax}, J_{max}, and R_{day} were 52.0, 82.0, and 0.63 µmol m^{-2} s^{-1} respectively. The corresponding ranges were 4.2 to 148.9, 14.0 to 203.6, and near-zero to 3.70 µmol m^{-2} s^{-1}. Average values of the chemical/structural traits LMA, N_{area} and P_{area} were 110.9 x 10^3, 0.19 and 0.013 mg m^{-2} with ranges of 12.04 to 610.3 x 10^3 (LMA), near-zero to 1.49 mg m^{-2} (N_{area}), and near-zero to 0.06 mg m^{-2} (P_{area}). Average values of c_i:c_a, H_{max} and WD were 0.71, 26.3 m and 0.55 g cm^{-3} with ranges of 0.39 to 0.94, 1.3 to 54.5 m, and 0.33 to 0.98 g cm^{-3} respectively.

Four orthogonal dimensions of trait variation were identified based on the PCA and correspond to the metabolic, chemical/structural, hydraulic and height trait groups described above (Figure 4.2, Table 4.2). Metabolic traits V_{cmax}, J_{max} and R_{day} varied continuously and in close correlation with one another. V_{cmax} and c_i:c_a were negatively correlated (not shown), but the correlation was weak. Table 4.2 makes it clear that c_i:c_a does not belong to the metabolic dimension. The chemical/structural traits LMA, N_{area} and P_{area} were positively correlated with one another ($p < 0.05$), the pairwise relationship of P_{area} to LMA however being weaker than that of N_{area}. The strong correlation between LMA and N_{area} suggests that much of the N content in the leaf is structural rather than metabolic in these plants. A PCA using mass- instead of area-based leaf nutrients similarly clustered LMA, N and P on the second axis (not shown). The third dimension was mostly represented by variation in WD, with some contribution from P_{area}. Finally H_{max} and c_i:c_a had a non-significant negative pairwise relationship and were associated with the fourth dimension, suggesting a trade-off between water loss and the length of the water-transport pathway. These dimensions of trait variation are slightly different from the ones found by Baraloto *et al.* (2010) but broadly in agreement with those described by Fyllas *et al.* (2012) and Reich (2014).

4.5.2 Contribution of climate variables to trait variation

Regression slopes between V_{cmax} and J_{max} for both high MI and low MI groups were statistically distinct ($p < 0.05$, Figure 4.3), and the same was true for high versus low mPAR and MAT groups (Figure 4.3). Regressions for V_{cmax} versus N_{area} were not significant within these climatic groups ($p < 0.05$, Figure 4.3) but the relationship was significant, albeit weak, when all of the data were considered together (not shown:

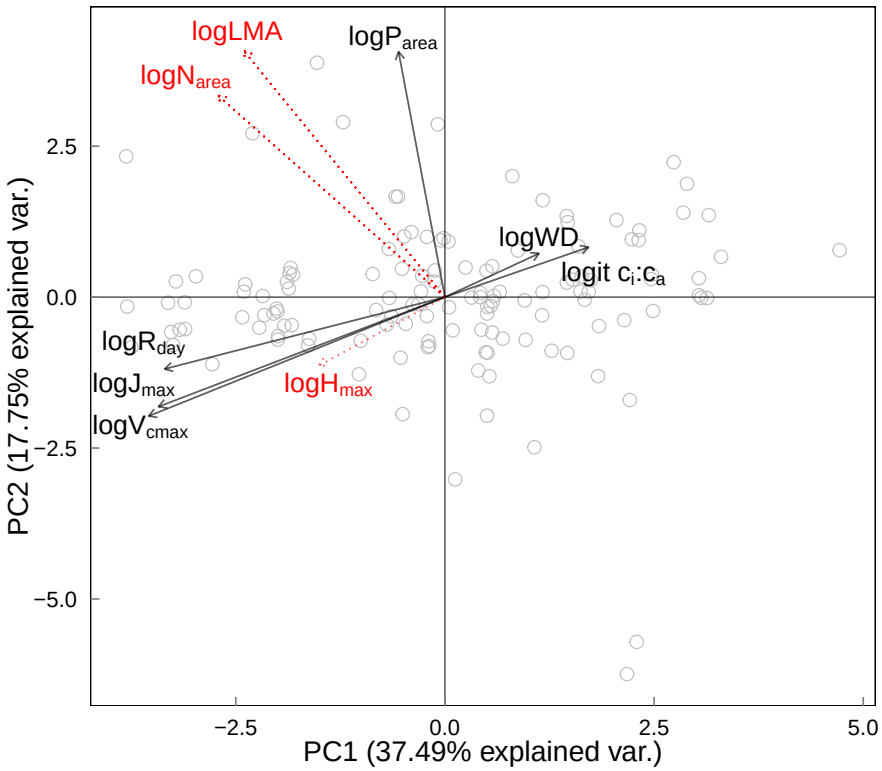

FIGURE 4.2: Principal component analysis (PCA) of nine traits in north-east Australia and south-east China ($n = 130$). Red dotted lines and names extend backwards from the plane of the paper; and black lines and names protrude forwards towards the observer.

TABLE 4.2: Principal Component Analysis (PCA) loadings for nine traits in north-east Australia and south-east China ($n = 130$). The highest correlations ($|> 0.45|$) are indicated with boldface.

	PC1	PC2	PC3	PC4
logV_{cmax}	**−0.48**	−0.27	0.21	0
logJ_{max}	**−0.46**	−0.25	0.18	0.04
logR_{day}	**−0.45**	−0.16	0.27	−0.01
logLMA	−0.32	**0.55**	−0.21	0.03
logN_{area}	−0.37	**0.45**	−0.24	−0.12
logP_{area}	−0.08	**0.54**	**0.45**	0.03
logWD	0.15	0.10	**0.68**	−0.16
logH_{max}	−0.20	−0.15	−0.24	**−0.74**
logitc_i:c_a	0.23	0.11	0.16	**−0.64**
	PC1	PC2	PC3	PC4
Standard deviation	1.84	1.26	1.09	0.98
Proportion of Variance	0.37	0.18	0.13	0.11
Cumulative Proportion	0.37	0.55	0.68	0.79

slope = 0.69, R2 = 0.10, $p < 0.05$). High MI and low mPAR were associated with high V_{cmax}, J_{max}, N_{area} (Figure 4.3), R_{day}, and LMA (not shown) individually. The remaining plant traits c_i:c_a, P_{area}, H_{max} and WD presented very scattered values for the same range of MI and mPAR. All traits had high and low values spanning the full range of MAT.

The clustered vectors for metabolic traits, MI and MAT in Figure 4.4 indicate that within this data set, higher moisture and air temperature favour species with higher metabolic rates (Figure 4.4). The RDA constrained by climate variables explained 35% of trait variation - with 20% and 11% on axes 1 and 2 respectively ($p < 0.05$, Figure 4.4) representing an unexpectedly large fraction of the trait variation, considering the relatively slight variation of MAT (19 to 24°C), mPAR (27.4 to 30.5 µmol m^{-2}) and MI (0.9 to 2.5) among these tropical moist forest sites. However, no individually significant trait-climate variable relationships were found. Association of high metabolic rates with aridity (Prentice *et al.*, 2011) is commonly found when considering longer climate gradients, but not within this data set. Thus, the analysis suggests that it is worthwhile to seek associations between the observed traits and dynamical roles, independent of climate.

4.5.3 Contribution of dynamical roles to trait variation

The decision regarding how the four groups clustered by K-means were associated to dynamic roles for A2 rested on the degree of correspondence of means of plant traits obtained by each group and the classification by Shugart (1984). H_{max} was the primary trait to determine if a cluster was climax - large pioneer or small pioneer - subcanopy. Higher photosynthetic traits defined tall trees as climax, as opposed to large pioneer, and small trees as small pioneer, as opposed to subcanopy.

Expert (A1) and quantitative (A2) role definitions explained 23% and 55% of total plant trait variance, respectively, as shown in Figure 4.5. The greater variance explained by the A2 classification is to be expected as the clustering was performed using the same trait data represented in the RDA. Nonetheless, the RDA results obtained with the two classifications are quite similar to one another. The major common patterns shown in the two RDA plots are as follows:

(1) The metabolic traits V_{cmax}, J_{max}, R_{day} and the structural-chemical traits N_{area} and LMA tending to be higher in climax species versus the rest;

(2) P_{area} tending to be greater in subcanopy species versus the rest; and

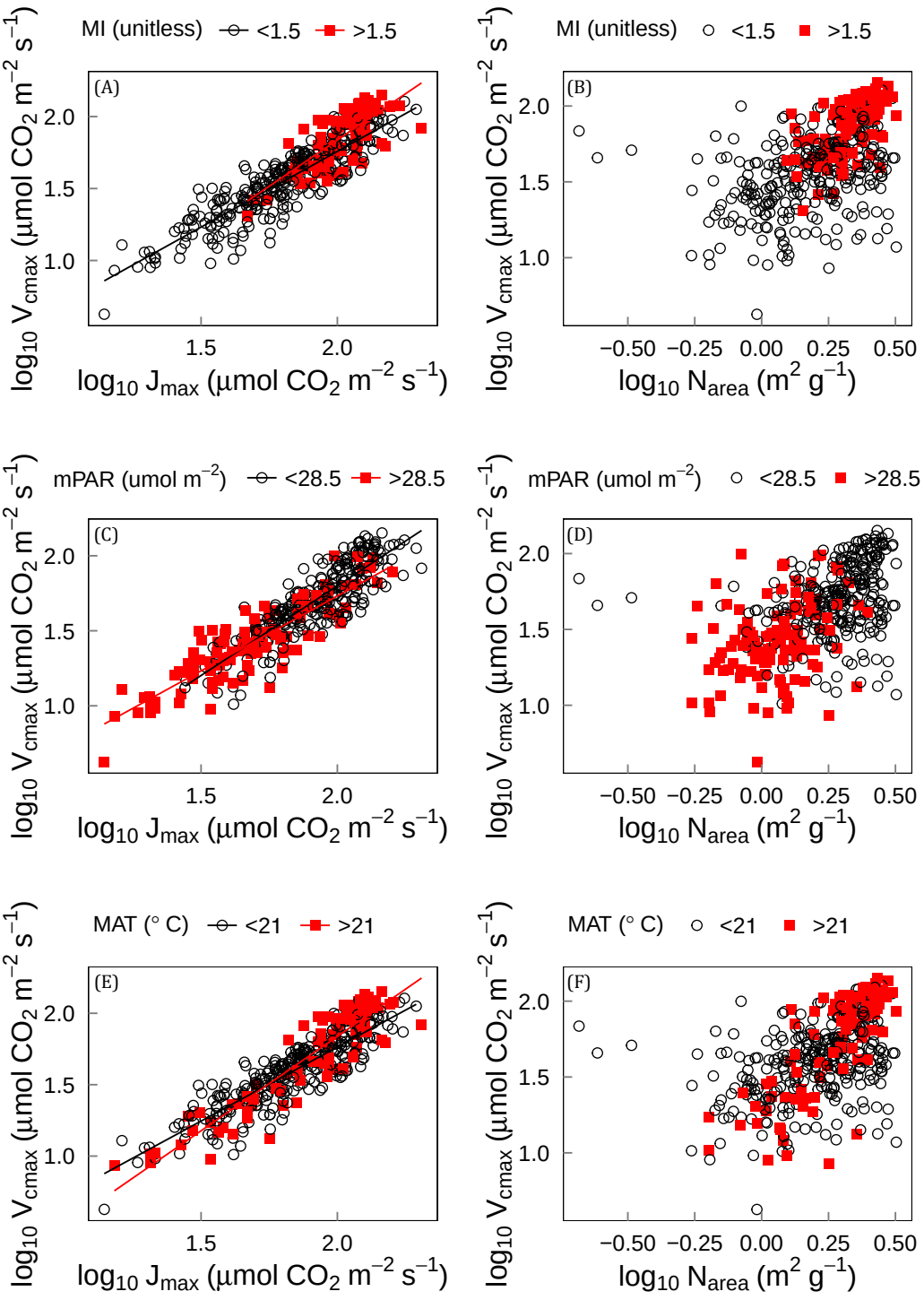

FIGURE 4.3: Bivariate relationships of $\log_{10}V_{cmax}$ versus $\log_{10}J_{max}$ and $\log_{10}V_{cmax}$ versus $\log_{10}N_{area}$, within groups defined by high and low values of climate variables (3A and 3B: MI; 3C and 3D: mPAR; 3E and 3F: MAT) ($n = 431$). Significant linear regressions ($p < 0.05$) are shown.

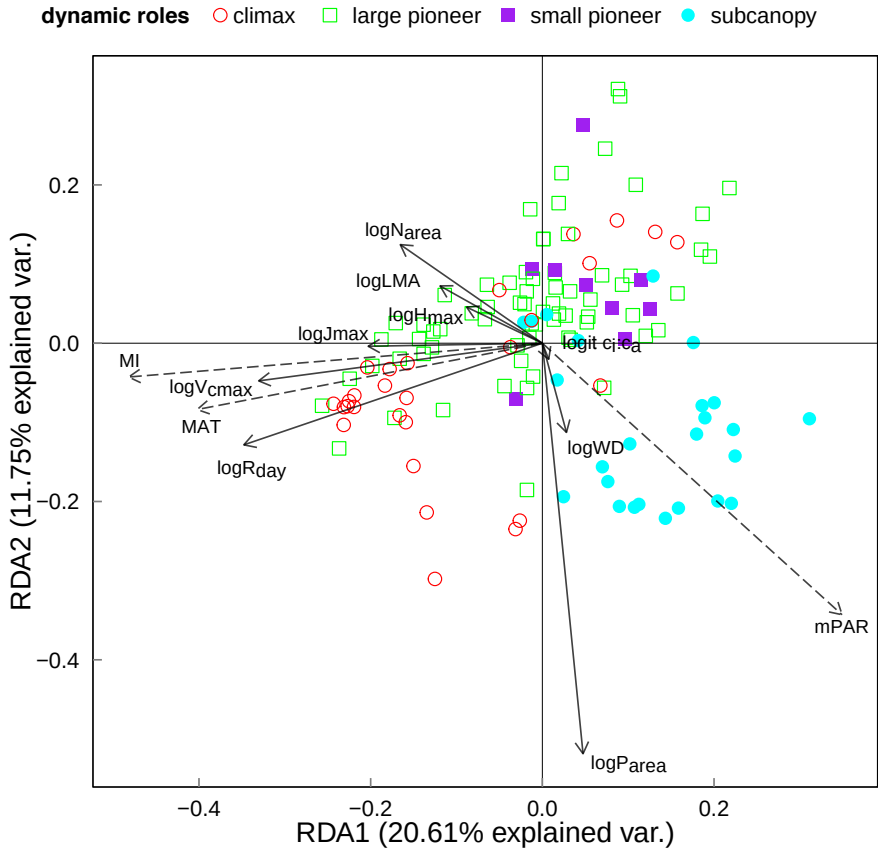

Figure 4.4: Redundancy analysis (RDA) of nine traits constrained by climate variables (MAT, MI, mPAR) in north-east Australia and south-east China ($n = 130$, $p < 0.05$). Dynamic roles do not participate in this RDA calculation and are shown for visual assessment.

(3) WD tending to be smaller in pioneer species versus the rest.

These distinctions are supported, and further information provided, by the summary statistics for trait variation within each group (Figure 4.6). Climax species consistently presented the highest values of V_{cmax}, J_{max}, R_{day}, LMA, N_{area}, and H_{max} (with large pioneer species sharing top position for H_{max}). High WD, consistent with slow growth, characterized the subcanopy species. The outstanding difference between the large and small pioneers was simply H_{max}. The c_i:c_a ratio was lowest in climax species. Gap-requiring and gap creating pioneers have lower V_{cmax} associated to higher c_i:c_a (higher stomatal conductance). The scaling slopes of the bivariate relationships between V_{cmax} and J_{max} and between V_{cmax} and N_{area} were largely similar within each group, whether the roles were defined quantitatively or by expert assessment (Figure

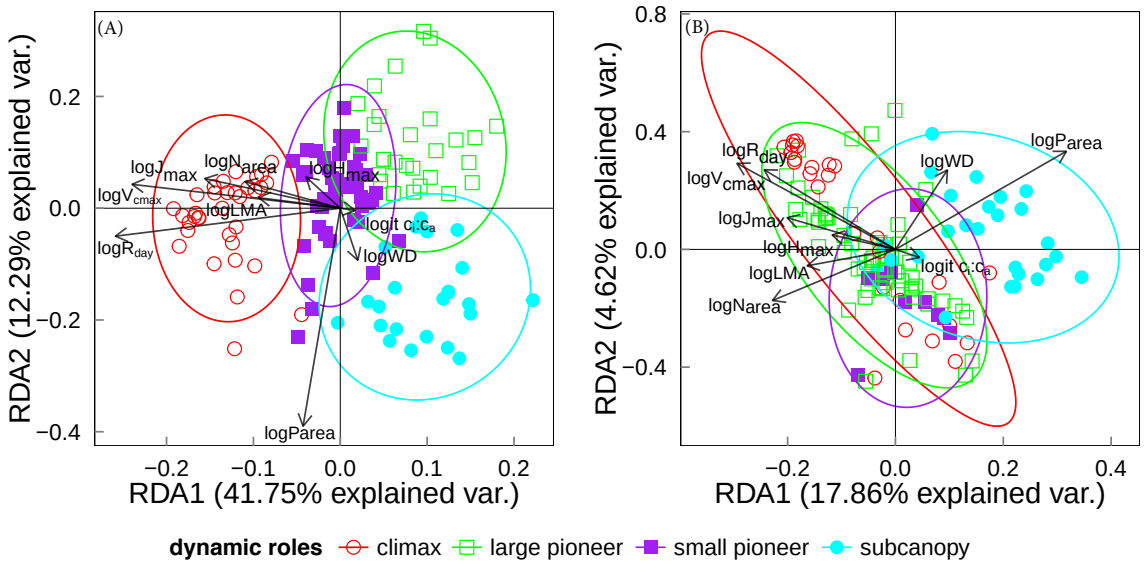

FIGURE 4.5: Redundancy analysis (RDA) of nine traits constrained by dynamic roles, defined by quantitative (5A) versus expert (5B) assessment in north-east Australia and south-east China($n = 130$). Ellipses represent 95% confidence intervals around the centroid of each group.

4.7).

4.5.4 Partitioning trait variance to climate variables versus dynamical roles

RDA constrained by the two sets of predictors both separately and collectively provides the necessary information to partition the total explained variation into the unique contributions of each set and a combined contribution associated with covariation of the two sets (not shown). Based on the quantitative assessment of dynamical roles (A2), RDA constrained by both sets of predictors explained 61% of trait variation, which could be partitioned as follows: 26% from dynamical roles alone, 6% from climate alone, and 29% from the combination. The corresponding figures based on expert assessment were as follows: 43% of trait variation explained, composed of 8% from dynamical roles alone, 20% from climate alone, and 15% from the combination.

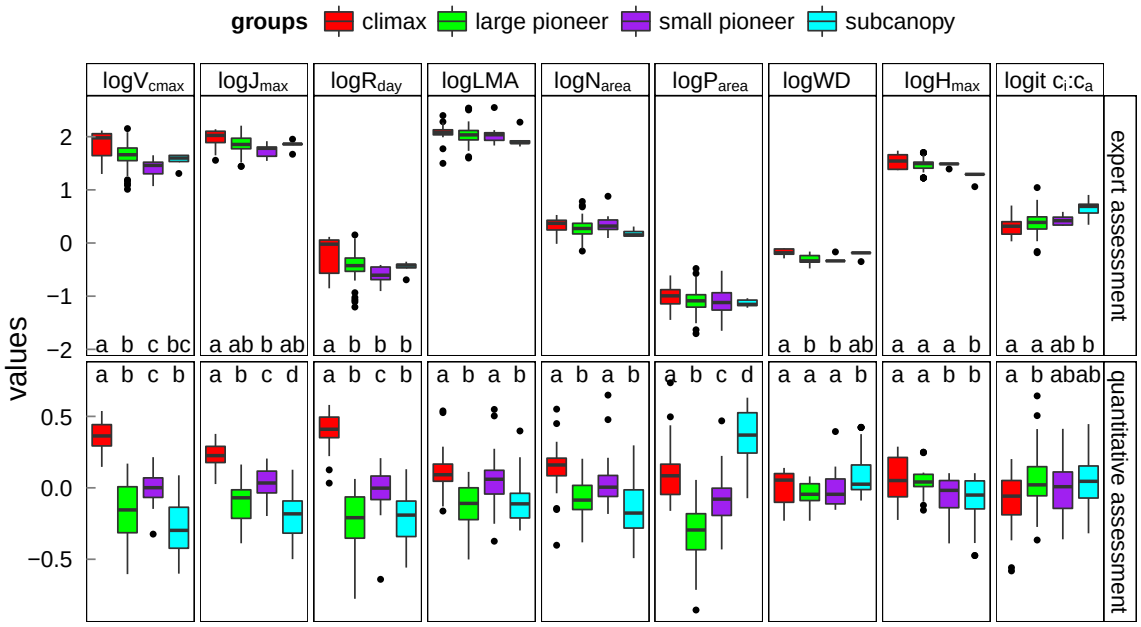

FIGURE 4.6: Box plots showing means and standard deviation of nine traits per four dynamic roles based on quantitative versus expert assessment ($n = 130$, $p < 0.05$). 'Expert' group averages of LMA, N_{area} land P_{area} are not significantly different (ANOVA). Dynamical roles of each trait sharing the same letter (Tukey *post hoc* test) are not significantly different.

4.6 Discussion

The existence of coordinated variation in plant traits is key to explaining species strategies, community assembly and ecosystem structure and function (Reich, 2014). Recent analyses have started to explore plant trait diversity and plasticity with a view to more realistic modelling of plant and vegetation processes, whether for local or global model applications (Fyllas *et al.*, 2009, 2012; Quesada *et al.*, 2012). Our study has provided support for the idea that forest dynamic roles, as described by Shugart (1984), might be systematically related to key biophysical and physiological traits that are used in DGVMs. Moreover, our results have supported certain specific predictions of the least-cost and coordination hypotheses, which collectively hold the promise of providing general, testable trait-environment relationships that could greatly reduce the excessive number of parameters required by most current DGVMs.

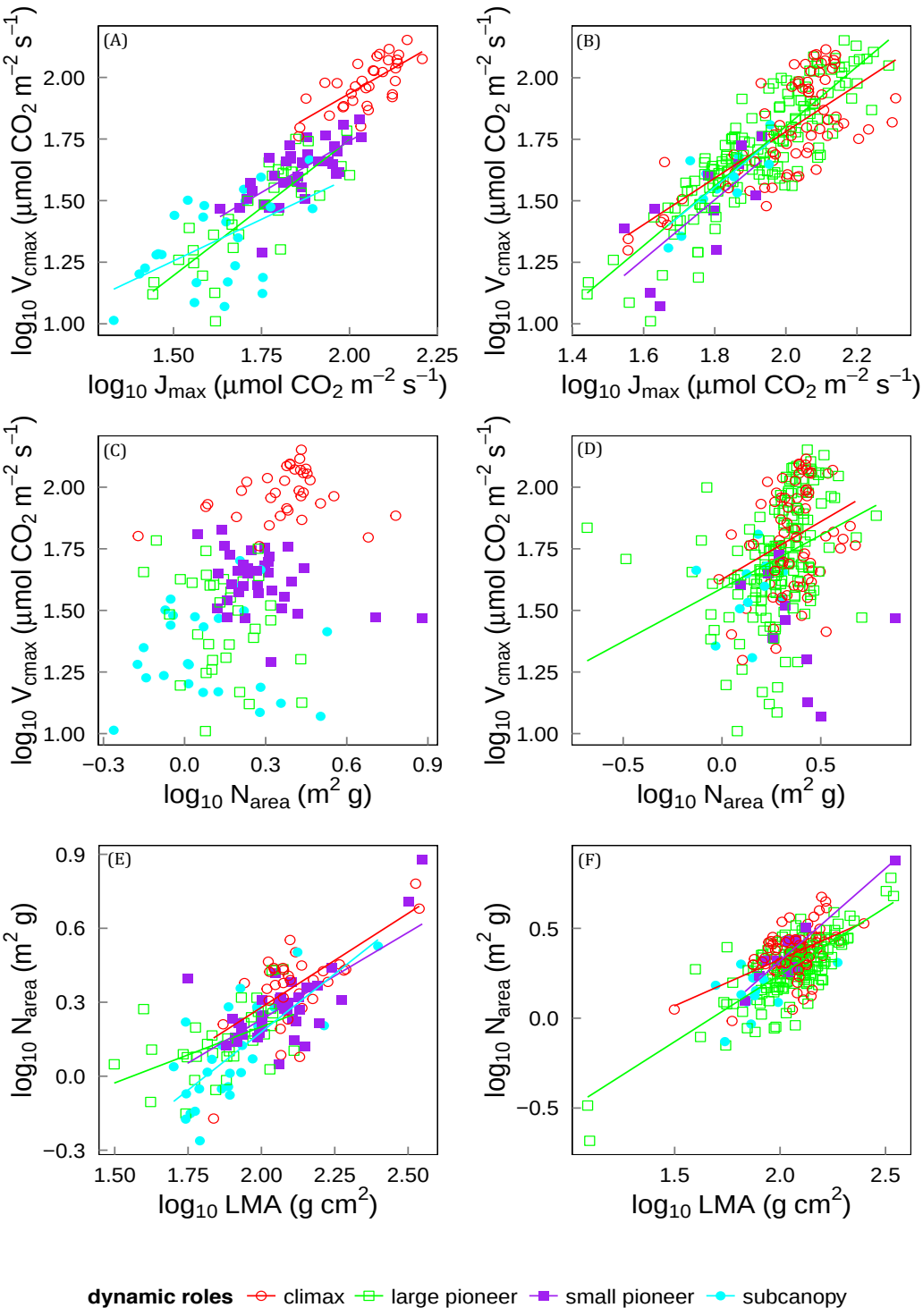

FIGURE 4.7: Bivariate relationships of V_{cmax} versus J_{max}, V_{cmax} versus N_{area} (upper panels) and N_{area} versus LMA (lower panels) within dynamical role groups, according to quantitative (left, $n = 130$) versus expert (right, $n = 262$) assessment. Significant linear regressions between $\log_{10}$-transformed variables are shown ($p < 0.05$).

4.6.1 Dynamic roles and the coordination hypothesis

A core prediction of the coordination hypothesis is that J_{max} and V_{cmax} should be higher under high illumination and lower in the shade, as seen both in the vertical gradient of light-saturated assimilation rates in dense canopies (Chen *et al.*, 1993) and more generally, in the solar radiation gradient across canopies situated in diverse environments (Maire *et al.*, 2012). Among dynamical roles, top-canopy climax species are expected to receive most PAR and therefore (optimally) should have the highest photosynthetic capacity, while subcanopy species should have the lowest. Our results support these predictions for tropical moist forests. Pioneer (gap-requiring) species would be expected to have intermediate photosynthetic capacity and this too is consistent with our findings. Additionally, the widely reported conservative ratio of J_{max} and V_{cmax} seems to be maintained, both within and across dynamic roles. The association of R_{day} with V_{cmax} and J_{max} was also found to be strong, with R_{day} maintaining a near constant ratio for leaves whether in sun-exposed or shade conditions, as previously reported (e.g. by Hirose and Werger, 1987; Weerasinghe *et al.*, 2014; Atkin *et al.*, 2015).

The observed relationships among N_{area}, P_{area} and LMA, and the weaker correlations of these traits with primary metabolic traits, reflect the fact that a substantial part of the N and P content of leaves is not tied to photosynthetic functions (Dong *et al.*, submitted). The photosynthetic component of N_{area} should also be proportional to incident PAR. Strong linear relationships between V_{cmax} and N_{area} seem to be widely expected (Evans, 1989; Chen *et al.* 1993, Domingues *et al.*, 2010) but are not always supported (Prentice *et al.*, 2014; Togashi *et al.*, in revision; this work), perhaps due to the overpowering effect of variation in structural and defensive components of leaf N. However, N_{area} often can be related to PAR, as confirmed by Dong *et al.* (submitted), and as suggested by our finding of highest N_{area} among climax species.

4.6.2 Dynamic roles and the least-cost hypothesis

It has been reported that c_i:c_a declines with tree height, and this too is a prediction of the least-cost hypothesis (Wang *et al.*, 2014) as the cost of maintaining the water transport pathway increases at with height; therefore, tall trees (and the top stratum of leaves in a tall tree: Koch *et al.*, 2015) should aim for a lower optimum c_i:c_a by investing more in the maintenance of biochemical capacity and less in transport capacity. Even if the 'path length' effect on stem hydraulic conductance is fully compensated by xylem tapering (Tyree and Ewers, 1991; Enquist and Bentley, 2012) as often seems to be the

case, it is still more expensive in terms of sapwood respiration to maintain a tall stem as opposed to a short stem (Prentice *et al.*, 2014). This prediction was confirmed by the low c_i:c_a ratios found here in climax species. However, large pioneer species (with H_{max} equivalent to climax species) did not show this adaptation. Subcanopy species, at least according to the expert classification, did nonetheless show high c_i:c_a ratios, consistent with their short stature. Given a reduced c_i:c_a ratio, the coordination hypothesis then predicts that V_{cmax} should be increased - a mechanism that may additionally contribute to high V_{cmax} found in climax species and low V_{cmax} in subcanopy species.

4.6.3 Dynamic roles, the leaf economics spectrum and the theory of forest dynamics

A third group of predictions broadly supported by our results comes from the framework presented in Shugart (1984), Turner (2001), and Fyllas *et al.* (2012). This approach considers two main axes of ecological specialization, one reflecting canopy position and access to light, the other life span and growth rate. The main advantage for large pioneers in rapidly achieving tall statures is to shade lower canopies nearby, while obtaining rapid access to full sunlight. Compared to climax species, large pioneers adopt a less conservative strategy regarding water use, and are likely to have a shorter lifespan (Shugart, 1984; Reich, 2014). One way to achieve fast growth is to invest in low-density conducting tissues, which implies lower WD. Subcanopy species by contrast are necessarily shade-tolerant and often have traits associated with slow growth. Our results support the existence of this tradeoff, with subcanopy trees having generally high WD (a trait often accompanied by a high density of short and narrow vessels: Reich, 2014).

According to the LES, across species globally, high LMA is linked to longevity of individual leaves; and it has generally been found that LMA varies as much or more within communities as with environmental gradients. Our data do not allow us to address the LMA-lifespan linkage directly. However, the distribution of LMA is not random across the dynamical roles, being greatest in climax species and associated with high V_{cmax} and least in subcanopy species where it is associated with low V_{cmax}. These findings suggest a more nuanced interpretation of the variation in LMA among dynamical roles. Namely: that thick, high-LMA leaves are a pre-requisite for a leaf to attain V_{cmax} commensurate with high levels of PAR at the top of a canopy (Niinemets and Tenhunen, 1997), while thin, low-LMA leaves provide optimum light capture for the least investment in leaves - a good strategy for subcanopy species. Fast-growing

pioneer species with their aggressive water-use strategy also require a low investment in leaf structure, developing thin, low-LMA leaves in order to obtain a quicker return on investment. The downside is that the leaves are likely to be more exposed to losses by herbivory while the low-density stems are subject to the risks of cavitation and embolism, shortening their life expectancy (Enquist and Bentley, 2012).

4.6.4 Partitioning of trait variation

Significant trait variation was found to be linked to climate, even within the narrow climatic range of tropical moist forests. But individual trait-climate relationships were weak and patterns observed across a wider range of climates, such as the widely reported increase of N_{area} with aridity, were not present. Variance partitioning showed that a significant fraction (between 8 and 26%) of trait variation could not be attributed to the temperature and moisture regime, but could be related uniquely to species' dynamical roles.

4.6.5 Implications for modelling

DGVMs based on continuous trait variation have recently emerged as a consequence of the growing realization that PFTs, as conventionally defined, do not adequately describe the genotypic or phenotypic plasticity of plant traits in the real world. However, DGVMs in general (including recent trait-based models) have paid minimal attention to the co-existing functional diversity of traits present in communities where climate variation is small but tree species diversity is large, such as tropical forests. Our results suggest that the framework provided by optimality concepts (the coordination and least-cost hypotheses) can be combined with classical forest dynamics theory, which differentiates complementary survival strategies for tree species in a highly competitive environment, to yield successful predictions that would allow vegetation dynamics to be represented more faithfully in DGVMs. The combination of these different research strands can be achieved quite simply, by extending existing predictions about trait-environment relationships based on optimality considerations to cover biotically induced microhabitat variation within complex plant communities. By providing information on the quantitative trait distinctions between different forest dynamical roles, we have made a first step towards the inclusion of these roles explicitly in the ecophysiological framework of most DGVMs. Next step should further test the methods presented in this work in different ecosystems.

The existence of systematic, adaptive trait variation within a narrow climate range

provides further support for the conclusion (e.g. Meng *et al.*, 2015) that models should avoid fixing PFT-specific values for most quantitative traits. In general, consideration of the adaptive function of trait differences among dynamic roles should contribute to reducing the multiplicity of uncertain parameters, and simultaneously increase the realism, of next-generation DGVMs.

Supporting Information: Dynamical roles dataset

All traits are $\log_{10}$ transformed with exception of logit transformed c_i:c_a.

Units ⇒ V_{cmax}, J_{max} and R_{day} (µmol m^{-2} s^{-1}); LMA (g cm^2); N_{area} and P_{area} (m^2 g^-1); WD (g m^{-3}); H_{max} (m); c_i:c_a (unitless)

As a condition for use of the dataset, we request that users agree:

(1) To notify the main author (Henrique Furstenau Togashi) if the dataset is to be used in any publication;

(2) To recognise that the researchers who gathered these data with formal recognition that may include co-authorship or acknowledgements on publications

Specie	V_{cmax}	J_{max}	R_{day}	LMA	N_{area}	P_{area}	WD	H_{max}	c_i:c_a	Expert	Quantitative
Acacia celsa	1.8	1.86	-0.3	2.54	0.68	-0.64	-0.19	1.43	0.27	large p.	climax
Acronychia acidula	1.63	1.87	-0.55	1.77	-0.02	-1.45	-0.28	1.48	0.13	climax	large p.
Actinodaphne henryi	1.7	1.96	-0.3	2.21	0.2	-0.43	-0.15	0.97	0.21	NA	subcanopy
Actinodaphne henryi	1.24	1.68	-0.76	1.89	-0.08	-0.46	-0.15	0.97	0.47	NA	subcanopy
Ailanthus fordii	1.5	1.7	-0.5	1.74	0.22	-0.94	0.13	1.34	0.59	NA	subcanopy
Albizia lucida	1.6	2	-0.4	1.63	0.11	-1.05	0.15	1.4	0.79	NA	large p.
Aleurites rockinghamensis	1.88	1.98	-0.18	2.02	0.35	-0.99	-0.41	1.66	0.49	large p.	climax
Alphitonia whitei	1.58	1.84	-0.42	2.07	0.32	-1.05	-0.2	1.5	0.41	large p.	small p.
Alphitonia whitei	1.62	1.83	-1.02	1.94	0.22	-1.12	-0.2	1.5	0.58	large p.	large p.
Alphitonia whitei	1.09	1.56	-0.59	2.04	0.28	-0.95	-0.2	1.5	0.32	large p.	subcanopy
Alphitonia whitei	1.75	1.99	-0.31	2	0.25	-1.13	-0.2	1.5	0.53	large p.	small p.
Alphitonia whitei	1.76	1.88	-0.33	2.09	0.3	-1.15	-0.2	1.5	0.5	large p.	small p.
Alphitonia whitei	1.64	1.82	-0.46	1.91	0.08	-1.2	-0.2	1.5	0.65	large p.	large p.
Alphitonia whitei	1.84	1.94	-0.17	2.17	0.31	-1.09	-0.2	1.5	-0.18	large p.	climax
Alstonia muelleriana	1.49	1.76	-0.29	2.05	0.42	-0.87	-0.17	1.43	0.36	large p.	small p.
Alstonia muelleriana	1.76	2.03	-1.07	2.1	0.38	-0.9	-0.17	1.43	0.55	large p.	small p.
Alstonia muelleriana	1.01	1.62	-0.49	1.75	0.08	-1.2	-0.17	1.43	0.5	large p.	large p.

continued on next page

continued from previous page

Specie	V_{cmax}	J_{max}	R_{day}	LMA	N_{area}	P_{area}	WD	H_{max}	c_i:c_a	Expert	Quantitative
Alstonia muelleriana	1.63	1.8	-0.49	1.97	0.14	-1.29	-0.17	1.43	0.37	large p.	large p.
Alstonia muelleriana	1.68	1.83	-0.44	2.06	0.3	-1.14	-0.17	1.43	0.32	large p.	small p.
Alstonia muelleriana	1.26	1.51	-1.11	1.89	0.1	-1.43	-0.17	1.43	0.51	large p.	large p.
Alstonia scholaris	2.15	2.16	0.15	2.05	0.43	-0.84	-0.48	1.7	0.3	large p.	climax
Alstonia scholaris	2.07	2.21	0.07	2.14	0.45	-0.64	-0.48	1.7	0.32	large p.	climax
Alstonia scholaris	1.91	1.88	-0.09	1.94	0.38	-0.98	-0.48	1.7	0.33	large p.	climax
Alstonia scholaris	2.09	2.08	0.09	2.07	0.38	-0.93	-0.48	1.7	0.32	large p.	climax
Alstonia scholaris	1.36	1.69	-0.64	1.73	0.09	-1.03	-0.48	1.7	1.04	large p.	large p.
Alstonia scholaris	1.74	1.88	-0.45	1.78	0.08	-1.26	-0.48	1.7	0.21	large p.	large p.
Antiaris toxicaria	1.12	1.75	-0.88	1.93	0.36	-0.69	0.06	1.16	0.85	NA	subcanopy
Argyrodendron peralatum	2.12	2.11	0.12	2.21	0.43	-0.88	-0.19	1.66	0.35	climax	climax
Argyrodendron peralatum	2.05	2.02	0.05	2.27	0.45	-0.88	-0.19	1.66	0.4	climax	climax
Argyrodendron peralatum	2.09	2.14	0.09	2.18	0.39	-0.81	-0.19	1.66	0.43	climax	climax
Argyrodendron peralatum	2.07	2.11	0.07	2.28	0.43	-0.84	-0.19	1.66	0.4	climax	climax
Baccaurea ramiflora	1.28	1.45	-0.72	1.82	0.02	-1.06	0.18	1.5	0.5	NA	subcanopy
Baccaurea ramiflora	1.55	1.7	-0.45	1.79	-0.05	-0.67	0.18	1.5	0.55	NA	subcanopy
Baccaurea ramiflora	1.01	1.33	-0.99	1.79	-0.26	-0.77	0.18	1.5	0.6	NA	subcanopy
Baccaurea ramiflora	1.35	1.68	-0.65	1.76	-0.15	-0.53	0.18	1.5	0.46	NA	subcanopy
Betula alnoides	1.99	2.13	-0.01	1.87	0.21	-0.73	-0.18	1.48	0.54	NA	climax
Bubbia semecarpoides	1.66	1.87	-0.42	2.27	0.31	-1.04	-0.35	1.06	0.34	subcanopy	small p.
Canarium album	1.36	1.61	-0.64	1.83	0.17	-1.85	-0.3	1.54	0.61	NA	large p.
Cardwellia sublimis	2.03	2.07	0.03	2.02	0.46	-0.99	-0.34	1.49	0.53	large p.	climax
Cardwellia sublimis	1.93	2.01	-0.07	2.12	0.5	-1.09	-0.34	1.49	0.51	large p.	climax
Cardwellia sublimis	1.96	2.06	-0.04	2.1	0.55	-1.03	-0.34	1.49	0.55	large p.	climax
Cardwellia sublimis	1.98	1.96	-0.02	2.13	0.34	-1.01	-0.34	1.49	0.48	large p.	climax
Cardwellia sublimis	1.47	1.69	-0.43	2.12	0.22	-1.05	-0.34	1.49	0.41	large p.	small p.
Cardwellia sublimis	1.58	1.85	-0.51	1.98	0.17	-1.08	-0.34	1.49	0.81	large p.	large p.
Cardwellia sublimis	1.55	1.79	-0.67	2.01	0.17	-1.08	-0.34	1.49	0.49	large p.	large p.
Cardwellia sublimis	1.67	1.83	-0.36	2.11	0.23	-1.21	-0.34	1.49	0.52	large p.	small p.
Cardwellia sublimis	1.76	1.86	0.09	2.14	0.28	-1.15	-0.34	1.49	0.06	large p.	climax
Cardwellia sublimis	1.17	1.44	-0.93	2.04	0.2	-1.13	-0.34	1.49	0.39	large p.	large p.
Cardwellia sublimis	1.76	1.93	-0.32	2.11	0.15	-1.24	-0.34	1.49	0.25	large p.	small p.
Cardwellia											

continued on next page

continued from previous page

Specie	V_{cmax}	J_{max}	R_{day}	LMA	N_{area}	P_{area}	WD	H_{max}	c_i:c_a	Expert	Quantitative
sublimis	1.66	1.77	-0.38	1.74	-0.15	-1.63	-0.34	1.49	0.48	large p.	large p.
Castanospora alphandii	1.43	1.66	-0.73	1.99	0.26	-1.34	-0.24	1.54	0.29	climax	large p.
Castanospora alphandii	1.41	1.65	-0.77	2.4	0.53	-0.61	-0.24	1.54	0.37	climax	subcanopy
Ceratopetalum succirubrum	1.51	1.71	-0.62	2.15	0.12	-1.22	-0.29	1.49	0.13	climax	small p.
Ceratopetalum succirubrum	1.3	1.56	-0.76	2.11	0.1	-1.3	-0.29	1.49	0.39	climax	large p.
Cinnamomum bejolghota	1.6	1.75	-0.4	1.99	0.2	-0.46	-0.22	1.4	0.22	NA	subcanopy
Cinnamomum bejolghota	1.48	1.59	-0.52	1.89	-0.04	-0.69	-0.22	1.4	0.38	NA	subcanopy
Duabanga grandiflora	1.93	2.12	-0.07	2.07	0.09	-0.49	-0.35	1.6	0.48	NA	climax
Engelhardia spicata	1.17	1.65	-0.83	1.93	0.12	-0.63	-0.25	1.3	0.34	NA	subcanopy
Engelhardia spicata	1.2	1.4	-0.8	1.93	0.01	-0.36	-0.25	1.3	0.53	NA	subcanopy
Ficus leptoclada	1.07	1.64	-0.52	2.12	0.5	-0.84	-0.34	1.49	0.55	small p.	subcanopy
Ficus leptoclada	1.52	1.92	-0.9	1.98	0.32	-0.96	-0.34	1.49	0.59	small p.	large p.
Ficus leptoclada	1.13	1.62	-0.69	2.07	0.43	-0.94	-0.34	1.49	0.49	small p.	large p.
Ficus leptoclada	1.3	1.8	-0.61	2.04	0.43	-1.65	-0.34	1.49	0.46	small p.	large p.
Ficus leptoclada	1.6	1.78	-0.41	1.83	0.09	-1.3	-0.34	1.49	0.33	small p.	large p.
Ficus leptoclada	1.47	1.63	-0.45	2.55	0.88	-0.52	-0.34	1.49	0.34	small p.	small p.
Ficus leptoclada	1.65	1.87	-0.44	1.9	0.23	-1.26	-0.34	1.49	0.32	small p.	small p.
Ficus leptoclada	1.46	1.8	-0.61	1.93	0.32	-1.12	-0.34	1.49	0.41	small p.	large p.
Flindersia bourjotiana	1.6	1.79	-0.53	2.13	0.27	-1.31	-0.28	1.52	0.19	large p.	small p.
Flindersia brayleyana	1.87	2.05	-0.4	2.29	0.43	-1.09	-0.32	1.54	0.06	large p.	climax
Flindersia pimenteliana	1.78	1.99	-0.49	1.62	-0.1	-1.5	-0.28	1.49	0.03	large p.	large p.
Garcinia cowa	1.2	1.58	-0.8	1.88	-0.02	-1.29	-0.26	1.36	0.81	NA	large p.
Garcinia cowa	1.28	1.47	-0.72	1.74	-0.17	-0.82	-0.26	1.36	0.55	NA	subcanopy
Garcinia cowa	1.23	1.42	-0.77	1.77	-0.14	-0.59	-0.26	1.36	0.58	NA	subcanopy
Garcinia cowa	1.28	1.46	-0.72	1.89	0.01	-0.64	-0.26	1.36	0.34	NA	subcanopy
Garuga floribunda	1.62	1.97	-0.38	1.75	0.39	-0.86	-0.16	1.45	0.08	large p.	small p.
Geissois biagiana	1.4	1.67	-0.85	1.5	0.05	-1.34	-0.28	1.56	0.32	climax	large p.
Lithocarpus grandifolius	1.44	1.5	-0.56	1.86	-0.05	-0.45	-0.12	1.18	0.43	NA	subcanopy
Litsea leefeana	1.19	1.75	-0.71	1.98	0.28	-0.89	-0.29	1.55	0.28	large p.	subcanopy
Litsea leefeana	1.12	1.44	-0.45	1.97	0.24	-1.51	-0.29	1.55	0.35	large p.	large p.
Litsea leefeana	1.64	1.98	-1.2	2.03	0.27	-1.7	-0.29	1.55	0.31	large p.	large p.
Litsea leefeana	1.57	1.81	-0.47	2.08	0.27	-1.06	-0.29	1.55	0.48	large p.	small p.
Litsea leefeana	1.55	1.86	-0.51	2.19	0.37	-0.97	-0.29	1.55	0.34	large p.	small p.

continued on next page

continued from previous page

Specie	V_{cmax}	J_{max}	R_{day}	LMA	N_{area}	P_{area}	WD	H_{max}	c_i:c_a	Expert	Quantitative
Litsea leefeana	1.5	1.71	-0.62	1.78	0.2	-1.21	-0.29	1.55	0.39	large p.	large p.
Litsea leefeana	1.54	1.72	-0.46	1.99	0.16	-1.01	-0.29	1.55	0.46	large p.	small p.
Litsea leefeana	1.47	1.77	-0.57	2.5	0.71	-0.77	-0.29	1.55	0.41	large p.	small p.
Litsea monopetala	1.47	1.89	-0.53	1.87	0.13	-0.56	-0.31	1.26	0.24	NA	subcanopy
Lomatia fraxinifolia	1.81	1.98	-0.36	2.06	0.05	-1.3	-0.1	1.37	0.16	climax	small p.
Macaranga inamoena	1.25	1.56	-0.99	1.88	0.08	-1.31	-0.34	1.69	0.4	NA	large p.
Magnolia henryi	1.17	1.57	-0.83	1.83	0.07	-0.68	-0.08	1.06	0.43	NA	subcanopy
Melicope vitiflora	1.75	1.85	-0.37	1.6	0.27	-1.26	-0.29	1.35	0.62	large p.	large p.
Meliosma arnottiana	1.8	2.03	-0.2	1.84	-0.17	-0.55	-0.14	1.3	0.27	NA	climax
Neolitsea dealbata	1.39	1.54	-0.73	2.04	0.26	-1.15	-0.17	1.39	0.42	small p.	large p.
Nephelium chryseum	1.5	1.54	-0.5	1.74	-0.07	-0.51	-0.14	1.47	0.23	NA	subcanopy
Phoebe puwenensis	1.43	1.58	-0.57	1.97	0.07	-0.39	-0.24	1.48	0.62	NA	subcanopy
Placospermum coriaceum	1.66	1.82	-0.38	2.2	0.22	-0.98	-0.25	1.51	0.41	large p.	small p.
Polyscias elegans	1.29	1.75	-0.33	2.13	0.32	-0.94	-0.4	1.33	0.19	large p.	small p.
Polyscias elegans	1.61	1.96	-0.54	1.99	0.18	-1.05	-0.4	1.33	0.5	large p.	small p.
Polyscias elegans	1.47	1.8	-0.51	1.91	0.16	-1.07	-0.4	1.33	0.26	large p.	small p.
Polyscias elegans	1.48	1.76	-0.62	1.84	-0.06	-1.22	-0.4	1.33	0.46	large p.	large p.
Polyscias elegans	1.88	2.05	-0.21	2.53	0.78	-0.57	-0.4	1.33	-0.16	large p.	climax
Polyscias elegans	1.83	2.03	-0.22	1.92	0.14	-1.19	-0.4	1.33	0.25	large p.	small p.
Polyscias elegans	1.88	1.98	-0.05	2.06	0.19	-1.14	-0.4	1.33	0.2	large p.	climax
Polyscias elegans	1.66	1.94	-0.45	1.93	0.2	-1.23	-0.4	1.33	0.35	large p.	small p.
Prunus turneriana	1.51	1.87	-0.27	2.16	0.36	-0.91	-0.36	1.22	0.4	large p.	small p.
Prunus turneriana	1.67	1.77	-0.31	2.24	0.44	-0.79	-0.36	1.22	0.55	large p.	small p.
Prunus turneriana	1.72	1.96	-0.6	2.06	0.31	-1.42	-0.36	1.22	0.18	large p.	small p.
Prunus turneriana	1.57	1.72	-0.48	2	0.2	-1.18	-0.36	1.22	0.42	large p.	small p.
Prunus turneriana	1.73	1.83	-0.32	1.94	0.17	-1.21	-0.36	1.22	0.45	large p.	small p.
Prunus turneriana	1.69	1.88	-0.59	2	0.22	-1.16	-0.36	1.22	0.04	large p.	small p.
Prunus turneriana	1.91	2.01	-0.11	2.23	0.38	-1.05	-0.36	1.22	0.42	large p.	climax
Pterospermum menglunense	1.47	1.78	-0.53	1.7	0.04	-0.44	-0.31	1.49	0.8	NA	subcanopy
Pullea stutzeri	1.61	1.81	-0.57	2.03	0.03	-1.42	-0.18	1.5	0.3	large p.	large p.
Rockinghamia angustifolia	1.6	1.85	-0.4	1.92	0.22	-1.15	-0.19	1.29	0.56	subcanopy	small p.
Rockinghamia angustifolia	1.53	1.86	-0.47	1.82	0.13	-1.07	-0.19	1.29	0.69	subcanopy	large p.
Rockinghamia											

continued on next page

continued from previous page

Specie	V_{cmax}	J_{max}	R_{day}	LMA	N_{area}	P_{area}	WD	H_{max}	c_i:c_a	Expert	Quantitative
angustifolia	1.31	1.67	-0.69	1.88	0.15	-1.22	-0.19	1.29	0.9	subcanopy	large p.
Rockinghamia angustifolia	1.65	1.95	-0.35	1.88	0.12	-1.18	-0.19	1.29	0.73	subcanopy	small p.
Sarcopteryx martyana	1.7	1.96	-0.58	2	0.31	-1.04	-0.18	1.54	0.06	climax	small p.
Synima cordierorum	1.98	1.93	-0.02	2.07	0.44	-0.91	-0.11	1.39	0.27	climax	climax
Synima cordierorum	2.03	2.07	0.03	2.05	0.37	-0.99	-0.11	1.39	0.4	climax	climax
Synima cordierorum	1.96	2.02	-0.04	2.08	0.43	-0.82	-0.11	1.39	0.44	climax	climax
Synima cordierorum	1.99	2.04	-0.01	2.03	0.42	-0.86	-0.11	1.39	0.45	climax	climax
Syzygium sayeri	2.1	2.09	0.1	2.1	0.39	-0.9	-0.11	1.74	0.17	climax	climax
Syzygium sayeri	2.07	2.13	0.07	2.09	0.41	-0.9	-0.11	1.74	0.13	climax	climax
Syzygium sayeri	2.06	2.14	0.06	2.04	0.44	-0.88	-0.11	1.74	0.23	climax	climax
Syzygium sayeri	2.04	2.13	0.04	2.03	0.31	-1.05	-0.11	1.74	0.19	climax	climax
Terminalia myriocarpa	1.92	2.12	-0.08	2.13	0.08	-0.26	-0.31	1.54	0.6	NA	climax
Toona ciliata	1.67	1.89	-0.33	1.89	0.28	-0.48	-0.31	1.45	0.08	large p.	subcanopy
Xanthophyllum octandrum	1.96	2.05	-0.04	2.07	0.32	-1.04	-0.19	1.38	0.03	climax	climax
Xanthophyllum octandrum	1.66	1.91	-0.34	2.09	0.27	-1.01	-0.19	1.38	0.7	climax	small p.
Xanthophyllum octandrum	2.02	2.09	0.02	2.09	0.23	-1.06	-0.19	1.38	0.39	climax	climax

4.7 Acknowledgments

This research was funded by the Terrestrial Ecosystem Research Network (TERN), Macquarie University and the Australian National University. H.F. Togashi is supported by an international Macquarie University International Research Scholarship (iMQRES). Prentice, Evans, and Togashi have been supported by the Ecosystem Modelling and Scaling Infrastructure (eMAST, http://www.emast.org.au), facility of TERN, supported by the Australian Government through the National Collaborative Research Infrastructure Strategy (NCRIS). Owen Atkin acknowledges the support of the Australian Research Council (DP130101252 and CE140100008). N and P were analysed at the Department of Forestry, ANU. We are grateful to Jinlong Zhang (Xishuangbanna Tropical Botanical Garden) for identifying plant species, and also to Jack Egerton (ANU), Li Guangqi (Macquarie), Lingling Zhu (ANU), Danielle Creek (University of Western Sydney), Lucy Hayes (ANU) and Stephanie McCaffery (ANU) for help with fieldwork and/or N and P digestions. We thank Tomas Ferreira Domingues (University of Sao Paulo) for comments that helped to improve this paper. We acknowledge Jon Lloyd, Zhu Hua and Jian Ni for data contribution. This paper is a contribution to the AXA Chair Program in Biosphere and Climate Impacts and the Imperial College initiative on Grand Challenges in Ecosystems and the Environment.

4.8 References

Allen, S. E, Grimshaw, H, Parkinson, J. A, and Quarmby, C. L. *Chemical analysis of ecological materials*. Blackwell Scientific Publications, 1974.

Atkin, O. K, Holly, C, and Ball, M. C. Acclimation of snow gum (*Eucalyptus pauciflora*) leaf respiration to seasonal and diurnal variations in temperature: the importance of changes in the capacity and temperature sensitivity of respiration. *Plant, Cell & Environment*, 23(1):15–26, 2000.

Atkin, O. K, Bloomfield, K. J, Reich, P. B, Tjoelker, M. G, Asner, G. P, Bonal, D, Bönisch, G, Bradford, M. G, Cernusak, L. A, Cosio, E. G, Creek, D, Crous, K. Y, Domingues, T. F, Dukes, J. S, Egerton, J. J. G, Evans, J. R, Farquhar, G. D, Fyllas, N. M, Gauthier, P. P. G, Gloor, E, Gimeno, T. E, Griffin, K. L, Guerrieri, R, Heskel, M. A, Huntingford, C, Ishida, F. Y, Kattge, J, Lambers, H, Liddell, M. J, Lloyd, J, Lusk, C. H, Martin, R. E, Maksimov, A. P, Maximov, T. C, Malhi, Y, Medlyn, B. E, Meir, P, Mercado, L. M, Mirotchnick, N, Ng, D, Niinemets, Ü, O'Sullivan, O. S, Phillips, O. L, Poorter, L, Poot, P, Prentice, I. C, Salinas, N, Rowland, L. M, Ryan, M. G, Sitch, S, Slot, M, Smith, N. G, Turnbull, M. H, VanderWel, M. C, Valladares, F, Veneklaas, E. J, Weerasinghe, L. K, Wirth, C, Wright, I. J, Wythers, K. R, Xiang, J, Xiang, S, and Zaragoza-Castells, J. Global variability in leaf respiration in relation to climate, plant functional types and leaf traits. *New Phytologist*, 206(2):614–636, 2015.

Baraloto, C, Timothy Paine, C, Poorter, L, Beauchene, J, Bonal, D, Domenach, A, Hérault, B, Patino, S, Roggy, J, and Chave, J. Decoupled leaf and stem economics in rain forest trees. *Ecology letters*, 13(11):1338–1347, 2010.

Bernacchi, C. J, Singsaas, E. L, Pimentel, C, Portis Jr, A. R, and Long, S. P. Improved temperature response functions for models of rubisco-limited photosynthesis. *Plant, Cell & Environment*, 24(2):253–259, 2001.

Bernacchi, C. J, Pimentel, C, and Long, S. P. *In vivo* temperature response functions of parameters required to model RuBP-limited photosynthesis. *Plant, Cell & Environment*, 26(9):1419–1430, 2003.

Bloomfield, K. J, Domingues, T. F, Saiz, G, Bird, M. I, Crayn, D. M, Ford, A, Metcalfe, D. J, Farquhar, G. D, and Lloyd, J. Contrasting photosynthetic characteristics of forest *vs*. savanna species (far north Queensland, Australia). *Biogeosciences Discuss.*, 11(6):8969–9011, 2014.

Botkin, D. B, Janak, J. F, and Wallis, J. R. Some ecological consequences of a computer model of forest growth. *The Journal of Ecology*, pages 849–872, 1972.

Box, E. O. Predicting physiognomic vegetation types with climate variables. *Vegetatio*, 45(2):127–139, 1981.

Bradford, M. G, Murphy, H. T, Ford, A. J, Hogan, D. L, and Metcalfe, D. J. Long-term stem inventory data from tropical rain forest plots in Australia. *Ecology*, 95(8): 2362–000, 2014.

Calvin, M and Benson, A. A. *The path of carbon in photosynthesis*. US Atomic Energy Commission, Technical Information Division, 1948.

Chen, J.-L, Reynolds, J, Harley, P, and Tenhunen, J. Coordination theory of leaf nitrogen distribution in a canopy. *Oecologia*, 93(1):63–69, 1993.

De Kauwe, M. G, Lin,Y-S, Wright, I. J, Medlyn, B. E, Crous, K. Y, Ellsworth, D. S, Maire, V, Prentice, I. C, Atkin, O. K, Rogers, A, Niinemets, Ü, Serbin, S, Meir, P, Uddling, J, Togashi, H. F, Tarvainen, L, Weerasinghe, L. K, Evans, B. J, Ishida, F. Y, and Domingues T. F. A test of the 'one-point method' for estimating maximum carboxylation capacity from field-measured, light-saturated photosynthesis V_{cmax}. *New Phytologist - Manuscript accepted for publication (copy on file with author)*, 2015.

Denslow, J. S. Tropical rainforest gaps and tree species diversity. *Annual review of ecology and systematics*, pages 431–451, 1987.

Díaz, S and Cabido, M. Plant functional types and ecosystem function in relation to global change. *Journal of vegetation science*, 8(4):463–474, 1997.

Domingues, T. F, Meir, P, Feldpausch, T. R, Saiz, G, Veenendaal, E. M, Schrodt, F, Bird, M, Djagbletey, G, Hien, F, Compaore, H, Diallo, A, Grace, J, and Lloyd, J. O. N. Co-limitation of photosynthetic capacity by nitrogen and phosphorus in west Africa woodlands. *Plant, Cell & Environment*, 33(6):959–980, 2010.

Dong, N, Prentice, I. C, Bradley, E. J, and Wright, I. J. Leaf nitrogen from first principles: Field evidence for optimal plant acclimation to environmental gradients. *Manuscript submitted for publication (copy on file with author)*, 2015.

Enquist, B. J and Bentley, L. P. Land plants: new theoretical directions and empirical prospects. *Metabolic Ecology: A Scaling Approach. Hoboken, NJ: Wiley-Blackwell*, pages 164–187, 2012.

Evans, J. Photosynthesis and nitrogen relationships in leaves of C_3 plants. *Oecologia*, 78(1):9–19, 1989.

Farquhar, G. D, von Caemmerer, S, and Berry, J. A. A biochemical model of photosynthetic CO_2 assimilation in leaves of C_3 species. *Planta*, 149(1):78–90, 1980.

Friend, A, Schugart, H, and Running, S. A physiology-based gap model of forest dynamics. *Ecology*, pages 792–797, 1993.

Fyllas, N. M, Patino, S, Baker, T, Bielefeld Nardoto, G, Martinelli, L, Quesada, C, Paiva, R, Schwarz, M, Horna, V, and Mercado, L. Basin-wide variations in foliar properties of Amazonian forest: phylogeny, soils and climate. *Biogeosciences*, 6(11): 2677–2708, 2009.

Fyllas, N. M, Quesada, C. A, and Lloyd, J. Deriving plant functional types for Amazonian forests for use in vegetation dynamics models. *Perspectives in Plant Ecology, Evolution and Systematics*, 14(2):97–110, 2012.

Hancock, P and Hutchinson, M. Spatial interpolation of large climate data sets using bivariate thin plate smoothing splines. *Environmental Modelling & Software*, 21(12): 1684–1694, 2006.

Harris, I, Jones, P. D, Osborn, T. J, and Lister, D. H. Updated high-resolution grids of monthly climatic observations – the CRU ts3.10 dataset. *International Journal of Climatology*, 34(3):623–642, 2014.

Harrison, S. P, Prentice, I. C, Barboni, D, Kohfeld, K. E, Ni, J, and Sutra, J. Ecophysiological and bioclimatic foundations for a global plant functional classification. *Journal of Vegetation Science*, 21(2):300–317, 2010.

Haxeltine, A and Prentice, I. C. A general model for the light-use efficiency of primary production. *Functional Ecology*, 10(5):551–561, 1996.

Hirose, T and Werger, M. J. Nitrogen use efficiency in instantaneous and daily photosynthesis of leaves in the canopy of a *Solidago altissima* stand. *Physiologia Plantarum*, 70(2):215–222, 1987.

Hutchinson, M. Daily maximum temperature: Anuclimate 1.0, 0.01 degree, Australian coverage, 1970-2012, 2014a. http://www.emast.org.au/

Hutchinson, M. Daily minimum temperature: Anuclimate 1.0, 0.01 degree, Australian coverage, 1970-2012, 2014b. http://www.emast.org.au/

Hutchinson, M. Daily precipitation: Anuclimate 1.0, 0.01 degree, Australian coverage, 1970-2012, 2014c. http://www.emast.org.au/

Koch, G. W, Sillett, S. C, Antoine, M. E, and Williams, C. B. Growth maximization trumps maintenance of leaf conductance in the tallest angiosperm. *Oecologia*, 177 (2):321–331, 2015.

Köppen, W. P. *Grundriss der klimakunde*. Walter de Gruyter, Berlin, 1931.

Kortschak, H. P, Hartt, C. E, and Burr, G. O. Carbon dioxide fixation in sugarcane leaves. *Plant Physiology*, 40(2):209, 1965.

Lavorel, S and Garnier, E. Predicting changes in community composition and ecosystem functioning from plant traits: revisiting the holy grail. *Functional ecology*, 16 (5):545–556, 2002.

Leemans, R and Prentice, I. C. FORSKA - A general forest succession model. *Meddelanden Från Växtbiologiska Institutionen*, pages 2–45, 1989.

Li, G, Harrison, S. P, Prentice, I. C, and Falster, D. Simulation of tree-ring widths with a model for primary production, carbon allocation, and growth. *Biogeosciences*, 11 (23):6711–6724, 2014.

Lin, Y-S, Medlyn, B. E, De Kauwe, M. G, and Ellsworth, D. S. Biochemical photosynthetic responses to temperature: how do interspecific differences compare with seasonal shifts? *Tree Physiology*, 33(8):793–806, 2013.

Lin, Y-S, Medlyn, B. E, Duursma, R. A, Prentice, I. C, Wang, H, Baig, S, Eamus, D, de Dios, V. R, Mitchell, P, Ellsworth, D. S, de Beeck, M. O, Wallin, G, Uddling, J, Tarvainen, L, Linderson, M.-L, Cernusak, L. A, Nippert, J. B, Ocheltree, T. W, Tissue, D. T, Martin-StPaul, N. K, Rogers, A, Warren, J. M, De Angelis, P, Hikosaka, K, Han, Q, Onoda, Y, Gimeno, T. E, Barton, C. V. M, Bennie, J, Bonal, D, Bosc, A, Low, M, Macinins-Ng, C, Rey, A, Rowland, L, Setterfield, S. A, Tausz-Posch, S, Zaragoza-Castells, J, Broadmeadow, M. S. J, Drake, J. E, Freeman, M, Ghannoum, O, Hutley, L. B, Kelly, J. W, Kikuzawa, K, Kolari, P, Koyama, K, Limousin, J.-M, Meir, P, Lola da Costa, A. C, Mikkelsen, T. N, Salinas, N, Sun, W, and Wingate, L. Optimal stomatal behaviour around the world. *Nature Climate Change*, 5(5): 459–464, 2015.

Lloyd, J, Bloomfield, K, Domingues, T. F, and Farquhar, G. D. Photosynthetically relevant foliar traits correlating better on a mass *vs* an area basis: of ecophysiological

relevance or just a case of mathematical imperatives and statistical quicksand? *New Phytologist*, 199(2):311–321, 2013.

Maire, V, Martre, P, Kattge, J, Gastal, F, Esser, G, Fontaine, S, and Soussana, J.-F. The coordination of leaf photosynthesis links C and N fluxes in C_3 plant species. *PLoS ONE*, 7(6):e38345, 2012.

Medlyn, B. E, Duursma, R. A, Eamus, D, Ellsworth, D. S, Prentice, I. C, Barton, C. V. M, Crous, K. Y, De Angelis, P, Freeman, M, and Wingate, L. Reconciling the optimal and empirical approaches to modelling stomatal conductance. *Global Change Biology*, 17(6):2134–2144, 2011.

Meng, T, Wang, H, Harrison, S, Prentice, I, Ni, J, and Wang, G. Responses of leaf traits to climatic gradients: adaptive variation *vs*. compositional shifts. *Biogeosciences Discussions*, 12(9), 2015.

Miyazawa, Y and Kikuzawa, K. Physiological basis of seasonal trend in leaf photosynthesis of five evergreen broad-leaved species in a temperate deciduous forest. *Tree Physiology*, 26(2):249–256, 2006.

Moorcroft, P. R, Hurtt, G. C, and Pacala, S. W. A method for scaling vegetation dynamics: The ecosystem demography model (ED). *Ecological Monographs*, 71(4): 557–586, 2001.

Niinemets, Ü and Tenhunen, J. D. A model separating leaf structural and physiological effects on carbon gain along light gradients for the shade-tolerant species *Acer saccharum*. *Plant, Cell & Environment*, 20(7):845–866, 1997.

Oksanen, J, Blanchet, F. G, Kindt, R, Legendre, P, Minchin, P. R, O'Hara, R, Simpson, G. L, Solymos, P, Stevens, M. H. H, and Wagner, H. Package 'vegan'. *Community ecology package, version*, pages 2.2–1, 2015.

Pavlick, R, Drewry, D. T, Bohn, K, Reu, B, and Kleidon, A. The jena diversity-dynamic global vegetation model (JeDi-DGVM): a diverse approach to representing terrestrial biogeography and biogeochemistry based on plant functional trade-offs. *Biogeosciences*, 10:4137–4177, 2013.

Prentice, I. C and Cowling, S. A. Dynamic Global Vegetation Models. *Encyclopedia of Biodiversity*, pages 607–689. Academic Press, Waltham, 2nd edition, 2013.

Prentice, I. C, Cramer, W, Harrison, S. P, Leemans, R, Monserud, R. A, and Solomon, A. M. Special paper: a global BIOME model based on plant physiology and dominance, soil properties and climate. *Journal of biogeography*, pages 117–134, 1992.

Prentice, I. C, Sykes, M. T, and Cramer, W. A simulation model for the transient effects of climate change on forest landscapes. *Ecological modelling*, 65(1):51–70, 1993.

Prentice, I. C, Bondeau, A, Cramer, W, Harrison, S. P, Hickler, T, Lucht, W, Sitch, S, Smith, B, and Sykes, M. T. *Dynamic global vegetation modeling: quantifying terrestrial ecosystem responses to large-scale environmental change*, pages 175–192. Springer, 2007.

Prentice, I. C, Meng, T, Wang, H, Harrison, S. P, Ni, J, and Wang, G. Evidence of a universal scaling relationship for leaf CO_2 drawdown along an aridity gradient. *New Phytologist*, 190(1):169–180, 2011.

Prentice, I. C, Dong, N, Gleason, S. M, Maire, V, and Wright, I. J. Balancing the costs of carbon gain and water transport: testing a new theoretical framework for plant functional ecology. *Ecology Letters*, 17(1):82–91, 2014.

Prentice, I and Leemans, R. Pattern and process and the dynamics of forest structure: a simulation approach. *The Journal of Ecology*, 78:340–355, 1990.

Quesada, C, Phillips, O, Schwarz, M, Czimczik, C, Baker, T, Patiãno, S, Fyllas, N, Hodnett, M, Herrera, R, and Almeida, S. Basin-wide variations in Amazon forest structure and function are mediated by both soils and climate. *Biogeosciences*, 9(6), 2012.

Ranson, S. L and Thomas, M. Crassulacean acid metabolism. *Annual Review of Plant Physiology*, 11(1):81–110, 1960.

Raunkiær, C. *The life forms of plants and statistical plant geography.* Clarendon Press, 1934.

R Core Team. R: A language and environment for statistical computing. R foundation for statistical computing, Vienna, Austria. http://www.r-project.org/. 2012.

Reich, P. B. The world-wide 'fast–slow' plant economics spectrum: a traits manifesto. *Journal of Ecology*, 102(2):275–301, 2014.

Reich, P. B, Walters, M. B, and Ellsworth, D. S. From tropics to tundra: global convergence in plant functioning. *Proceedings of the National Academy of Sciences*, 94(25):13730–13734, 1997.

Reid, D. E. B, Silins, U, Mendoza, C, and Lieffers, V. J. A unified nomenclature for quantification and description of water conducting properties of sapwood xylem based on Darcy's law. *Tree Physiology*, 25(8):993–1000, 2005.

Scheiter, S, Langan, L, and Higgins, S. I. Next-generation dynamic global vegetation models: learning from community ecology. *New Phytologist*, 198(3):957–969, 2013.

Sharkey, T. D, Bernacchi, C. J, Farquhar, G. D, and Singsaas, E. L. Fitting photosynthetic carbon dioxide response curves for C_3 leaves. *Plant, Cell & Environment*, 30 (9):1035–1040, 2007.

Shugart, H. H. *A Theory of Forest Dynamics*. Springer-Verlag, New York, 1984.

Sitch, S, Smith, B, Prentice, I. C, Arneth, A, Bondeau, A, Cramer, W, Kaplan, J. O, Levis, S, Lucht, W, Sykes, M. T, Thonicke, K, and Venevsky, S. Evaluation of ecosystem dynamics, plant geography and terrestrial carbon cycling in the LPJ dynamic global vegetation model. *Global Change Biology*, 9(2):161–185, 2003.

Smith, B, Prentice, I. C, and Sykes, M. T. Representation of vegetation dynamics in the modelling of terrestrial ecosystems: comparing two contrasting approaches within European climate space. *Global Ecology and Biogeography*, 10(6):621–637, 2001.

Sperry, J. S. Evolution of water transport and xylem structure. *International Journal of Plant Sciences*, 164(S3):S115–S127, 2003.

Swaine, M and Whitmore, T. On the definition of ecological species groups in tropical rain forests. *Vegetatio*, 75(1-2):81–86, 1988.

Ter Braak, C. J and Prentice, I. C. A theory of gradient analysis. *Advances in Ecological Research*, pages 235-282. Academic Press, 1988.

Togashi, H. F, Prentice, I. C, Atkin, O. K, Macfarlane, C, Prober, S. M, Bloomfield, K. J, and Evans, B. J. Thermal acclimation of leaf photosynthetic traits in an evergreen woodland, consistent with the co-ordination hypothesis. *Manuscript in revision (copy on file with author)*, 2015a.

Togashi, H. F, Prentice, I. C, Evans, B. J, Forrester, D. I, Drake, P, Feikema, P, Brooksbank, K, Eamus, D, and Taylor, D. Morphological and moisture availability controls of the leaf area-to-sapwood area ratio: analysis of measurements on Australian trees. *Ecology and Evolution*, 5(6):1263–1270, 2015b.

Turner, I. M. *The ecology of trees in the tropical rain forest*. Cambridge University Press, 2001.

Tyree, M and Ewers, F. The hydraulic architecture of trees and other woody plants. *New Phytologist*, 119(3):345–360, 1991.

Verheijen, L, Brovkin, V, Aerts, R, Bönish, G, Cornelissen, J, Kattge, J, Reich, P, Wright, I, and Van Bodegom, P. Impacts of trait variation through observed trait-climate relationships of performance of a representative Earth system model: a conceptual analysis. *Biogeosciences*, 10:5497–5515, 2013.

Wang, H, Prentice, I. C, and Davis, T. W. Biophysical constraints on gross primary production by the terrestrial biosphere. *Biogeosciences Discussions*, 11:3209–3240, 2014.

Warton, D, Wright, I, Falster, D, and Westoby, M. Bivariate line-fitting methods for allometry. *Biological Reviews*, 81(2):259–291, 2006.

Weerasinghe, L. K, Creek, D, Crous, K. Y, Xiang, S, Liddell, M. J, Turnbull, M. H, and Atkin, O. K. Canopy position affects the relationships between leaf respiration and associated traits in a tropical rainforest in far north Queensland. *Tree physiology*, 34 (6):564–584, 2014.

Whitehead, D, Edwards, W. R. N, and Jarvis, P. G. Conducting sapwood area, foliage area, and permeability in mature trees of *Picea sitchensis* and *Pinus contorta*. *Canadian Journal of Forest Research*, 14(6):940–947, 1984.

Whitmore, T. On pattern and process in forests. *Special publications series of the British Ecological Society*, 1982.

Wickham, H. *ggplot2: elegant graphics for data analysis*. Springer, 2010.

Woodward, F. I. *Climate and plant distribution*. Cambridge University Press, 1987.

Wright, I. J, Reich, P. B, Westoby, M, Ackerly, D. D, Baruch, Z, Bongers, F, Cavender-Bares, J, Chapin, T, Cornelissen, J. H. C, Diemer, M, Flexas, J, Garnier, E, Groom,

P. K, Gulias, J, Hikosaka, K, Lamont, B. B, Lee, T, Lee, W, Lusk, C, Midgley, J. J, Navas, M.-L, Niinemets, U, Oleksyn, J, Osada, N, Poorter, H, Poot, P, Prior, L, Pyankov, V. I, Roumet, C, Thomas, S. C, Tjoelker, M. G, Veneklaas, E. J, and Villar, R. The worldwide leaf economics spectrum. *Nature*, 428(6985):821–827, 2004.

5

Conclusion

This thesis has focused on processes important for improving the representation of primary production, plant growth and vegetation changes in dynamic global vegetation models (DGVMs). Leaf- and plant-level data were compiled and analysed, combining new fieldwork with existing data sources, in order to address three issues that are either neglected or treated simplistically in the majority of current models. A simple theoretical framework, based on a combination of the least-cost theory (Prentice et al., 2014) with the coordination hypothesis (Maire et al., 2012), provides a basis for interpreting and generalizing the results. This framework is applied to variation in plant functional traits across species and climates (chapter 2), within species through time (chapter 3), and between species occupying different spatial and temporal niches (chapter 4). The wider analysis of field measurements in an explicit theoretical framework, as demonstrated in this thesis, should help eventually to increase the realism and predictive capability of next-generation DGVMs.

Chapter 2 tested the 'pipe model' relating leaf area (LA) to sapwood area (SA) in trees and branches, and investigated the extent to which the LA:SA ratio in angiosperm trees relates to hydroclimatic variation (quantified using the Cramer-Prentice α index of plant-available moisture). Decreasing LA:SA with increasing aridity has previously been shown for gymnosperms (Warton *et al.*, 2006; Mencuccini and Grace, 1995; Schfer

et al., 2000; Delucia *et al.*, 2000) but not for angiosperms (Gleason et al., 2012). The pipe model was supported by the finding of a near-isometric relationship between LA and SA. LA:SA however was found to show some relationship to tree height, consistent with the observation that taller plants tend to present larger vessel diameters and lower vessel densities (Gleason et al., 2012; Olson and Rosell, 2013), presumed to be a means of maintaining hydraulic conductivity with increasing height. Across species, the maximum and minimum observed values of LA:SA varied with α but within the (large) range of values shown the relationship was very weak. Leaf-specific hydraulic conductivity went some way towards explaining this large range of variation, with lower conductivity compensated by greater sapwood area (smaller LA:SA). The strong relationship between LA:SA *vs.* hydroclimate in gymnosperms and the much weaker relationship shown here for angiosperms are contrasting, and can be explained by the many-fold greater diversity of xylem conduit diameters in angiosperms (Sperry et al., 2006) combined with the steep (fourth-power) dependence of hydraulic conductivity on diameter, according to Poiseuille's law. Chapter 4 results, derived from the analysis of 130 leaves of individual angiosperm tropical trees, suggests that tall climax species have a great inclination for higher wood density, trait linked to hydraulic conductivity. Increasing hydraulic conductivity associated with increasing height (a consequence of tapering of the xylem elements) sits with the expectation that tall climax species have dense wood, and this should be a difference among species strategies rather than an ontogenetic change.

Chapter 2 follow up work should explore a wider global synthesis of data on LA:SA ratios, wood density and hydraulic properties, in order to advance the understanding regarding the relationship between LA:SA (a trait that can be easily collected in the field and also provides powerful associations with other traits) in angiosperms and climate. This wider dataset must contain representative number of species in different climates and information in dynamic roles/ successional stages; which is crucial to further test the dynamic role approach.

Chapter 3 evaluated a major (and *a priori*, probably unrealistic) simplification frequently adopted in DGVMs, namely that key photosynthetic traits (including the leaf-level capacities for carboxylation (V_{cmax}) and electron transport (J_{max}), measured at a standard temperature) are constant through the seasonal cycle. The coordination hypothesis is physiologically based in plants response to environmental conditions, where the short term balance is regulated in the chloroplast to modulate Rubisco limited rate of carboxylation (W_c) and RuBP limited rate of carboxylation (W_j) (Chen *et al.*, 1993). If W_c and W_j remain out of balance for prolonged periods, nitrogen has

to be reallocated to leaves (increasing with irradiance and decreasing with air temperature) to restore balance (Maire et al., 2012). Plants respond to environment constantly changes by attempting to restore their balance through coordination to achieve optimal (or near-optimal) behaviour (Chen *et al.*, 1993). This assumption of fixed photosynthetic parameters is at odds with optimal allocation theory, which predicts that such traits should acclimate over time to changing environmental conditions. In particular, this assumption would imply that the temperature response of photosynthesis over monthly time scales is the same as the instantaneous temperature response, which is governed by enzyme kinetics. Short-term variation of temperature (and irradiance) should be large enough to significantly modify leaf physiology, and long-term acclimation may result in different assimilation among short distances in plant canopies only if they become exposed to diverse microclimates such as unequal irradiation or temperature in various heights of a canopy (Niinemets and Valladares, 2004). The thermal acclimation of assimilation was tested by repeated sampling of evergreen angiosperm trees in a highly seasonal, semi-arid environment during the warm and the cool seasons. It was found that the photosynthetic traits (V_{cmax}, J_{max}) and the rate of leaf dark respiration (R_{dark}) increased with ambient temperature from the cool season to the warm season, but less steeply than would be predicted by enzyme kinetics - such that the values when standardized to 25°C decreased with ambient temperature. The N:P ratio was also lower in the warm season, consistent with a reduced allocation of N to photosynthetic functions at higher temperatures (Way and Sage, 2008). These findings suggest that there is active seasonal acclimation consistent with the coordination hypothesis (co-limitation of photosythesis by Rubisco and electron transport), which predicts lower allocation of N to Rubisco and other photosynthetic enzymes at higher temperatures - counterbalancing the effect of enzyme kinetics. V_{cmax} and J_{max} were strongly correlated, as also predicted by the coordination hypothesis, and further supported by measurements in chapter 4. R_{dark} was correlated with V_{cmax} and J_{max}, consistent with results presented by Weerasinghe et al. (2014) and Atkin et al. (2015). V_{cmax} and J_{max} were negatively correlated with c_i:c_a (in both chapter 3 and 4), a further prediction of the coordination hypothesis, as higher photosynthetic capacity is required to offset reduced c_i.

To my knowledge, chapter 3 represents the first attempt to apply the Farquhar et al. (1980) model of carbon assimilation in order to quantify (and test for) the optimal acclimation of V_{cmax}, J_{max} and R_{dark} according to the coordination hypothesis. (The alternative of no acclimation predicts a steeper response, governed by enzyme kinetics alone). Field-observed responses to ambient temperature were shown to be closer to the

responses predicted by the coordination hypothesis. The response of c_i:c_a to ambient temperature was positive (as predicted by the least-cost hypothesis) but only about half as large as predicted, probably due to reduction in c_i:c_a associated with higher vapour pressure deficits in the warm season (Prentice et al., 2014). Overall, these findings support the idea that metabolic rate parameters in DGVMs should be allowed to acclimate temporally to environmental conditions, as in the LPJ family of models [e.g. LPJ-GUESS (Smith et al., 2001); LPJ (Sitch et al., 2003); LPJ 2.1 (Gerten et al., 2004); LPJ-SPITFIRE (Thonicke et al., 2010); LPX (Prentice et al., 2011)], rather than being fixed characteristics of PFTs. Testing these findings in models that do not account for V_{cmax}, J_{max} and R_{dark} acclimation could demonstrate the magnitude of error relative to this process and it would provide information to improve future models.

Chapter 4 considered another aspect of plant functional trait variation that is not considered by most current DGVMs, namely the functional basis for spatial and temporal niche differentiation within complex communities. Data on more than 200 evergreen angiosperm tree species from intact moist tropical forests in both northeastern Australia and southwestern China were assembled, including metabolic, structural, hydraulic and height variables. Within the relatively narrow range of climatic variation represented by these tropical forest sites, it was possible to identify syndromes of traits linked to species' 'dynamical roles' as defined by the fourfold classification of Shugart (1984). This classification distinguishes climax, large pioneer, small pioneer, and subcanopy taxa based on canopy position and life span. Other classifications make essentially the same distinctions. The differences among species in different role groups were found to be broadly consistent with theoretical expectations. In particular, climax species were characterized by greatest maximum height (H_{max}) accompanied by relatively low c_i:c_a - a consequence of the increasing cost of water transport with increasing height (Koch et al., 2015) and high values of V_{cmax}, J_{max}, R_{day} and leaf nitrogen content per unit area (N_{area}), consistent both with high exposure to light and with low c_i:c_a. Subcanopy species showed generally the opposite combinations of traits. Climax species were also found to have the thickest leaves (highest leaf mass per area, LMA), which is a requirement for high V_{cmax} (Niinemets and Tenhunen, 1997); conversely, thin leaves (low LMA) were found in subcanopy species, optimizing the use of limited carbon supplies for light capture. It was also expected, and found, that fast-growing pioneer species should adopt low investment in leaf structure, developing thin leaves (low LMA) along with low wood density, consistent with a non-conservative water use strategy. Wood density was greater for slow growers (climax and subcanopy species):

a trait presumed to confer longer life, for example through resistance to embolism and mechanical damage (Enquist and Bentley, 2012), but at a greater carbon cost.

Thus, chapter 4 provides pointers towards the integration of classical forest dynamic theory with contemporary plant functional ecology. It also suggests how species' dynamical roles might be represented in next-generation DGVMs, by implementing quantitative distinctions in both metabolic and biophysical traits. Future research building on this work should try to identify dynamical roles in other ecosystems and compare them to the functional trait combinations identified for tropical forests in this study. This is an outstanding research need that should produce crucial information to improve the representation of current DGVMs.

This thesis has discussed and has examined a set of theories, evaluating them by using state-of-the art methods and originally assembled data sets. These articles have potential to have a significant impact on DGVM practice, as well as the representation of PFTs and traits in ESMs. This work addresses complex natural processes in a simple way that matches fundamental ecological insights. I hope the findings in this thesis stimulate the ecological community (theorists as well as field scientists) to further test and support, extend or falsify the many other assumptions derived from the evolutionary attractor framework.

5.1 References

Atkin, O. K, Bloomfield, K. J, Reich, P. B, Tjoelker, M. G, Asner, G. P, Bonal, D, Bönisch, G, Bradford, M. G, Cernusak, L. A, Cosio, E. G, Creek, D, Crous, K. Y, Domingues, T. F, Dukes, J. S, Egerton, J. J. G, Evans, J. R, Farquhar, G. D, Fyllas, N. M, Gauthier, P. P. G, Gloor, E, Gimeno, T. E, Griffin, K. L, Guerrieri, R, Heskel, M. A, Huntingford, C, Ishida, F. Y, Kattge, J, Lambers, H, Liddell, M. J, Lloyd, J, Lusk, C. H, Martin, R. E, Maksimov, A. P, Maximov, T. C, Malhi, Y, Medlyn, B. E, Meir, P, Mercado, L. M, Mirotchnick, N, Ng, D, Niinemets, Ü, O'Sullivan, O. S, Phillips, O. L, Poorter, L, Poot, P, Prentice, I. C, Salinas, N, Rowland, L. M, Ryan, M. G, Sitch, S, Slot, M, Smith, N. G, Turnbull, M. H, VanderWel, M. C, Valladares, F, Veneklaas, E. J, Weerasinghe, L. K, Wirth, C, Wright, I. J, Wythers, K. R, Xiang, J, Xiang, S, and Zaragoza-Castells, J. Global variability in leaf respiration in relation to climate, plant functional types and leaf traits. *New Phytologist*, 206(2):614–636, 2015.

Chen, J-L, Reynolds, J, Harley, P, and Tenhunen, J. Coordination theory of leaf

nitrogen distribution in a canopy. *Oecologia*, 93(1):63–69, 1993.

Delucia, E. H, Maherali, H, and Carey, E. V. Climate-driven changes in biomass allocation in pines. *Global Change Biology*, 6(5):587–593, 2000.

Enquist, B. J and Bentley, L. P. Land plants: new theoretical directions and empirical prospects. *Metabolic Ecology: A Scaling Approach. Hoboken, NJ: Wiley-Blackwell*, pages 164–187, 2012.

Farquhar, G. D, von Caemmerer, S, and Berry, J. A. A biochemical model of photosynthetic CO_2 assimilation in leaves of C_3 species. *Planta*, 149(1):78–90, 1980.

Gerten, D, Schaphoff, S, Haberlandt, U, Lucht, W, and Sitch, S. Terrestrial vegetation and water balance-hydrological evaluation of a Dynamic Global Vegetation Model. *Journal of Hydrology*, 286(1):249–270, 2004.

Gleason, S. M, Butler, D. W, Ziemińska, K, Waryszak, P, and Westoby, M. Stem xylem conductivity is key to plant water balance across Australian angiosperm species. *Functional Ecology*, 26(2):343–352, 2012.

Koch, G. W, Sillett, S. C, Antoine, M. E, and Williams, C. B. Growth maximization trumps maintenance of leaf conductance in the tallest angiosperm. *Oecologia*, 177 (2):321–331, 2015.

Maire, V, Martre, P, Kattge, J, Gastal, F, Esser, G, Fontaine, S, and Soussana, J.-F. The coordination of leaf photosynthesis links C and N fluxes in C_3 plant species. *PLoS ONE*, 7(6):e38345, 2012.

Mencuccini, M and Grace, J. Climate influences the leaf area/sapwood area ratio in scots pine. *Tree Physiology*, 15(1):1–10, 1995.

Niinemets, Ü and Tenhunen, J. D. A model separating leaf structural and physiological effects on carbon gain along light gradients for the shade-tolerant species *Acer saccharum*. *Plant, Cell & Environment*, 20(7):845–866, 1997.

Niinemets, Ü and Valladares, F. Photosynthetic acclimation to simultaneous and interacting environmental stresses along natural light gradients: optimality and constraints. *Plant Biology*, 254(6):254–268, 2004.

Olson, M. E and Rosell, J. A. Vessel diameter–stem diameter scaling across woody angiosperms and the ecological causes of xylem vessel diameter variation. *New Phytologist*, 197(4):1204–1213, 2013.

Prentice, I. C, Harrison, S. P, and Bartlein, P. J. Global vegetation and terrestrial carbon cycle changes after the last ice age. *New Phytologist*, 189(4):988–998, 2011.

Prentice, I. C, Dong, N, Gleason, S. M, Maire, V, and Wright, I. J. Balancing the costs of carbon gain and water transport: testing a new theoretical framework for plant functional ecology. *Ecology Letters*, 17(1):82–91, 2014.

Schäfer, K. V. R, Oren, R, and Tenhunen, J. D. The effect of tree height on crown level stomatal conductance. *Plant Cell & Environment*, 23(4):365–375, 2000.

Shugart, H. H. *A Theory of Forest Dynamics*. Springer-Verlag, New York, 1984.

Sitch, S, Smith, B, Prentice, I. C, Arneth, A, Bondeau, A, Cramer, W, Kaplan, J. O, Levis, S, Lucht, W, Sykes, M. T, Thonicke, K, and Venevsky, S. Evaluation of ecosystem dynamics, plant geography and terrestrial carbon cycling in the LPJ dynamic global vegetation model. *Global Change Biology*, 9(2):161–185, 2003.

Smith, B, Prentice, I. C, and Sykes, M. T. Representation of vegetation dynamics in the modelling of terrestrial ecosystems: comparing two contrasting approaches within European climate space. *Global Ecology and Biogeography*, 10(6):621–637, 2001.

Sperry, J. S, Hacke, U. G, and Pittermann, J. Size and function in conifer tracheids and angiosperm vessels. *American Journal of Botany*, 93(10):1490–1500, 2006.

Thonicke, K, Spessa, A, Prentice, I, Harrison, S, Dong, L, and Carmona-Moreno, C. The influence of vegetation, fire spread and fire behaviour on biomass burning and trace gas emissions: results from a process-based model. *Biogeosciences*, 7(6):1991–2011, 2010.

Warton, D, Wright, I, Falster, D, and Westoby, M. Bivariate line-fitting methods for allometry. *Biological Reviews*, 81(2):259–291, 2006.

Way, D. A and Sage, R. F. Thermal acclimation of photosynthesis in black spruce. *Picea mariana*. *Plant, Cell & Environment*, 31(9):1250–1262, 2008.

Weerasinghe, L. K, Creek, D, Crous, K. Y, Xiang, S, Liddell, M. J, Turnbull, M. H, and Atkin, O. K. Canopy position affects the relationships between leaf respiration and associated traits in a tropical rainforest in far north Queensland. *Tree physiology*, 34 (6):564–584, 2014.